Checkpoint-mediated regulations of meiotic double-strand-break repair and crossover formation in *Drosophila melanogaster*

by

ERIC F. JOYCE

A Dissertation submitted to the

Graduate School-New Brunswick

Rutgers, The State University of New Jersey

and

The Graduate School of Biomedical Sciences

University of Medicine and Dentistry of New Jersey

in partial fulfillment of the requirements

for the degree of

Doctor of Philosophy

Graduate Program in Microbiology and Molecular Genetics

written under the direction of

Kim S. McKim, Ph. D.

and approved by

_____

_____

_____

_____

New Brunswick, New Jersey

May, 2010

ABSTRACT OF THE DISSERTATION

Checkpoint-mediated regulations of meiotic double-strand break repair and crossover formation in *Drosophila melanogaster*

By ERIC F. JOYCE

Dissertation Director:

Kim S. McKim

During meiotic prophase, programmed DNA double-strand breaks (DSBs) are required to initiate recombination between homologous chromosomes and are repaired as either crossovers or noncrossovers. Crossovers provide a link between the homologs and facilitate their orientation on the meiosis I spindle and segregation at anaphase. Although studies in a variety of experiment systems have identified and characterized numerous factors necessary for crossover formation, far less is known about how the distribution and number of crossovers are controlled.

The process of repairing meiotic DSBs is monitored by at least two surveillance mechanisms: the canonical DSB repair checkpoint that responds to DNA damage and another that requires the widely conserved AAA+ ATPase Pch2, hereafter referred to as the "pachytene checkpoint." In *Saccharomyces cerevisiae* and *Caenorhabditis elegans,* pachytene checkpoint activity has been detected with mutations in genes encoding structural proteins required for crossing over; however, it remains unclear what the underlying process is that the pachytene checkpoint is monitoring.

I identified the Drosophila pachytene checkpoint by conducting a phenotypic analysis of different classes of recombination-defective mutants. Specifically, the Drosophila pachytene checkpoint delays prophase progression when genes necessary for DSB repair and crossover formation are defective, but surprisingly functions independently of DSB formation. In addition, I investigated the relationship between chromosome structure and the pachytene checkpoint and found that defects in chromosome axis components also cause *pch2*-dependent delays. These findings suggest the pachytene checkpoint monitors two genetically distinct events: an early function of DSB repair proteins and the organization of chromosome axes. In support of this model, heterozygous chromosome aberrations result in a pachytene delay and interchromosomal increase in crossovers that are both dependent on *pch2*.

My studies have led to a model where the sites and/or conditions required to promote crossovers are established independent of DSB formation early in meiotic prophase. The pachytene checkpoint may function to promote an optimal number of crossovers by regulating the duration of PCH2 expression, which defines the crossover determination phase. These results have provided new insights into this highly conserved surveillance mechanism as well as its relationship to pachytene progression and crossover control.

ACKNOWLEDGMENTS

First and foremost, I would like to thank my advisor, Dr. Kim McKim. In addition to being an outstanding mentor, Kim has been a true friend. His passion for science and genetics, in particular, is infectious and is something that I now share. I am forever grateful for the opportunity to have worked with Kim and have learned so much. The experience has shaped my scientific career goals and will drive me for the rest of my life. For these reasons and many more, I will sorely miss my time in the McKim lab.

I have benefited from working with many exceptional colleagues. I owe special thanks to Janet McKim, not only for the time she spent teaching me cytology and microscopy but also for being such a caring and true friend. I would like to thank Rajal Bhagat and former graduate student Dr. Sonam Mehrotra for initially training me in molecular biology and fly genetics. I'd also like to thank fellow graduate student Jeff Cesario for late-night study sessions, moral support, and for making this sometimes grueling process always seem fun. I am grateful to Dr. Sarah Radford for helpful comments on manuscripts as well as providing stimulating discussions. I would also like to thank my lab "best friend" Andrew Harrison for entertaining conversations and the various undergraduates that have worked with me: Matt Hanlon, Audrey Reusch, Sona Jasani, and Katie Landy. In particular, I'd like to thank Shree Tanneti for all her hard work, for putting up with all my tantrums when experiments go wrong, and of course for all the laughs (some of which at her expense). Altogether, you have helped make lab fun as well as productive.

I owe much gratitude to my thesis committee, Drs. Ruth Steward, Nancy Walworth and Jay Tischfield. They provided much needed advice and encouragement on

my research as well as helpful comments on the manuscripts. I would also like to thank Drs. Jeff Sekelsky, Tom Kusch and Scott Hawley for providing reagents, antibodies and insightful criticisms on manuscripts.

To my friends and family, thank you for supporting me since the beginning of my studies and for putting up with my absence on so many occasions. I owe a very special thank you to my parents for their guidance and unconditional support and to my brother Danny, who has stood by me during the best and worst moments of my academic pursuits. To Katherine, you have been a great source of motivation and inspiration. Without you, the past and busiest year of my life would not have been so enjoyable.

This work was supported in part by the Charles and Johanna Busch pre-Doctoral fellowship.

DEDICATION

This thesis is dedicated to my father Ray, who taught me the importance of hard work and how it can help overcome a lot of obstacles and to my mother Judy, who taught me to follow what I love and was the first to encourage me to get a PhD. I also dedicate this to my grandfathers Frank Vaccaro and Edward Joyce who might not have understood what I was doing but were always terribly proud of me.

Last but not least, I dedicate this thesis to the many fruit flies who sacrificed their lives for the advancement of science.

TABLE OF CONTENTS

LIST OF TABLES

LIST OF ILLUSTRATIONS

CHAPTER 1: Introduction

I. Preface

This chapter was published, as presented here, as an invited review in *Bioessays*, March 2007 with the title "When specialized sites are important for synapsis and the distribution of crossovers."

Meiosis: juggling synapsis and recombination

Meiotic prophase involves two striking interactions between the homologous chromosomes. The first is the tight alignment, or synapsis, of homologs along their entire length and the second is the recombination of genetic material. Instead of thinking about these two as parallel processes, it has become clear that the interaction between genetic recombination and synapsis is complex. Meiotic recombination initiates with a double strand break (DSB) in probably all organisms. Furthermore, it is so far without exception that Spo11, a TopoVI-like protein, is required for meiotic DSB formation (Keeney 2001). The pathway of meiotic DSB repair has been reviewed extensively (Bishop et al. 2004; Neale et al. 2006) but two important features are i) single stranded DNA from the broken chromatid undergoes a homology search for a repair template and ii) progression into the repair process leads to recombination intermediates that can be resolved into either simple gene conversions or crossovers. Crossovers are important due to their role in chromosome segregation. At diplotene, crossovers appear as chiasmata and provide a link between the homologs, facilitating homolog orientation and segregation on the meiosis I spindle.

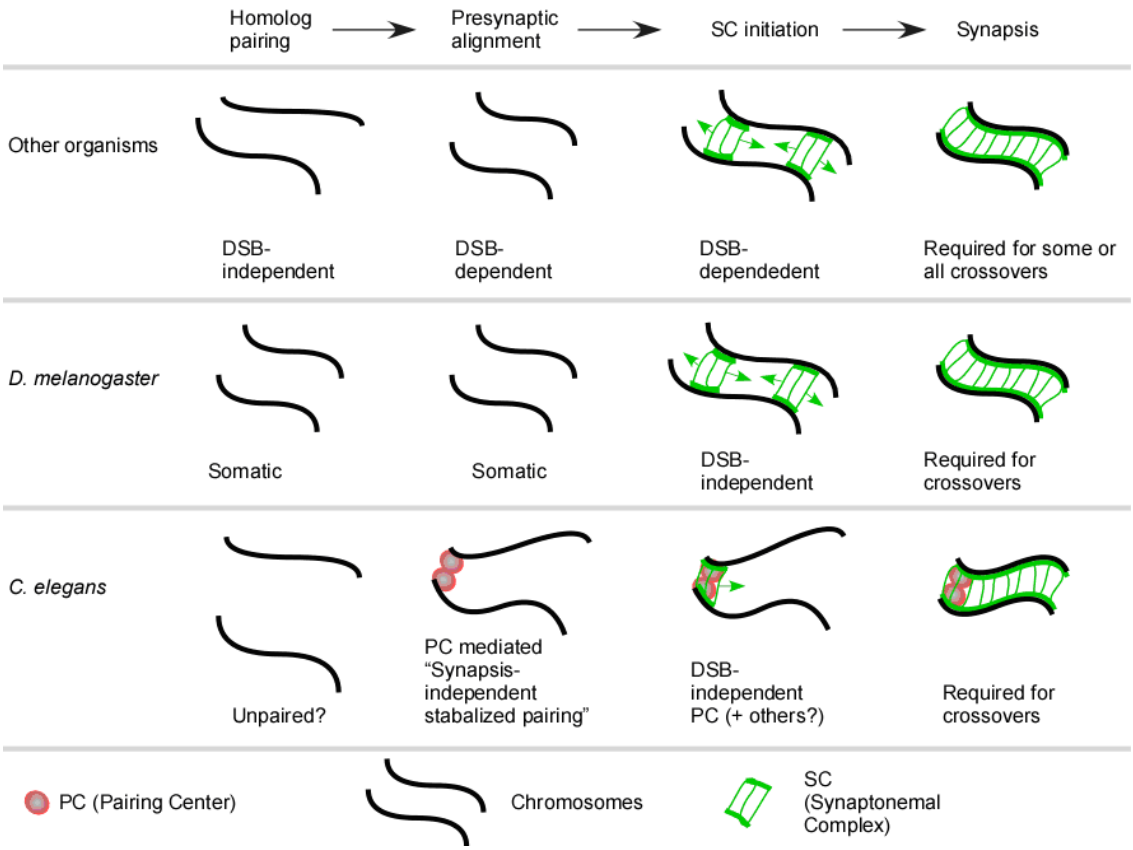

Figure 1: General concepts and the requirements for chromosome alignment, SC formation and crossing over.

The pathway to synapsis can involve DSB-independent pairing, DSB-dependent pairing and finally the establishment of SC initiation sites. However, it is not clear whether the first two stages are obligatory to SC initiation in every organism. In Drosophila, these first two steps have likely been replaced by accurate somatic pairing mechanisms. Similar to other organisms, however, SC initiation probably occurs at multiple sites per chromosome with the main difference being these initiations do not depend on DSBs. There may even be a preference for distal SC initiation sites in Drosophila (Roberts 1972; Sherizen et al. 2005). These models could be modified to include two types of SC initiation site, primary sites and secondary sites which depend on success at a primary site. *C. elegans* may have combined the functions of presynaptic alignment and SC initiation at the PC but there is no evidence of DSB-independent homolog pairing. Not shown is that the PC/HIM-8 complex is located at the nuclear envelope. Although SC initiation is shown to occur at the PC, this has not been directly shown and even if the PC is the predominant site of SC initiation, other sites may have this capacity with lower efficiency.

The whole process may begin with a type of DSB-independent homolog interaction (Zickler et al. 1998; Gerton et al. 2005; Zickler 2006), which could include events near the telomeres (Bass 2003; Harper et al. 2004) and whose relationship to the later DSB-dependent events is poorly defined. Subsequently, but prior to synapsis, it is often possible to identify a stage of presynaptic alignment which may depend on DSBs and serves to align the axis of homologous chromosomes at a distance of 300-400nm (von Wettstein et al. 1984; Zickler 2006). Finally, synapsis stabilizes the homologs at a distance of approximately 100nm as they are held together by the SC, a meiosis specific structure conserved in most organisms (Zickler et al. 1999; Page et al. 2004). Organisms with SC depend on its components for many or all of their crossovers. For example, all crossing over is eliminated in mutants lacking transverse element components of the SC in *C. elegans* (MacQueen et al. 2002; Colaiacovo et al. 2003) and *D. melanogaster* (Hall 1972; Page et al. 2001).

It might have been expected that the close pairing of the homologs would precede DSBs in order to promote recombinational repair between homologs. In fact, the opposite approach appears to be the favored mechanism as a recombination based process stimulates synapsis in a variety of organisms, such as budding yeast and other fungi, mice, and plants such as Arabidopsis (Keeney 2001; Henderson et al. 2005). While DSBs can generate a substrate for homology searching and a mechanism for aligning chromosomes (Carpenter 1987), synapsis initiation appears to be more complicated. Studies in fungi have suggested that there are two stages of DSB-dependent pairing, presynaptic alignment and synapsis, and that each require a different number of DSBs (Storlazzi et al. 2003; Tesse et al. 2003; Henderson et al. 2004) (Figure 1). Presynaptic

alignment requires fewer DSBs than synapsis. To explain the requirement for additional DSBs to promote synapsis, is has been suggested that SC only initiates at a subset of DSB sites (see below) (Zickler 2006).

Some organisms, however, do not require DSBs for synapsis. Studying meiosis in these systems has the advantage that the mechanism of SC formation has been uncoupled from DSB formation. Here we will discuss two well studied cases, in *C. elegans* and *D. melanogaster,* where it has been shown that synapsis occurs without delay in the absence of DSBs (Dernburg et al. 1998; McKim et al. 1998). Two important questions to address are: how is synapsis initiated when it does not require DSBs, and are there common features in the mechanism for SC initiation among those organisms that require DSBs for synapsis and those that do not? If there are similarities, studying the arguably simpler synapsis initiation mechanism in *C. elegans* and *D. melanogaster* may provide insights into the core of the synapsis initiation mechanism. These two organisms have another feature which has not been described in other organisms. In both organisms, special sites are required for normal levels of crossing over. Here we will review the evidence for specialized meiotic sites and ask why they exist. Is their presence in these organisms related to the fact that they do not require DSBs for synapsis?

Translocations and inversions provide evidence for specialized meiotic sites in *D. melanogaster*

Translocations are region specific crossover suppressors (as assessed by progeny counts) in *D. melanogaster*. A long held belief has been that crossover suppression in

translocation heterozygotes was due to defects in homolog pairing or synapsis (Dobzhansky 1931; Roberts 1970). Since heterozygosity for a single breakpoint reduces crossing over between two discrete boundaries, it has been proposed that there are pairing sites which mediate homolog interactions. This idea was also inspired by the characterization of collochores in Drosophila males, which are sites where the X and Y chromosomes are attached in the absence of chiasmata (Cooper 1964; McKee et al. 1990), and of heterochromatic sequences in Drosophila females, where achiasmate chromosomes pair (Dernburg et al. 1996). As described below, however, the sites important for crossing over do not appear to be required for homolog pairing.

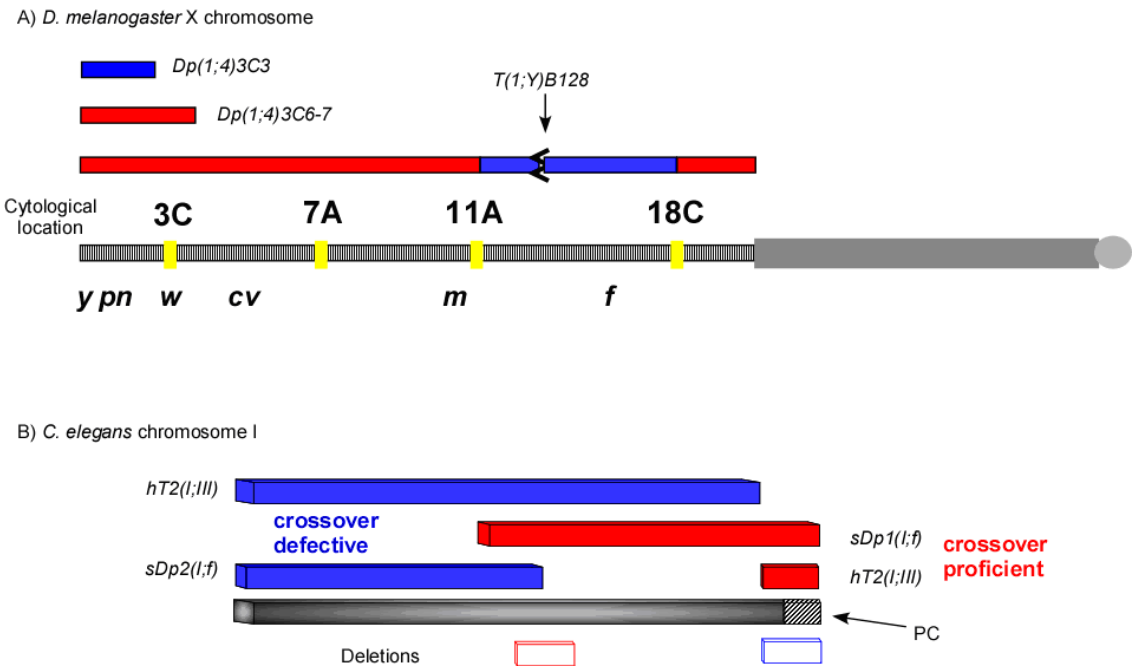

Figure 2: Genetics of meiotic boundary sites.

A) The *D. melanogaster* X chromosome and the structure of the duplication and translocation chromosomes. The euchromatin, where all crossing over occurs, is striped and the heterochromatin is solid grey. The regions shown in red engage in crossing over normally, the blue regions do not and the breakpoints are determined by cytological banding. The translocation *T(1;Y)B128* involves a break at cytological location 13A and the X-chromosome sequences have been joined to portions of the Y chromosome. The duplications are present as fragments of a chromosome in addition to the normal chromosomes (e.g. *Dp*/+/+) and are either attached to another chromosome (to the 4th in these examples from *D. melanogaster*). B) Pattern of rearrangements and crossover suppression on *C. elegans* chromosome I, a typical autosome. The chromosome is shown in grey shading and the location of the PC is hatched. Chromosomes composed of fragments without the PC (blue filled boxes) and some deletions (open blue boxes) are defective for crossing over. In contrast, chromosomes composed of fragments with the PC (red filled boxes) are competent for crossing over. The *C. elegans* duplications are considered to be free, not known to be attached to any other chromosome. Note that the deletion shown to suppress crossing over is hypothetical and drawn by analogy to the X-chromosome PC deletions. No such autosomal PC deletion has been described.

Whether involved in pairing or not, comparing the pattern of crossover suppression to the location of rearrangement breakpoints has been a successful method for identifying sites important for meiotic recombination. Based on the pattern of crossover suppression in translocation heterozygotes, Hawley (1980) mapped four "pairing sites" on the X-chromosome (Figure 2A). For example, the translocation *T(1;Y)B128*, with a break in cytological band 13A, exhibited 8.8% of wild-type crossing over in the *m – f* interval while having 82.0% of wild-type crossing over in the *w – m* interval (Figure 2A). Indeed, X-chromosome translocations with breaks anywhere between cytological divisions 11A and 18C suppressed crossing over between *m* and *f* but not between others markers. Experiments with free duplications showed that these sites did not act only in cis, but could compete with each other as well. A duplication *Dp(1;4)/X/X* which included the site at 3C suppressed crossing over between *w* and *m* on two full length X-chromosomes, even though the duplication included almost no material in this interval (Figure 2A). A slightly shorter duplication, differing only by the lack of the 3C sequences, did not affect *w – m* crossing over. This result suggested that, by interacting with a normal X-chromosome in the 3C region, the longer duplication could prevent the other X-chromosome from engaging in crossovers between *w* and *m.*

Sherizen et al. (2005) extended this type of study, using the extent of crossover suppression in translocation heterozygotes to map four sites on chromosome 3R. The most surprising result came from fluorescent in situ hybridization (FISH) experiments which showed that homolog pairing in translocation heterozygotes was normal throughout the crossover suppressed region. This result was confirmed with the analysis of inversions on the X chromosomes by Gong et al (2005). These results lead to the

conclusion that homolog pairing defects are not the cause of the crossover suppression in translocation or inversion heterozygotes. For this reason, we now refer to these chromosome locations as boundary sites to represent the observation that a rearrangement breakpoint causes crossover suppression only between two sites (with one exception, see below). Indeed, both Sherizen et al. (2005) and Gong et al (2005) found that homologs most likely enter meiotic prophase paired at multiple sites along their lengths. This highly accurate homolog pairing may be mechanistically related to similar events in somatic cells (Hiraoka et al. 1993; Fung et al. 1998) and the mitotically dividing oogonial cells of the female germline (Grell et al. 1970). It has not been determined if pairing is established rapidly after pre-meiotic DNA replication since pairing may be lost at S-phase (Csink et al. 1998), or if pairing is maintained from an event earlier in development. Interestingly, the somatic pairing mechanism(s) is not sufficient to hold the homologs together throughout meiotic prophase. In *c(3)G* mutants, which lack SC, the homologs begin to separate as prophase progresses (Gong et al. 2005; Sherizen et al. 2005). In short, *D. melanogaster* females initiate SC between homologs that are already precisely aligned and require synapsis to stabilize homolog pairing later in meiotic prophase.

To date, no DNA sequences have been associated with boundary sites. Hawley (1980) suggested that the locations of the X-chromosome *D. melanogaster* sites corresponded to the known sites of intercalary heterochromatin (IH). The sites mapped by Sherizen et al. (2005) may also correspond to these locations. IH contains repetitive DNA, is late replicating, enriched for certain proteins like HP1 and associates with the nuclear envelope (Zhimulev et al. 2003). Indeed, upwards of 15 sites per chromosome

arm are predicted to interact with the nuclear envelope in somatic cells (Marshall et al. 1996). Although these sites have not been shown to correspond to known locations of IH and IH has only been described in somatic cells, all IH sites have probably not yet been identified. The suggestion by Hawley is intriguing, however, because it raises the possibility that the *D. melanogaster* boundary sites have some common characteristics to the *C. elegans* sites described below, such as interactions with the nuclear envelope.

The *C. elegans* pairing center and its role in synapsis and crossing over

As in *D. melanogaster*, crossover suppression is observed for a long distance from a *C. elegans* translocation breakpoint (Rosenbluth et al. 1981; McKim et al. 1988). Unlike *D. melanogaster*, however, each *C. elegans* chromosome has only a single specialized site located near one end of each chromosome, referred to as a *Pairing Center* (PC). Chromosome fragments require only the PC end of a chromosome to be able to crossover with the homolog, while the complementary fragment lacking the PC, no matter how large, rarely experiences a crossover (Figure 2B). The degree of crossover suppression is quite impressive. In the study of *eT1(III;V),* an interval of 8.6 cM was reduced to less than 0.3 cM (Rosenbluth et al. 1981). Similar observations were made with duplications of the X chromosome (Herman et al. 1989) and the autosomes (Rose et al. 1984; McKim et al. 1993). For example, crossing over between the free duplication *sDp2(1:f)* and the regular chromosome I was rare, occurring at a frequency of $<10^4$ even though the expected frequency based on the genetic length of the same interval on the intact chromosome I was ~25% (Rose et al. 1984). Conversely, a duplication carrying the PC end of chromosome I engaged in crossing over frequently. These results show

that long regions of homology are not sufficient to promote crossing over and the PC is required for crossing over between homologs.

The most detailed studies on the *C. elegans* PC function have been conducted on the X-chromosome. These studies revealed a dual role for the X-chromosome PC. The first is in homolog pairing as revealed by the observation of "synapsis–independent stabilization of pairing" which refers to the ability of the PC region of the chromosome to maintain pairing in the absence of synapsis (MacQueen et al. 2002; Colaiacovo et al. 2003). Since synapsis–independent stabilization of pairing involves the interaction of two homologously paired copies of the PC in the absence of SC proteins, it may have similarities to presynaptic alignment observed in other organisms (Figure 1). The second function is the promotion of synapsis. A deletion of the X-chromosome PC results in a disruption in synapsis, as shown by lack of staining with SC proteins like SYP-1 (Macqueen et al. 2005). Unlike the pairing function, it appears that one copy of the PC can initiate a low level of synapsis (see below). One consequence of these defects is that the PC deletions cause a decrease in crossing over and an increase in nondisjunction that is specific to the X-chromosome (Villeneuve 1994).

The genetic evidence for the PC has been confirmed with the molecular analysis of *him-8* (Phillips et al. 2005). HIM-8 is a C2H2 zinc-finger protein required for synapsis and crossing over on the X-chromosome but not the autosomes. Since both *him-8* mutants and PC deficiencies have similar effects on pairing, synapsis and crossing over, HIM-8 may be a protein required for PC activity. Indeed, HIM-8 localizes to the end of the X-chromosome containing the PC and this complex is closely associated with the nuclear envelope. These results raise the interesting possibility that pairing and synapsis

in *C. elegans* involves the PC interacting with several proteins at the nuclear envelope. Interactions between telomeres and the nuclear envelope are thought to be important for homolog pairing in other organisms as well, but the link to synapsis is poorly understood (Bass 2003; Harper et al. 2004). These results in *C. elegans* may be the best current example linking chromosome contacts at the nuclear envelope to synapsis. There are, however, several important questions to be answered. For example, is the nuclear envelope association of the PC important for synapsis and does it depend on HIM-8? Although HIM-8 may primarily function at the PC, there is a small but significant increase in the severity of the synaptic defects in *him-8* mutants compared to a PC deficiency and synapsis is occasionally observed in PC deficiency heterozygotes. This could be explained by HIM-8 interacting with X-chromosome sequences other than those in the PC to promote synapsis and crossing over.

Do the specialized sites in *C. elegans* and *D. melanogaster* function in SC initiation?

An attractive model for both *C. elegans* and *D. melanogaster* is that these specialized pairing sites are locations for SC initiation. Since PC deletions severely disrupt SC formation in *C. elegans*, the primary location of synapsis initiation may be at or near the PC (Macqueen et al. 2005). While synapsis may initiate at additional locations on a *C. elegans* chromosome, these events are relatively infrequent. Furthermore, *C. elegans* may have combined the steps of pairing (presynaptic alignment) and synapsis initiation at the PC. Unlike Drosophila, there is little evidence for premeiotic or DSB-independent homolog pairing mechanisms as a force for the meiotic alignment of homologs (Figure 1). In *him-8* mutants, there is no difference in pairing of

X-chromosome sites in premeiotic and meiotic cells (Phillips et al. 2005). Interestingly, when SC forms between homologs in the absence of the PC, synapsis is complete, suggesting that once initiated, SC formation is highly processive. This is supported by the synapsis behavior of translocation heterozygotes. The results of FISH studies indicate that the translocations do not form a classical quadrivalent structure. Instead, six bivalents are formed because the crossover suppressed regions (those sequences "distal" to the breakpoint relative to the PC) nonhomologously synapse (Macqueen et al. 2005).

The idea that homologous synapsis proceeds from the PC up to the breakpoint nicely explains the close correspondence between crossover suppression boundaries and the translocation breakpoint (McKim et al. 1988; McKim et al. 1993). The continuation of synapsis into nonhomologous regions is both a striking example of processive synapsis and a failure to respect any constraints that prevent nonhomologous synapsis. These mechanisms depend on the *hop2* and *mnd1* gene products in yeast and mammals and prevent SC formation between nonhomologous sequences (Petukhova et al. 2003; Tsubouchi et al. 2003; Page et al. 2004). While these genes are not present in *C. elegans*, a similar mechanism to block nonhomologous synapsis probably exists, as shown by the recent findings that *htp-1* mutants exhibit nonhomologous synapsis (Couteau et al. 2005; Martinez-Perez et al. 2005). In contrast, the PC appears to give sequences a license to synapse. Since synapsis occurs rapidly between homologous and nonhomologous sequences in translocation heterozygotes, then homology may not be checked once initiated by the PC. The consequence of PC function, therefore, appears to promote synapsis regardless of proteins, like HTP-1, that function to prevent nonhomologous synapsis.

The relationship between the boundary sites in *D. melanogaster* and synapsis is less clear than in *C. elegans*. In *D. melanogaster*, SC is usually present in the crossover suppressed regions of translocation (Sherizen et al. 2005) and inversion (Gong et al. 2005) heterozygotes. Part of the reason why crossover suppression is usually more severe in *C. elegans* could be the more extensive SC formation in *D. melanogaster* translocation heterozygotes. However, the resolution of these immunofluorescence studies could not rule out that SC structure is affected in *D. melanogaster*. The failure to observe frequent disruptions in synapsis could be explained if SC assembly progresses bidirectional from the initiation sites in *D. melanogaster*. Thus, even if SC assembly initiates at boundary sites, most regions in a translocation heterozygote would be associated with SC because either side of the breakpoint is still linked to an SC initiation site. The breakpoint will, however, prevent the SC from becoming continuous between two boundary sites. The fact that breakpoints cause defects in synapsis is also supported by the observation that, in a low frequency of oocytes, the staining of the SC protein C(3)G was missing or reduced in the crossover suppressed regions of translocation (Sherizen et al. 2005) or inversion (Gong et al. 2005) heterozygotes. As described below, crossover suppression may occur due to the break in the chromosome axis, rather than simply the absence of SC.

Missing from the analysis of synapsis initiation in *C. elegans* and *D. melanogaster* is cytological observations of homolog pairing during zygotene. Part of the problem is that zygotene, when one would expect to observe evidence of SC initiation sites, is rapid in both organisms. In *D. melanogaster*, the axial elements do not form prior to assembly of transverse filaments (Carpenter 1975). Therefore, while zygotene

has been described, the location of synaptic initiation sites cannot be determined by EM. Similarly, immunofluorescence studies have shown that two SC proteins, C(2)M and C(3)G, appear simultaneously during zygotene (Manheim et al. 2003). Since C(2)M is a Rec-8 family member and C(3)G is a transverse filament protein, these results are consistent with the EM data that lateral and transverse elements assemble at the same time in *D. melanogaster*. Based on immunofluorescence studies of zygotene in wild-type or early prophase in *c(2)M* mutants (Page et al. 2001; Manheim et al. 2003), there is definitely more than one SC initiation site per arm in *D. melanogaster*, consistent with the mapping of approximately four sites per arm from the genetic studies. In *C. elegans,* there appears to be a brief time where the axial elements (detected using antibodies to Hop1 homologs HIM-3 and HTP-3 or REC-8) (MacQueen et al. 2002; Colaiacovo et al. 2003) form prior to the transverse filaments, making it formally possible to map SC initiation sites.

Chromosomal rearrangements create crossover suppression without affecting the initiation of recombination

In neither *C. elegans* nor *D. melanogaster* is the crossover suppression in rearrangement heterozygotes due to reductions in the initiation of recombination. Using γ-His2Av staining as a marker for DSBs in *D. melanogaster*, Gong et al (2005) demonstrated that DSBs are induced in the crossover suppressed regions. Similarly, Rad51 staining has been used to show that DSBs are induced when synapsis fails due to a PC deletion in *C. elegans* (Macqueen et al. 2005). Therefore, in both organisms, the crossover defects may be a secondary consequence of a synapsis defect. Consistent with

this conclusion is the observation that mutants lacking SC in *C. elegans* (MacQueen et al. 2002; Colaiacovo et al. 2003) and *D. melanogaster* (Hall 1972; Page et al. 2001) lack crossovers. Nonetheless, it is unclear how the DSBs induced in crossover suppressed regions are repaired. Sherizen et al. (2005) reported that gene conversion was also reduced in the crossover suppressed regions. To reconcile this with the observation that DSBs are induced, it is possible that DSBs are repaired using the sister chromatids. This could explain what happens to the *C. elegans* DSBs in the crossover suppressed regions, since they are present on unsynapsed chromosomes. Normally there are barriers to sister chromatid exchanges, such as axial element proteins such as HIM-3 (Couteau et al. 2004) and HTP-1 (Couteau et al. 2005; Martinez-Perez et al. 2005). But since at least some of these axial element proteins localize in synapsis defective mutants and PC deletions (Macqueen et al. 2005; Phillips et al. 2005), DSB repair involving the sister chromatids would be occurring despite the presence of proteins which are supposed to prevent it.

The absence of crossing over can be attributed to the lack of SC in *C. elegans.* In *D. melanogaster,* however, the effect on crossing over in translocation heterozygotes is more severe than the synapsis defect. As described above, extensive SC may form in the crossover suppressed regions, but it is not continuous between two boundary sites (Sherizen et al. 2005). This could be critical. There is circumstantial evidence that crossover suppression can be caused by breaks in the structure of the SC. For example, in either a *c(3)G* mutant with a internal deletion of its coiled-coil (Page et al. 2001) or *c(2)M* mutants (Manheim et al. 2003), many small segments of SC are assembled but never joined into long continuous threads and crossing over is severely reduced. One interpretation of these results is that repair of a DSB into a crossover requires long

continuous segments of SC. A similar idea has been proposed by Zickler and Kleckner (Zickler et al. 1999) based on the transmission of physical stresses, such as tension, along the chromosome cores. A role for properly assembled chromosome axes has also been suggested in studies of *C. elegans* (Nabeshima et al. 2004). Since crossover suppression occurs despite the presence of SC proteins, continuity of SC structure, and not simply having SC proteins assembled, may be critical to stimulate crossing over in *D. melanogaster* (Sherizen et al. 2005).

SC initiation sites in other organisms

A link between synapsis initiation and crossover sites has been proposed in several organisms. The evidence for this is strongest in budding yeast (Borner et al. 2004; Fung et al. 2004; Henderson et al. 2004) and has been extensively reviewed (Bishop et al. 2004; Page et al. 2004; Henderson et al. 2005; Zickler 2006). The ZMM complex of proteins (including budding yeast Zip1, Zip2, Zip3, Mer3, Msh4, Msh5) is thought to be involved in both crossover-specific processing of DSBs and the nucleation of SC (Borner et al. 2004). Consistent with this idea, crossover specification in *S. cerevisiae* occurs very early in the recombination pathway, prior to DSB formation or during the initial stages of strand exchange (Bishop et al. 2004).

Some ZMM proteins are conserved in other organisms (such as Mer3, Msh4 and Msh5) but the link between crossovers and SC initiation has not been characterized to the same level of detail. Interestingly, mouse *msh4* and *msh5* mutants exhibit defects in synapsis (de Vries et al. 1999; Edelmann et al. 1999; Kneitz et al. 2000). Furthermore, some interesting correlations have been found between the cytologically observed

distribution of recombination sites and patterns of synapsis. Recombination nodules (RNs) as seen through EM analysis are associated with meiotic chromosomes and SC during prophase. They are believed to be the sites of initiation and continuation of recombination and contain the appropriate proteins for the molecular events leading to crossover formation as well as other products of DSB repair. There are two types of RN based on morphology and timing: early RNs may be the sites of the earliest stages of DSB repair while late RNs are less frequent, have a distribution similar to crossovers and may indeed be those DSB sites which become crossovers (Carpenter 1979). Since RNs and the stages of SC assembly can be visualized simultaneously, the study of RN distribution has provided insights into the processes by which SC initiation and meiotic recombination is regulated. This type of analysis is not informative in Drosophila, however, since both types of RN do not appear until pachytene (Carpenter 1979).

SC often first initiates in distal regions (Zickler et al. 1999), although in many cases, particularly in plants, there are secondary interstitial initiations as well. In mammals, SC initiation may occur at fewer sites. A recent study of meiosis in human males concluded that SC initiation is reproducible, occurring at one site per chromosome arm at a subtelomeric location (Brown et al. 2005). Similarly, a large fraction of the crossovers occur in these distal regions. Studies of early and late RNs in maize have shown a correlation between where synapsis initiates and crossovers form. This could also be related to the placement of early RNs, which show distal enrichment in some cases (Anderson et al. 2001). Interestingly, early RNs often appear at synaptic forks, providing evidence that sites engaged in the early stages of DSB repair can be synapsis initiation sites (Anderson et al. 2001; Moens et al. 2002). It is not known, however, if

these are the subset which will become crossovers. Since it is only the earliest appearing RNs that are associated with synaptic forks, and if the first appearing early RNs are also the ones to become crossover sites, it is possible that the relationship between crossover distribution and synapsis initiation is indirect.

Synapsis initiation is not always associated with a crossover site. Particularly in plants, there are more initiation sites than crossover sites, and the distribution of chiasmata does not always reflect the pattern of SC initiation (Jones 1984; Zickler et al. 1999; Stack et al. 2002). Thus in these cases, there must be mechanisms for SC initiation that do not proceed through the crossover specification mechanism. There are also situations in organisms with the recombination-dependent pathway, such as yeast, where SC can occur in the absence of DSBs (Bhuiyan et al. 2004; Zickler 2006). Together, these results show that SC can initiate independently of crossovers and possibly DSBs.

If SC initiates in distal regions, it might be predicted that chromosome rearrangements in these regions could have long distance effects on synapsis and crossing over. An observation like this was made by Burnham et al (1972), who cytologically characterized pairing in translocation heterozygotes of maize and concluded that the probability for an initial pairing between homologs was highest in the distal regions of each arm. Remarkably, almost identical conclusions were made by Roberts (1972) in *D. melanogaster* based on the observation that translocations with distal break points suppressed crossing over throughout the arm of a chromosome (this phenomenon does not occur with X-chromosome translocations). These results were confirmed by Sherizen et al (2005). Why an organism that does not require DSBs for synapsis shows such a similarity with one that may require DSBs (although it has not been confirmed that maize

requires DSBs for synapsis) is yet to be determined. One possibility is that there are dominant SC initiation sites even in organisms that have the potential to initiate SC at many (crossover or noncrossover) sites. Once SC is initiated at these presumably distal sites, subsequent events of SC initiation can occur at secondary sites.

In summary, there are several types of sites that may initiate SC in different organisms. Recombination sites destined to be crossovers, the earliest recombination sites to be initiated, recombination sites in a particular region of the chromosome or some other subset of recombination sites have been proposed to be sites where SC assembly can initiate. In addition, particularly in organisms where DSBs are not required, SC could be initiated by other types of sites, such as those at defined locations. In any of these cases, however, the connection between selecting a site to initiate SC formation and actually triggering the assembly of SC proteins has not yet been determined.

Specialized sites for checking homology

The studies in *C. elegans* and *D. melanogaster* summarized above emphasize the importance of chromosome structure on synapsis and meiotic crossing over. It has been demonstrated in these two organisms that the function of specialized sites can be disrupted by breaking the axial backbone of the meiotic chromosomes. We propose that specialized sites evolve for different reasons (see below) but their function is related to a requirement for all organisms to check for homology before the initiation of SC assembly (Figure 1). Secondarily, this can have an effect on crossover control since the strength of interference or the distance for which SC can assemble from an initiation site can influence the distribution of crossovers.

In most organisms, SC may initiate at a select group of sites such as a subset of recombination sites and, in some cases, sites determined to become crossovers. These sites, however, are not at specific locations because DSBs occur at many sites. Linking synapsis to a select group of recombination sites, such as crossover sites, could be a method to regulate SC initiation and ensure its formation between aligned homologs. In contrast, specialized sites at defined locations could be the basis for initiating SC without DSBs. In either case, this process generates a small number of SC initiation sites at a stage in prophase when SC formation is strictly homologous. In contrast, nonhomologous synapsis occurs in some organisms at later stages of prophase and may reflect a relaxation of the constraints limiting SC formation to a homology check (von Wettstein et al. 1984; Zickler et al. 1999). Therefore, in early prophase there may be blocks to forming SC which are alleviated at specific initiation sites providing a "license" to synapse.

As proposed by MacQueen et al. (MacQueen et al. 2005), the PC could have a role in the check for homology between chromosomes. Transient stabilization at the PC end of the chromosome might allow homology to be checked, either in the region of the PC or chromosome wide. It remains to be determined whether homologous PCs preferentially interact or any two PCs can interact prior to a check for homology. The former would be consistent with the finding that other chromosomes probably use different HIM-8 – like proteins. Although there is less supporting data in *D. melanogaster*, the current evidence does not rule out a role for the boundary sites at the interface between a homology check and SC initiation. Even in *D. melanogaster* when

the chromosomes are prealigned, it may be necessary to check homology prior to SC formation.

The number of SC initiation sites may have an important impact on crossover frequency. This is based on the suggestion that interference is related to the capacity to assemble continuous SC for a long distance from the initiation point (Zickler 2006). Below, we invoke this to explain why *C. elegans* has only a single specialized site. For example, highly processive SC formation in *C. elegans* could lead to the high levels of interference observed in this organism (Meneely et al. 2002; Hillers et al. 2003). This leads to a 1:1 relationship between SC initiation and crossover sites even though the two occur at distinctly separate locations.

Conclusion

We suggest that the specialized sites in *D. melanogaster* and *C. elegans* substitute for the function of recombination (or crossover) sites in providing a homology check prior to initiating SC formation (Figure 1). This is a level of control that is probably present in all organisms, and involves restricting SC formation in early prophase to occur only between homologous regions of a chromosome. We also suggest that there are features of the mechanism of SC initiation in *D. melanogaster* and *C. elegans* which are conserved in many organisms. While in the minority when it comes to synapsis in the absence of DSBs, *C. elegans* and *D. melanogaster* are unlikely to be alone. There are several examples of organisms that form SC in the absence of crossovers, such as *B. mori* females (Rasmussen 1977) and several others, mostly insects (Zickler et al. 1999; Zickler 2006). Therefore, mechanisms for SC formation in the absence of recombination must be

present in these organisms. Finally, the experiments to determine if there are specialized sites that mediate synapsis or crossing over have not often been performed. Therefore, is not known how widespread these specialized sites are for synapsis and recombination.

In *C. elegans*, the presence of a single PC could be related to the lack of defined and localized centromeres. MacQueen et al (2005) suggested that a single pairing center on each chromosome could ensure that chromosome fragments are not efficiently segregated. One problem with this model is that many large free duplications are almost as stable as full chromosomes (being transmitted at close to 50% of gametes) (McKim et al. 1990). Alternatively, the presence of a single PC may be related to the problems associated with segregating chromosomes that are holokinetic. There must be a mechanism to restrict centromere activity to one side of a crossover site at meiosis I or a bivalent could be pulled in two directions at anaphase (Rosenbluth et al. 1981; Albertson et al. 1993). Restriction of centromere activity has clearly been shown to occur in other mitotically holokinetic organisms (Goday et al. 1989). In addition, recent studies have shown that SC disassembly and AIR-2 (an Aurora B homolog) localization is asymmetric relative to crossover position (Nabeshima et al. 2005). Perhaps a single pairing site is part of the mechanism that ensures a single crossover occurs (through high interference – see above), or to regulate the restriction of microtubule attachment sites, or both.

D. melanogaster has no need for a stage equivalent to presynaptic alignment and its recombination dependent mechanisms. Therefore, a major role for DSBs has been negated. In the future, it will be important to determine if the boundary sites are the locations where SC initiates or whether they define domains where the SC must be uninterrupted for normal levels of crossing over. While these are not mutually exclusive

possibilities, there are several implications if the former is correct. SC does not initiate simply because the homologs are in close proximity. Instead, SC formation is regulated by initiating only at specialized sites.

It is simplest to presume that the mechanisms regulating synapsis in *D. melanogaster* and *C. elegans* evolved independently and for different reasons. Interestingly, both of these organisms have apparently lost three proteins during their evolution– Hop2, Mnd1 and Dmc1, which have roles in promoting strand exchange and DSB-dependent pairing (Ramesh et al. 2005). This loss may not be a difficult transition, however, since it is possible to compensate for the loss of these proteins by over expressing Rad51(Tsubouchi et al. 2003). Conversely, it is not known why other organisms need to use a DSB-dependent mechanism to align chromosomes prior to synapsis. Although highly speculative, it may be necessary to override forces which normally prevent pairing of homologs in somatic cells. Despite the initial differences in how SC formation is initiated, our ignorance of the mechanism that starts the polymerization of SC subunits leaves the possibility open that once a site for SC initiation has been established, the mechanism to carry out synapsis could be conserved amongst organisms that depend on DSBs and those that do not.

CHAPTER 2: Drosophila Hold'em is required for a subset of meiotic crossovers and interacts with DNA repair endonuclease complex subunits MEI-9 and ERCC1

I. Preface

This chapter was published, as presented here, in Genetics, January 2009. Materials and methods are described in the figure legends and table footnotes. My contributions to the project and paper were: writing of the paper as well as all the experiments with the exception of *hdm; Ercc1* nondisjunction analysis.

II. Abstract

Three Drosophila proteins, ERCC1, MUS312 and MEI-9, function in a complex proposed to resolve double-Holliday junction intermediates into crossovers during meiosis. We report here the characterization of *hold'em* (*hdm*), whose protein product belongs to a ssDNA-binding superfamily of proteins. Mutations in *hdm* result in reduced meiotic crossover formation and sensitivity to DNA damaging agent MMS. Furthermore, HDM physically interacts with both MEI-9 and ERCC1 in a yeast two-hybrid assay. We conclude that HDM, MEI-9, MUS312 and ERCC1 form a complex that resolves meiotic recombination intermediates into crossovers.

III. Introduction

Repairing DNA damage is critical for genomic stability. In meiosis, programmed DNA double-strand breaks (DSBs) induce recombination between homologous chromosomes that are resolved as either crossovers or noncrossovers (McKim et al. 1998; Keeney 2001). Several genes in *Drosophila melanogaster* have been identified that are required for meiotic crossing over but not for DSB or noncrossover formation.

A subset of these genes, *mei-9, Ercc1* and *mus312,* form a discrete group known as the exchange class based on two criteria. First, while most recombination-defective mutations have a polar reduction in the frequency of meiotic crossing over, mutations in exchange class genes reduce crossing over uniformly along the chromosomes, leaving the nonrandom wild-type distribution of crossovers intact (Carpenter et al. 1974; Sekelsky et al. 1995). Second, all three of the identified exchange gene products interact in a yeast two-hybrid assay (Yildiz et al. 2002; Radford et al. 2005). Based on these findings, exchange class proteins have been proposed to be directly involved in the reaction that generates crossovers (Carpenter et al. 1974; Baker et al. 1976). For example, *mei-9* is required for 90% of all meiotic crossovers as well as some types of somatic DNA repair such as nucleotide excision repair (NER) (Boyd et al. 1976). MEI-9 is the Drosophila homolog of the human and yeast NER proteins XPF and Rad1p, respectively, which contain a highly conserved structure-specific endonuclease domain (Sekelsky et al. 1995; Sijbers et al. 1996). These data have led to a model that predicts MEI-9, ERCC1 and MUS312 function in a complex with endonuclease activity that is required during DSB repair to generate crossovers (Yildiz et al. 2004). We have now identified a fourth

member of the exchange class of genes, *hold'em* (*hdm*), whose protein product belongs to a superfamily of proteins with ssDNA-binding activity.

IV. Results and Discussion

hdm mutants have reduced levels of crossing over without altering the distribution of residual crossovers

In a screen for ethyl methane sulfonate (EMS)-induced mutations that increased X-chromosome nondisjunction, we recovered three alleles of *hdm* (*hdm*^{g6}, *hdm*^{g7}, and *hdm*^{g8}*)* that failed to complement each other and exhibited approximately 7% X-chromosome nondisjunction (Liu et al. 2000). *hdm*^{g7} mutants have 28.9% and 47.5% of wild-type crossover levels on the X and 2nd chromosome, respectively, suggesting that the increase in nondisjunction is a secondary consequence of a decrease in crossing over (Table 1,Table 2) (Baker et al. 1976). As described below, all three mutations appear to be null alleles and had similar effects on nondisjunction and crossing over.

Exchange class mutants are defined by their uniform reduction in the frequency of crossing over along the chromosomes. Most other crossover-defective mutations, such as *mei-218* (Carpenter et al. 1974; McKim et al. 1996), reduce crossing over less drastically in the euchromatic regions closest to the centromeric heterochromatin, resulting in map distances more proportional to the physical distances. To examine crossover distribution, we compared the percentage of wild-type crossing over in the centromere-proximal interval (*pr-cn*) to the percentage of wild-type crossing over across the entire 2nd chromosome arm (*al-cn*) (Blanton et al. 2005) (Table 1). *mei-218* mutants had a ratio of

4.86 due to the relatively mild crossover reduction in the interval near the centromere. *hdm* mutants had a ratio of 0.97, similar to the exchange mutant *mei-9* (1.18), both indicating a uniform crossover reduction across the entire chromosome (Table 1). The implication of this result is that *hdm* joins *mei-9*, *mus312* and *Ercc1* as a member of the exchange class of crossover genes.

hdm is not required to make DSBs

To determine if *hdm* mutants have decreased crossover levels due to a reduction in DSBs, we analyzed the staining pattern of an antibody generated against the phosphorylated form of the histone variant, HIS2AV (γ-HIS2AV), which accumulates at DSBs during meiotic prophase (Mehrotra et al. 2006). Since asynchrony of DSB formation can complicate measuring their total numbers, we utilized a mutation in *spn-B*, which encodes a Rad51 paralog required for DSB repair. A *spn-B* mutation forces DSBs, and thus γ-HIS2AV foci, to accumulate into late pachytene (region 3) oocytes (Jang et al. 2003). The number of foci at late pachytene in DSB repair mutants like *spn-B* is expected to be close to the total number of DSBs induced throughout meiotic prophase.

Late pachytene (region 3) oocytes in *spn-B* mutant females displayed an average of 20.3 (SD=3.6) γ-HIS2AV foci, which is similar to previous estimates for the total number of DSBs per nucleus (McKim et al. 2002; Mehrotra et al. 2006). Similarly, *hdm; spn-B* double mutant late pachytene oocytes had an average of 23.0 (SD=1.4) γ-HIS2AV foci (Figure 3). This result suggests that *hdm* mutants do not have a decrease in the total number of DSBs, consistent with other mutants in the exchange class of crossover-specific genes (Joyce et al. 2009). We also examined *hdm* single mutants and found that

few γ-HIS2AV foci persisted into late pachytene oocytes, indicating DSB repair was not blocked (Figure 3; (Joyce et al. 2009).

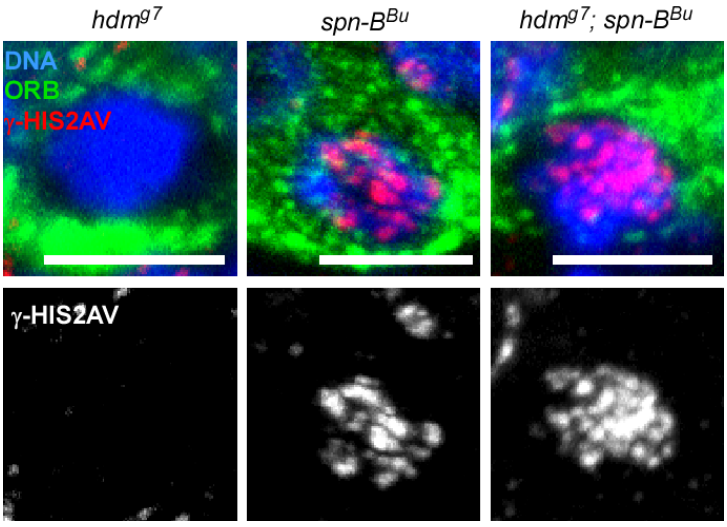

Figure 3: γ-HIS2AV foci in DSB repair-defective background.

Representative examples of γ-HIS2AV staining (red) in late pachytene (region 3) oocytes *in hdm, spnB* and *hdm; spnB* mutants. The cytoplasmic ORB protein (green) is enriched around the oocytes and DNA is in blue. In wild-type (not shown) and *hdm* single mutants, γ-HIS2AV foci are present in region 2 but not in region 3, which is indicative of efficient DSB repair. *spnB* mutants are defective in DSB repair, resulting in the accumulation of foci in later stage oocytes such as in region 3. Each image shows a projection of all confocal sections through the oocyte nucleus. The foci were counted manually by examining each section in a full series of optical sections containing complete pro-oocyte nucleus. The scale bars are 5 μM. Details for the γ-HIS2AV staining experiments can be found in (Joyce et al. 2009).

Mapping and molecular identification of *hdm*

We genetically mapped *hdm* between two P-element insertions located at 7A and 8C. Furthermore, we were unable to recover a crossover between *hdm* and *P[EP]CG10777*^{EP1347} located at 7C3, suggesting a close physical link.

All available X-chromosome deficiencies complemented the *hdm*^{g7} mutation, however a small gap defined at the distal end by *Df(1)ct4b1* (7B2 to 7C3) and at the proximal end by *Df(1)C128* (7D1 to 7D5-6) was left that also contained

P[EP]CG10777^{EP1347} at 7C3. This gap between 7C3 and 7D1 contains 10 predicted coding sequences. Sequencing of candidate coding sequences in the three *hdm* mutants revealed that all alleles had mutations in predicted coding sequence CG15329 (Figure 4). *hdm*^{g6} is a nonsense mutation at the beginning of exon 2 that changes a Gln to a stop codon, *hdm*^{g7} is a 161-base-pair deletion at the end of exon 1, and *hdm*^{g8} is a point mutation at the 3' splice acceptor site in the second intron. All three mutations are putative null alleles, predicted to eliminate full length protein, and behaved similarly in the assays discussed below. RT-PCR confirmed that the CG15329 transcript was expressed in the ovaries, consistent with a meiotic function (data not shown).

HDM's amino acid sequence is conserved in all sequenced Drosophila species, mosquitos, and mammals, but we have not found any obvious homologs in fungi, plants or nematodes (Figure 4). The HDM protein is predicted by the alignment and fold recognition program, Phyre (Bennett-Lovsey et al. 2008), to contain an OB-fold (oligonucleotide binding) that is related to the single stranded DNA-binding domain of human replication protein, RPA70 subunit 3. Therefore, HDM's function may include binding to ssDNA substrates.

A)

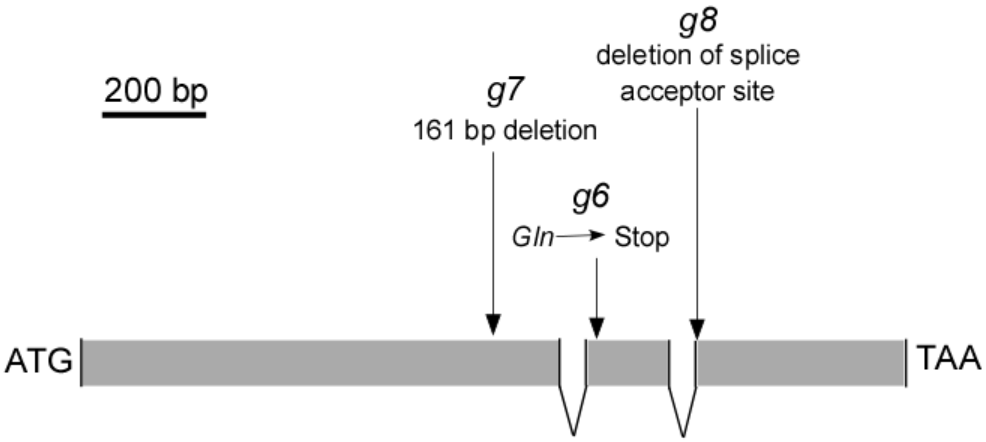

B)

```
                                      1                                                  50
                        HDM     (1) MARRIKFQR----LAEMRPTMTRFSTVALIVSKSSPNIFYDKMSG-TERGV
ENSANGP00000015919 (A. gambiae)     (1) ------------------------------------------DTSHE-TARGV
MGC35212 isoform c (H. sapiens)     (1) MANSFAARIFTTLSDLQPNMANLKVIGIVIGKTDVKGFPDRKNIGSERYT
                          Consensus (1) MA          LADL P M     IAIII KS    F DK    TERGV
                                      51                                                 100
                        HDM    (47) LSLTIRDSPNHLTNCKCWGQRDCVDEYAAMLQIGHVVDIVGAKVMSIPFA
ENSANGP00000015919 (A. gambiae)    (11) LTLTLRDSNRDTINCTVWGKADTIIHYDGAFAIGDVIDVNRPQVAASMFG
MGC35212 isoform c (H. sapiens)    (51) FSFTIRDSPAHFVNAASWGNEDYIKSLSDSFRVGDCVIIENPLIQRKEIE
                          Consensus (51) LSLTIRDSP H INC  WGN D I  YAAAF IGDVVDI  P V A  FA
                                     101                                                 150
                        HDM    (97) APGEQRYQPQATVSCALVVNEG---SGYVVRHDNDDFGQITILQQLLHQPI
ENSANGP00000015919 (A. gambiae)    (61) R---SEQYSPTVTSPYCLTVNDQTVQGAQITRHDGPAQELQRFRALLRVPL
MGC35212 isoform c (H. sapiens)   (101) R---EEKFSPATPSNCKLLLSEN----HSTVKVCSSYEVDTKLLSLIHLPV
                          Consensus (101) R  EEKYSP  TS C LLVNEN   GH I K    F  ITKL ALLHLPI
                                     151                                                 200
                        HDM   (145) RPLGAVLKLADVRSGLGFPDKIITTNVNLLVVVAAVRPVRQIKRKLQGPL
ENSANGP00000015919 (A. gambiae)    (109) VQPGETIPLADIVAS-G---SGCNGETFNVLVVVRAVRAKRDVRVARS----
MGC35212 isoform c (H. sapiens)   (145) KESHDYYSLGDIVAN----GHSLNGRIINVLAAVKSVGEPKYFTTSDR----
                          Consensus (151) K  GD I LADIVA  G    ING  INVLVVVKAVR  R IK A
                                     201                                                 250
                        HDM   (195) SEVQELLQCLEVIVIDASYPEGMLLSVWQPDWIQRAQQWQPRRTVLHLID
ENSANGP00000015919 (A. gambiae)    (153) ----NQVKTFREVILMDGSH-GGVLMKLWSDSYIRWSEQWVPLKTTLLIVD
MGC35212 isoform c (H. sapiens)   (189) ----RKGQ-RCEVRLYDETE-SSFAMICWDNESILLAQSWMPRETVIFASD
                          Consensus (201)    N L    EVILIDASH  GMLMSLW  DWI  AQQWMPRKTVL IID
                                     251                                                 300
                        HDM   (245) VRVSYSNFHRSLVLSHSNCTLICENFQ---AAGDDCRLLLAFAATVPLTTF
ENSANGP00000015919 (A. gambiae)    (199) TRAEFNAYYKTICLAVDRKTIITQEPAHPNAGDRCRMLASYSICYFLIIY
MGC35212 isoform c (H. sapiens)   (234) VRINFDKFRNCMTATVISKTIITTNPDIPEANILLNFIRENKEINVLDDE
                          Consensus (251) VRI F  FHKSI LSV  KTIIT NP  P AGD CRLL AFA T  L  F
                                     301                                                 350
                        HDM   (293) SGCDQAELDNMPAVASIQAQMTVRQIYSRAEGELQDPSIHQFTAVLYGMV
ENSANGP00000015919 (A. gambiae)    (249) SNTNPIAYL-IPTASTINTVMTVQQILDRTEGDLVQ-EEDQFTALCYAVI
MGC35212 isoform c (H. sapiens)   (284) IDSYFKESINLSTIVDVYTVEQLKGKALKNEGKADP----SYGILYAYIS
                          Consensus (301) S S   E INIPTIASINTVMTVKQI  R EGDL      QFTAL YAII
                                     351                                                 400
                        HDM   (343) TKFDLDGLTSHVNRKCIAQQQHIPRNLQDCASDACQQYFSLDNDEPRSIS
ENSANGP00000015919 (A. gambiae)    (297) TRFDLDGCSRLVSERCAHCRSLVREPNGTCGKYDCPGQTTAPDAREP----
MGC35212 isoform c (H. sapiens)   (330) ILNIDDETTKVVRNRCSSCGYIVNEASNMCTTCNKN-----SLDFKSVFL
                          Consensus (351) TKFDLDG TKLV  RCAAC  IV E  N CAS  CN   S   D
                                     401                                                 450
                        HDM   (393) YFNINIHLSDQTGTLVEARLAGHPAERILGLRAEDFERLAEREKSELKWR
ENSANGP00000015919 (A. gambiae)    (344) FFDIAVDVTDHTGTLTGCRMASRVAETVLCCDVATFLRQTDTQRTVLKWK
MGC35212 isoform c (H. sapiens)   (375) SFHVLIDLTDHTGTLHSCSLTGSVAEETLGCTVHEFLAMTDEQKTALKWQ
                          Consensus (401) FF I IDLTDHTGTL  CRLAG VAE ILGC V DFLRLTD QKT LKWR
                                     451                                                 497
                        HDM   (443) FLLKYFEVRLMIKKPVGVRNHLVIVVVDMQAIPLEKLVANMVVF----
ENSANGP00000015919 (A. gambiae)    (394) YLLDRCAVRLIVKRRSAVRFQHLYSIVDCAIADPAEVEAKLKVY----
MGC35212 isoform c (H. sapiens)   (425) FLLERSKIYLKFVLSHRARSGLKISVLSCKLADPTEASRNLSGQKHV
                          Consensus (451) FLLDR  VRLIIKK  AVR  LLISVVDC IADP EL ANL VF
```

Figure 4: Molecular analysis of *hdm*

(A) A schematic of the *hdm* coding region with start and stop codons and splicing pattern resulting in three exons and two introns. The nature of the mutation or amino acid change for the hdm^{g6}, hdm^{g7}, and hdm^{g8} alleles are indicated. B) Full-length protein sequence alignment of HDM to homologs from *A. gambiae* (43.1% similar, 26.7% identical to HDM) and *H. Sapiens* (predicted from cosmid MGC35212 isoform c) (36.9% similar, 22.7% identical to HDM). Identical amino acids are marked with a dark grey background. Conservative and similar changes are noted with a light grey background. The predicted OB-fold is located within the first 290 amino acids (Bennett-Lovsey et al. 2008).

hdm mutants are sensitive to DNA damaging agent MMS

All previously described genes in the exchange class have a role in repairing somatic DNA damage. For example, *mei-9* and *Ercc1* mutants are hypersensitive to DNA damaging agent Methyl Methane Sulfonate (MMS) and both are required for NER (Sekelsky et al. 1995; Radford et al. 2005). To test the possibility that HDM functions in somatic DNA repair, we measured the survival of *hdm* mutants after MMS treatment. Sensitivity to MMS was assayed as described previously (Radford et al. 2005), with mutant and control flies laying eggs in vials for two days followed by addition of MMS on the third day. The relative survival rate following a treatment was measured as the ratio of mutant to wild-type flies. Sensitivity to MMS was expressed as the survival of treated flies divided by the survival of untreated flies. *hdm* mutant larvae administered with a 0.08% or 0.1% dose of MMS exhibited a relative survival rate of 26% and 23% of wild-type, respectively. These results were not as severe as *mei-9* mutants, which exhibited 0% survival after being administered with the same doses of MMS. Therefore, HDM is likely involved in the repair of somatic DNA damage in addition to its role in meiotic crossover formation.

hdm and *Ercc1* are partially redundant in crossover formation

Our results show that crossing over in *hdm* mutants occur at 28.9%-47.5% of wild-type frequencies, depending on the chromosome, whereas *mei-9* mutants only exhibit approximately 10% (Table 1; Table 2). This indicates that *hdm* is required for only a subset of *mei-9*-dependent crossovers. A similar mild effect on crossover formation has previously been shown in the exchange class mutant, *Ercc1,* which exhibits 33.9% of wild-type crossing over on the X-chromosome (Radford et al. 2005). To determine if *hdm* and *Ercc1* have redundant functions in the formation of crossovers, we constructed a double mutant and measured nondisjunction and crossover frequencies on the X-chromosome. *hdm* and *Ercc1* single mutants had 7.2% and 14.2% nondisjunction, respectively (Table 2). The *hdm; Ercc1* double mutant, however, exhibited 21.0% nondisjunction, which is comparable to the effects of *mus312* and *mei-9* alleles (Yildiz et al. 2004). Furthermore, *hdm; Ercc1* double mutants had reduced levels of crossing over, to 14.8% of wild-type, similar in severity to various *mei-9* mutants (Carpenter et al. 1982; Yildiz et al. 2004).

In a *hdm mei-9* double mutant we observed 10.7% of wild-type crossovers, indicating that the residual crossovers in *mei-9* mutants did not require *hdm* (Table 1). A similar result with *mei-9; Ercc1* double mutants has previously been reported (Radford et al. 2005). Together, these results indicate that exchange class genes, *hdm* and *Ercc1*, are partially redundant for the formation of *mei-9*-dependent crossovers.

HDM physically interacts with MEI-9 and ERCC1

MEI-9, ERCC1 and MUS312 physically interact in a two-hybrid assay (Yildiz et al. 2002; Radford et al. 2005). Since HDM is a new member of the exchange class of gene products, we sought to determine if this protein interacts with the other known members of this complex in a yeast two-hybrid assay. An interaction was detected between HDM and MEI-9 as well as with HDM and ERCC1 (Figure 5). An interaction between HDM and MUS312 could not be tested since they both self-activate in a yeast-two-hybrid assay. These results support the hypothesis that all four members of the exchange class, HDM, MEI-9, MUS312 and ERCC1, form a complex required for crossover formation.

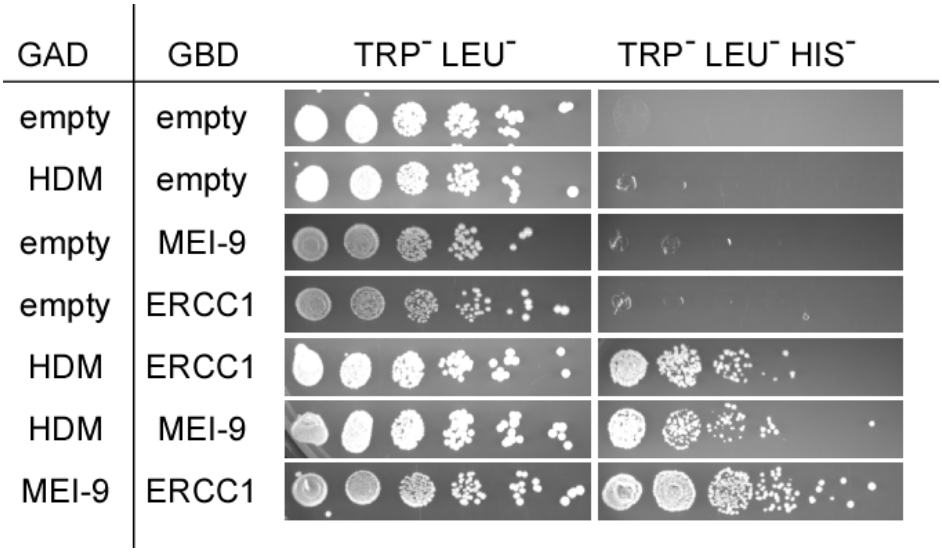

Figure 5: Yeast two-hybrid assay with HDM, ERCC1 and MEI-9.

The two-hybrid experiments were performed as described (James et al. 1996). A full-length *hdm* cDNA was cloned into pGADT7 (Gal4 activation domain) and pGBKT7 (Gal4 binding domain) to create pGADT7-*hdm* and pGBKT7-*hdm*. pGBKT7-*hdm* self-activated and was not used further. pGBKT7-*mei-9*, pGBKT7-*Ercc1*, pGADT7-*mei-9*, and pGADT7-*Ercc1* were described previously (Yildiz et al. 2002; Radford et al. 2005). Clones in the pGADT7 vector containing the Gal4 activation domain (GAD) are noted in the left column and clones in the pGBKT7 vector containing the Gal4 binding domain (GBD) are noted in the right column. Yeast transformed with an empty vector are also shown. Growth with serial dilutions on the TRP- LEU- dropout media indicates both pGBKT7 and pGADT7 vectors were present. Growth with serial dilutions on the TRP- LEU- HIS- dropout media, which also contained 5mM 3-amino-1,2,4-triazole, indicates a physical interaction between the GBD and GAD fusion proteins.

Concluding Remarks

Here we have presented evidence that HDM is physically associated with ERCC1, MEI-9 and MUS312, and that this complex functions in the meiotic recombination pathway to resolve DSB-repair intermediates into crossovers. Like the other exchange class genes, *hdm* also has a role in somatic DNA repair, although this function does not necessarily involve the complex required for meiotic crossing over. In contrast to MEI-9 and ERCC1, HDM and MUS312 probably do not function in NER. Indeed, the interaction between MUS312 and MEI-9 depends on an amino acid required for the meiotic but not DNA repair function of *mei-9* (Yildiz et al. 2002), suggesting the complex required for meiotic crossing over is distinct from the complex required for NER. HDM has a putative ssDNA binding domain and therefore may function as a bridge between endonuclease activity and substrate specificity. HDM may only enhance the complex's affinity to potential recombination intermediate cleavage sites given that it is not required for all *mei-9*-dependent crossovers. *Ercc1* and *hdm* mutants might have additive effects due to a partially redundant role in cleavage site recognition or resolvase activity. Alternatively, ERCC1 and HDM may be required at different crossover sites.

Table 1: Crossing over in precondition and exchange mutants

	Crossing over on the Second Chromosome (cM)						
Mutant [a]	*al-dp*	*dp-b*	*b-pr*	*pr-cn*	Total *al-cn*	Ratio [b]	N [c]
Wild-type	15.6 (100)	22.2 (100)	5.1 (100)	1.4 (100)	44.3 (100)	1.00	886
hdm^{g7}	3.3 (20.9)	7.4 (33.5)	1.7 (33.1)	0.39 (28.0)	12.8 (28.9)	0.97	1251
$mei\text{-}9^{a}$	0.67 (4.3)	3.0 (13.6)	0.50 (9.8)	0.16 (11.5)	4.33 (9.78)	1.18	1192
$mei\text{-}218^{1}$	0.86 (5.5)	1.1 (4.8)	0.51 (10.0)	0.45 (32.0)	2.92 (6.59)	4.86	1018
$mei\text{-}9^{a}$ hdm^{g7}	0.51 (3.3)	3.1 (14.0)	0.81 (15.9)	0.31 (22.1)	4.73 (10.7)	2.07	983

[a] Second chromosome crossing over was assayed by crossing *al dp b pr cn/+* females to *al dp b pr cn/ CyO* males in the indicated backgrounds. The Cy^{+} progeny were scored for recombinants. Crossing over is expressed as cM across the intervals shown. Numbers in parentheses denote the percentage of wild-type crossing over.

[b] The ratio of the percentage of wild-type crossing over across the centromere-proximal interval (*pr-cn*) compared to the percentage of wild-type crossing over across the entire chromosome arm (*al-cn*). Exchange mutants have ratios close to one, while precondition mutants have ratios greater than three (Blanton et al. 2005).

[c] N= total flies counted

Table 2: Crossing over and nondisjunction in *hdm* and *Ercc1* mutants

	Nondisjunction and crossing over on the X-Chromosome						
Mutant [a]	% X-ND [b]	*pn-cv*	*cv-m*	*m-f*	*f-y+*	Total *pn-y+*	N [c]
Wild-type	0.0	15.3 (100)	21.6 (100)	19.1 (100)	6.9 (100)	62.9 (100)	1479
$Ercc1^{X}$	14.2	2.5 (16.3)	10.3 (47.7)	6.0 (31.4)	2.5 (33.9)	21.3 (33.9)	1405
hdm^{g7}	7.2	3.9 (25.5)	15.0 (69.2)	6.8 (35.3)	4.2 (60.1)	29.9 (47.5)	1656
hdm^{g7}; $Ercc1^{X}$	21.0	1.2 (7.8)	4.1 (19.0)	0.91 (4.8)	3.1 (44.9)	9.31 (14.8)	1433

[a] Actual crosses: *y/y pn cv m f • y+ or cy/y pn cv m f • y+ ; Ercc1*^{x} or *y pn cv* hdm^{g7}*/ y* hdm^{g7} *m f y+* or *y pn cv* hdm^{g7}*/ y* hdm^{g7} *m f y+ ; Ercc1*^{X} females crossed to *C(1:Y)1, v f B; C(4)RM, ci ey* males and recombinants were scored among the male progeny. Crossing over is expressed as cM across the intervals shown. Numbers in parentheses denote the percentage of wild-type crossing over.

[b] ND = nondisjunction. The frequency of X-chromosome nondisjunction is calculated as 2(Bar+ females + Bar males)/ [2(Bar+ females + Bar males) + Bar females + Bar+ males].

[c] N= total flies counted

CHAPTER 3: Drosophila PCH2 is required for a pachytene checkpoint that monitors DSB-independent events leading to meiotic crossover formation

I. Preface

This chapter was published, as presented here, in *Genetics*, January 2009. My contributions to the project and paper were: writing of the paper and performing all the experiments.

II. Abstract

During meiosis, programmed DNA double-strand breaks (DSBs) are repaired to create at least one crossover per chromosome arm. Crossovers mature into chiasmata which hold and orient the homologous chromosomes on the meiotic spindle to ensure proper segregation at meiosis I. This process is usually monitored by one or more checkpoints that ensure DSBs are repaired prior to the meiotic divisions. We show here that mutations in Drosophila genes required to process DSBs into crossovers delay two important steps in meiotic progression: a chromatin remodeling process associated with DSB formation and the final steps of oocyte selection. Consistent with the hypothesis that a checkpoint has been activated; the delays in meiotic progression are suppressed by a mutation in the Drosophila homolog of *pch2*. The PCH2-dependent delays also require proteins thought to regulate the number and distribution of crossovers, suggesting that this checkpoint monitors events leading to crossover formation. Surprisingly, two lines

of evidence suggest that the PCH2-dependent checkpoint does not reflect the accumulation of unprocessed recombination intermediates: the delays in meiotic progression do not depend on DSB formation or on *mei-41,* the Drosophila ATR homolog, which is required for the checkpoint response to unrepaired DSBs. We propose that the sites and/or conditions required to promote crossovers are established independent of DSB formation early in meiotic prophase. Furthermore, the PCH2-dependent checkpoint is activated by these events and pachytene progression is delayed until the DSB repair complexes required to generate crossovers are assembled. Interestingly, the PCH2-dependent delays in prophase may, in some situations, allow additional crossovers to form.

III. Introduction

Meiotic crossovers promote genetic variation and mature into chiasmata, which hold the homologous chromosomes together at metaphase I and direct their segregation at anaphase I. In the absence of chiasmata, homologs may segregate randomly, resulting in aneuploidy, which can lead to infertility, severe developmental consequences, or lethality. Therefore, it is not surprising that crossover formation is a tightly regulated process. The formation of crossovers depends on the repair of programmed DNA double-strand breaks (DSBs) through homologous recombination (McKim et al. 1998; Keeney 2001). DSBs are believed to be catalyzed by the Spo11 protein, a suspected paralog of a type II topoisomerase from archaebacteria. DSBs that do not become crossovers are repaired as noncrossovers, often referred to as “gene conversions”.

The mechanism for repairing DSBs to generate crossovers during meiotic prophase probably involves some kind of double Holliday Junction intermediate (Stahl 1996; Heyer et al. 2003; Hollingsworth et al. 2004; Whitby 2005). By contrast, noncrossovers can be generated by a combination of repair pathways such as synthesis dependent strand annealing (SDSA). The meiotic DSB repair program involves proteins specialized for the generation of crossovers as well as generic DSB repair proteins. In Drosophila, the former group of "crossover proteins" have been identified by mutations that cause reductions in the frequency of crossovers but not noncrossovers (reviewed in Mehrotra et al. 2007). The latter group includes proteins such as members of the Rad51 family, required to repair all DSBs (Hoffmann et al. 2004; Kunz et al. 2004).

Drosophila genes required for crossing over have been divided into two general classes: precondition and exchange genes (Sandler et al. 1968; Carpenter et al. 1974). The distinction between the precondition and exchange classes has been mainly based on the effects of mutations on the distribution of crossovers. The few crossovers observed in the progeny of females homozygous for precondition mutants show an altered distribution, while the few crossovers generated by mothers homozygous for exchange mutants show a relatively normal distribution. Therefore, precondition genes may have a role in establishing the crossover distribution, while exchange genes are required later, to carry out the reaction which generates crossovers.

Meiotic DSB repair in Drosophila is monitored by at least one checkpoint. When there is a defect in repairing meiotic DSBs in Drosophila females, the ATR/MEI-41-dependent DSB repair checkpoint is activated (Jang et al. 2003), resulting in a variety of developmental defects including the failure of the oocyte to establish dorsal-ventral

polarity (Ghabrial et al. 1999). This checkpoint pathway may also have a more direct role in DSB repair since mutations in the *mei-41* gene cause a reduction in crossing over (Baker et al. 1972). In budding yeast, checkpoint proteins may also have a role in determining whether repair occurs using the sister chromatid or the homolog (Grushcow et al. 1999).

We have found evidence for a new meiotic prophase checkpoint in Drosophila females. Mutations in DSB repair genes and exchange genes cause delays in two meiotic events: a chromatin remodeling response to DSBs and oocyte selection. Both of these phenotypes may be a consequence of a general delay in pachytene progression, suggestive of an activated checkpoint. Surprisingly, the delay in pachytene progression in DSB repair and exchange mutants is independent of DSB formation but requires precondition genes like *mei-218* and *rec*. This suggests that the checkpoint is not the canonical DSB-repair checkpoint that depends on ATR/MEI-41 (Ghabrial et al. 1999). Instead, we propose that this delay is the result of a second checkpoint associated with the pathway leading to crossovers. We show that this DSB-independent checkpoint requires the Drosophila homolog of PCH2, a AAA-adenosine triphosphatase.

In *Saccharomyces cerevisiae* and *Caenorhabditis elegans*, it has been suggested that a PCH2-dependent checkpoint pathway responds to synapsis defects independent of DSBs (Bhalla et al. 2005; Wu et al. 2006). However, some Drosophila mutants with PCH2-dependent delays in pachytene do not have obvious defects in synapsis. Thus, our results point to a defect in the pathway leading to crossover formation as the trigger which activates the checkpoint. Interestingly, the synapsis mutants analyzed in other

organisms also have crossover defects, suggesting there may be a common mechanism related to crossover specification for triggering the checkpoint in all three species.

IV. Materials and Methods

Fly Stocks and genetic techniques*:* The following mutations were used and have been previously described: *hdm*^{g7} (Joyce et al. 2009), *mei-W68*^{4572} (Bhagat et al. 2004), *mei-P22*^{103} (Liu et al. 2002), *okr*^{WS}, *spn-A*^{1}*, spn-B*^{BU}, and *spn-D*^{349} (Ghabrial et al. 1998; Abdu et al. 2003; Jang et al. 2003; Staeva-Vieira et al. 2003), *mei-41*^{D3} (Sibon et al. 1999), *mei-218*^{1} (Carpenter et al. 1974; McKim et al. 1996), *rec*^{1} and *rec*^{2} (Blanton et al. 2005), *mei-9*^{a}*, mei-9*^{A2}, *mei-9*^{12} and *mei-9*^{RT1} (Yildiz et al. 2004) and *mus312*^{D1} (Yildiz et al. 2002). Experiments were done with both *mei-9*^{a} and *mei-9*^{A2} since they are both genetic null alleles. Experiments with *rec* were done with *rec*^{1} */ rec*^{2} heterozygotes. The deficiency of *pch2, Df(3R)p-XT103,* deletes cytological bands 85A2-85C2. All crosses were raised at 25 ^{o}C. The frequency of *X*-chromosome nondisjunction is calculated as 2(Bar^{+} females + Bar males)/ [2(Bar^{+} females + Bar males) + Bar females + Bar^{+} males].

Irradiation of oocytes*:* Females were exposed to a dose of 10 Gy of X-rays (at a dose rate of 1 Gy/min) and were dissected and fixed at 1, 5 or 24 hours after irradiation.

Cytology and Immunofluorescence*:* For immunolocalization experiments, females were aged at room temperature for about 16 hours and ovaries were dissected and fixed using using Buffer A (Belmont et al. 1989; McKim et al. 2008). The antibody to γ-HIS2AV was described by Mehrotra et al. (2006) and used at a 1:500 dilution. Additional primary

antibodies included mouse anti-C(3)G antibody used at 1:500 (Page et al. 2001), rabbit anti-C(2)M antibody used at 1:400 (Manheim et al. 2003), and a combination of two mouse anti-ORB antibodies (4H8 and 6H4) used at 1:100 (Lantz et al. 1994).

The secondary antibodies were Cy3 labeled goat anti-rabbit (Jackson Labs) used at 1:250 and FITC labeled goat anti-mouse (Vector labs) used at 1:125. Chromosomes were stained with Hoechst at 1:5000 (10mg/ml solution) for seven minutes at room temperature. Images were collected using a Leica TCS SP2 confocal microscope with a 63X, N.A. 1.3 lens. In most cases, whole germaria were imaged by collecting optical sections through the entire tissue. These data sets are shown as maximum intensity projections. The analysis of the images, however, was performed by examining one section at a time.

Counting two-oocytes and calculating p-values: The oocytes were observed using an anti-C(3)G antibody. A cell was scored as an oocyte if complete SC filaments were clear and distinct. P-values were calculated using the Fisher's exact test. The p-value from the test compares the ratio of one-oocyte to two-oocyte cysts that were observed in two genotypes. In experiments where C(3)G staining was not visible (such as in the *c(3)G* null mutant), a concentration of ORB staining in the cytoplasm of a cell was used to identify the oocytes (Gonzalez-Reyes et al. 1997).

Counting γ-HIS2AV foci: The γ-HIS2AV foci were counted from germaria where the foci were clear and distinct. Foci numbers in wild-type were at a maximum in region 2a (early pachytene) and few foci were visible by region 2b (mid pachytene). Therefore, to

compare foci numbers in different genotypes, we used a method that includes all cysts with γ-HIS2AV foci, averaging the number in each pair of pro-oocytes. We compared the average number of foci in all the pro-oocytes or oocytes of each germarium, starting with the youngest cysts at the anterior end, by examining a full series of optical sections.

Plotting γ-HIS2AV foci as a function of relative cyst age: Since the position of a cyst in the germarium is only a rough estimate of its meiotic stage, the foci were first counted in all the pro-oocytes/ oocytes (identified by C(3)G staining) in the germarium. The meiotic stage of each pro-oocyte was then normalized according to the relative position of the entire cyst within the germarium since the relative position is more important than absolute position. The pro-oocytes from 13 wild-type germaria, 18 hdm^{g7}, 6 $mei\text{-}218^{1}$, 5 hdm^{g7} $mei\text{-}218^{1}$, 5 $spn\text{-}D^{349}$, 4 $mei\text{-}218^{1}$; $spn\text{-}D^{349}$, 5 $pch2^{EY01788a}$, 6 hdm^{g7}; $pch2^{EY01788a}$, 5 $mei\text{-}9^{A2}$; and 5 $mei\text{-}9^{A2}$; $pch2^{EY01788a}$ were arranged according to their relative age. The average number of γ-HIS2AV foci per pro-oocyte at each stage was then calculated and plotted as a function of relative cyst age.

Isolation of a *pch2* insertion allele: We used an allele of *pch2* in which the coding region was disrupted by 473 bp of a partially deleted P-element (*P[EPgy2]CG31453[EY01788a]*) inserted toward the end of the first exon (Bellen et al. 2004). This $pch2^{EY01788a}$ mutation causes a frame-shift early in the protein and is therefore likely a null allele. The original stock contained two third chromosome insertions ($P[EPgy2]CG31453^{EY01788a}$ *P[EPgy2]EY01788b*). One insertion, *EY01788a*, was located inside the coding region of CG31453 at 85A3. The other insertion,

EY01788b, was located at 95F1 near CG5524. To isolate the *pch2* (CG31453) insertion, we crossed y^1 w^{67c23}*; P[EPgy2]CG31453*^{EY01788a} *P[EPgy2]EY01788b* males to *cu e ca/ TM6B* females. The Tb^+ female progeny were then crossed to *cu e Pr ca/ TM6B* males and cu^+ *e ca* recombinants were collected and crossed individually to *yw; Dr/ TM3* females. Five stocks were made from crossing Pr^+ *Sb* females to their Pr^+ *Sb* brothers. We confirmed the presence of *EY01788a* by isolating DNA from homozygote *pch2*^{EY01788a} *e ca* females. In all 5 lines, PCR revealed an approximately 500bp insertion in the *pch2* locus. Sequence analysis showed that there was 473bp of a deleted *P[Epgy2]* element inserted into the coding region of *pch2*, which is expected to cause a frame-shift mutation.

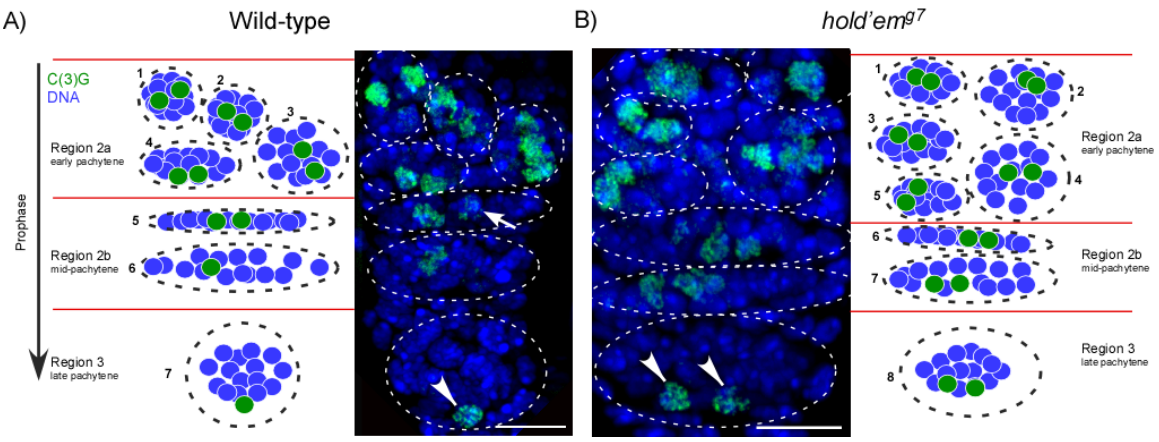

Figure 6: SC formation and the two-oocyte phenotype in *hdm* mutants.

A–B) Maximum intensity projections showing a merge of all the confocal optical sections through a wild-type and *hdm* mutant germarium stained for SC (C(3)G) in green and DNA in blue. A cartoon depiction of oocyte development in wild-type and *hdm* mutant germaria is shown next to its corresponding image. Oocyte development begins in the germarium, where 4 incomplete divisions form a 16-cell cyst (region 1, not shown). Two of the cells in each cyst have four interconnections, or ring canals, and become the pro-oocytes. Changes in cyst morphology differentiate regions 2a, 2b, and 3. In region 2a, both pro-oocytes enter meiosis, including zygotene and early pachytene, where the SC assembles between homologs and meiotic recombination initiates. Region 2a cysts are round, region 2b cysts flatten out and region 3 cysts become round again before leaving the germarium into the vitellarium (stages 2-14). A) In some region 2b and most region 3 wild-type cysts, one cell is identifiable as the oocyte by robust localization of the SC component C(3)G protein. The white arrow indicates the 'loser' pro-oocyte in region 2b which shows trace amounts of C(3)G staining and the white arrowhead indicates a region 3 oocyte with robust C(3)G staining. B) In *hdm* mutants, there are two late pachytene cells (oocytes) with robust C(3)G staining in most region 3 cysts (white arrowheads). Scale bars are 10 μM.

V. Results

Many of the exchange genes have been shown to encode proteins with informative biochemical functions. MEI-9 and ERCC1 form an endonuclease, supporting the hypothesis that exchange proteins play direct roles in the recombination process. In contrast, the function of precondition genes has been ambiguous and confusing because their biochemical functions are not known. Furthermore, the distinction between the precondition and exchange genes is based mostly on the distribution of crossing over in the mutants although the mechanistic basis for this difference is not known.

To establish meaningful parameters to distinguish precondition from exchange genes and gain insights into how these genes promote crossover formation, we used cytological tools to characterize synaptonemal complex (SC) formation and DSB repair in mutations required for crossing over. This was done by comparing the progression through meiotic pachytene in wild-type and mutant females. Whole-mounted ovaries were stained with antibodies recognizing SC components C(3)G and C(2)M to observe synapsis, identify the pro-oocytes and estimate the meiotic stage of each nucleus. DSB formation and repair was monitored using an antibody to γ-HIS2AV. Phosphorylation of HIS2AV (or H2AX in mammals) is a rapid chromatin remodeling response to DSBs that appears during pachytene stage in Drosophila female meiosis (Rogakou et al. 1999; Madigan et al. 2002; Jang et al. 2003).

Meiotic progression in wild-type females

During wild-type oogenesis, oocytes differentiate within a 16-cell germline cyst (see Figure 6 for description of oogenesis). Several cysts are contained in each germarium and are arranged in temporal order, with the earliest cysts located in the most anterior positions. These germarium cysts can be separated into three stages based on their morphology. First, within region 2a cysts, two pro-oocytes initially appear equivalent as both enter meiosis and reach early pachytene. At this time the SC forms and is observed as complete filaments of C(3)G or C(2)M staining in each pair of pro-oocytes. Second, within region 2b cysts, one of the two pro-oocytes begins to exit meiosis, converts to a nurse cell fate, and loses staining of SC proteins. Third, within region 3 cysts, located in the most posterior position of the germarium, oocyte selection

has occurred. This is characterized by the presence of only a single oocyte with SC staining (Figure 6).

In the progression from early (region 2a) to late (region 3) pachytene, there is also a characteristic pattern of γ-HIS2AV staining in the pro-oocytes and oocyte (Mehrotra et al. 2006). γ-HIS2AV foci are most abundant at early pachytene (region 2a) and by late pachytene (region 3) no γ-HIS2AV foci are observed. We used cyst morphology, SC and γ-HIS2AV staining to compare relative timing of progression through pachytene in wild-type and recombination-defective mutants (summarized in Table 3).

Mutations in the exchange and DSB repair classes of genes result in a delay in oocyte selection during pachytene

Meiotic progression was examined in females homozygous for mutations in each of three exchange class genes: two previously characterized, *mei-9* and *mus312*, and *hold'em* (*hdm),* a new member of the exchange class that we recently identified (Joyce et al. 2009). Ovaries from these exchange mutant females were stained for C(3)G. As in wild-type, zygotene was an infrequently observed stage, and complete threads of C(3)G staining were observed in most region 2a pro-oocytes of each exchange mutant (Figure 6). This indicates that SC formation and synapsis occurred rapidly and without noticeable delay, as expected from previous electron microscopy studies of SC formation in *mei-9* homozygotes (CARPENTER 1979).

In all three exchange mutants, however, oocyte selection was delayed; the choice between the two pro-oocytes occurred later than in wild-type. For example, in *hdm* mutant females, two pro-oocytes were visible by C(3)G staining in 62.5% of region 3

cysts (Figure 6; Figure 7), which was significantly greater than the frequency of 9.5% observed in wild-type (p =0.0005, Fisher's exact test). Similarly, both the *mei-9* and *mus312* mutants showed a high frequency of two-oocytes in region 3 cysts (69.6% p=0.00006 and 75.0% p=0.00002 respectively, Figure 7). The presence of two oocytes was associated with the failure of either pro-oocyte to localize to the posterior end of the cyst and frequently showed weaker C(3)G staining in region 3 compared to either wild-type region 3 oocytes or to earlier stage oocytes in the same mutant germarium (Figure 8A). These two observations indicate that the delay affects both pro-oocytes. The presence of two pro-oocytes in region 3 cysts will be referred to as the "two-oocyte" phenotype in this paper.

All known exchange gene products have roles in both somatic DNA repair and meiotic crossover production. To examine whether the two-oocyte phenotype reflected the loss of the meiotic recombination functions, we tested two special *mei-9* alleles (Yildiz et al. 2004). The $mei\text{-}9^{12}$ mutant, which is defective for meiotic crossover formation but proficient in somatic DNA repair, had a high frequency of the two-oocyte phenotype (52.9%, p=0.005). The $mei\text{-}9^{RT1}$ mutant, which is proficient in meiotic crossover formation but is defective in somatic DNA repair, had a low frequency of the two-oocyte phenotype (28.6%, p=0.21). These results suggest that the delay in oocyte selection is due to a defect in a meiotic function of the exchange genes.

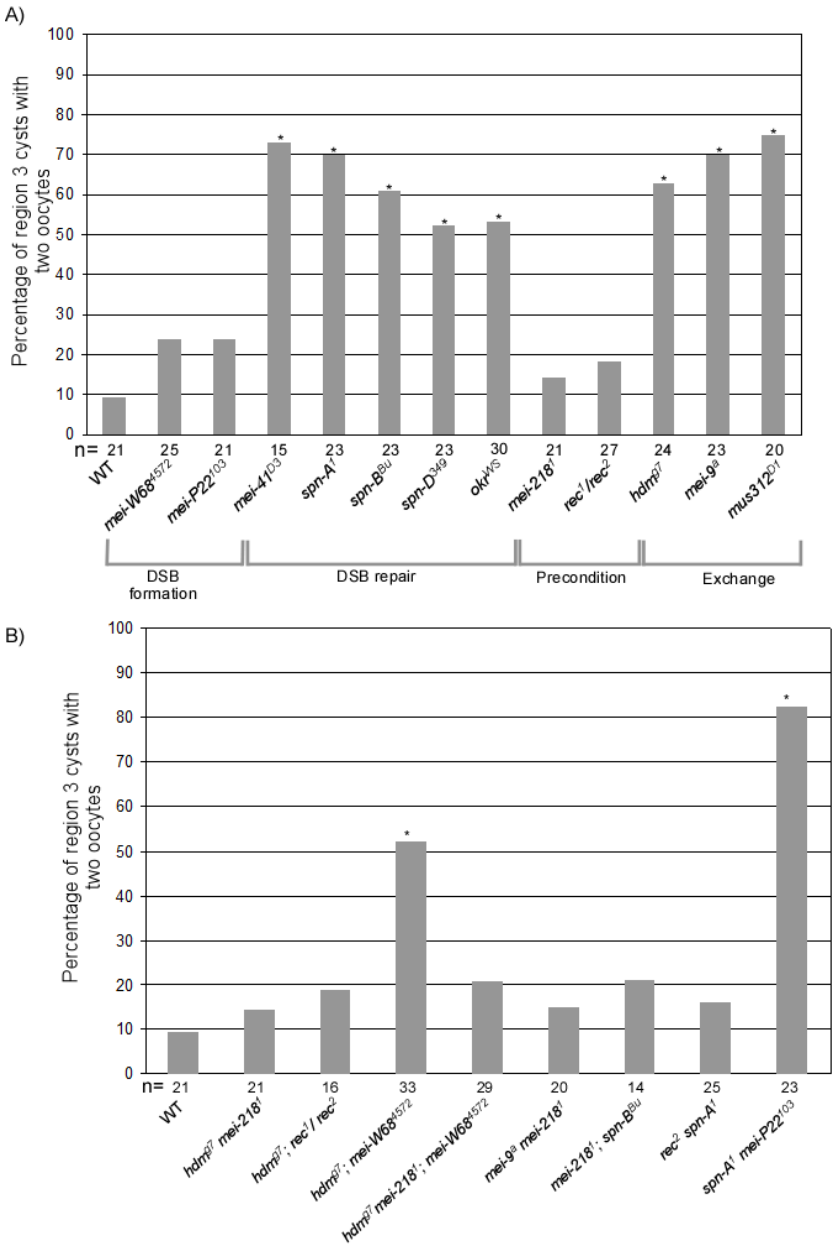

Figure 7: Two-oocyte phenotype in region 3 cysts of wild-type and crossover-defective single mutant females.

The percentage of region 3 cysts with two-oocytes based on C(3)G staining. Asterisks are located above each bar corresponding to a genotype which gave a p-value less than 0.05 when compared to wild-type. The number of cysts (which is equivalent to the number of germaria) counted is shown at the bottom of each bar. A) Two-oocyte phenotype in single mutant females. The mutants are grouped by their primary defect in recombination. A significantly high frequency of the two-oocyte phenotype was found in DSB repair and exchange class mutants, but not in mutants of the DSB formation and precondition groups. The two-oocyte phenotype appears to be robust and reproducible. The frequencies reported here are similar to those in Huynh and St. Johnston (2000). B) Two-oocyte phenotype in double mutant females. The high frequency of two-oocytes observed in exchange mutants (*hdm*^{g7} or *mei-9*^{a}) was suppressed by *mei-218*^{1} or *rec*^{1}/*rec*^{2} but not *mei-W68*^{4572}. Similarly, the two-oocyte phenotypes of DSB repair mutants (*spn-A*^{1} or *spn-B*^{BU}) were suppressed by *rec*^{1}/*rec*^{2} and *mei-218*^{1} but not by *mei-P22*^{103}.

We next examined mutations in four genes required for meiotic DSB repair for the two-oocyte phenotype: the *Rad51* ortholog *spn-A*, *Rad51* paralogs *spn-B* and *spn-D* and the *Rad54* ortholog *okr*. In all of these DSB repair mutants, complete threads of C(3)G staining were observed in most region 2a pro-oocytes, indicating that SC formation and synapsis occurred normally. Like the exchange mutants, each DSB repair mutant exhibited a high frequency of the two-oocyte phenotype (52.5-69.6%, each $p<0.05$ compared to wild-type, Figure 7). Indeed, a two-oocyte phenotype has previously been described in some of these mutants using different markers for the oocyte, such as the cytoplasmic ORB protein (Gonzalez-Reyes et al. 1997; McCaffrey et al. 2006) or a different SC antibody (Huynh et al. 2000). In all mutant females analyzed, SC staining was limited to one cell at stage 2 of oogenesis, which is shortly after a cyst leaves the germarium. Thus, one of the two pro-oocytes does eventually become a nurse cell. These results suggest that exchange and DSB repair mutations delay but do not block the pro-oocyte-to-oocyte decision, causing region 3 oocytes to be in mid-pachytene rather than late pachytene.

In contrast to exchange and DSB repair mutants, the two precondition class mutants we examined, *mei-218* and *rec,* showed a frequency of two-oocytes in region 3 that was not significantly greater than wild-type (14.3%, $p=1$ and 18.5%, $p=0.44$, respectively) (Figure 7). Similarly, mutants with defects in DSB formation, *mei-W68* and *mei-P22*, also showed a low frequency of two-oocytes in region 3 (24.0%, $p=0.26$ and 23.8%, $p=0.41$, respectively). Taken together, our results indicate that only mutations in DSB repair and exchange class genes induce a significant delay in oocyte selection. In contrast, neither defects in DSB formation or precondition genes cause such a delay.

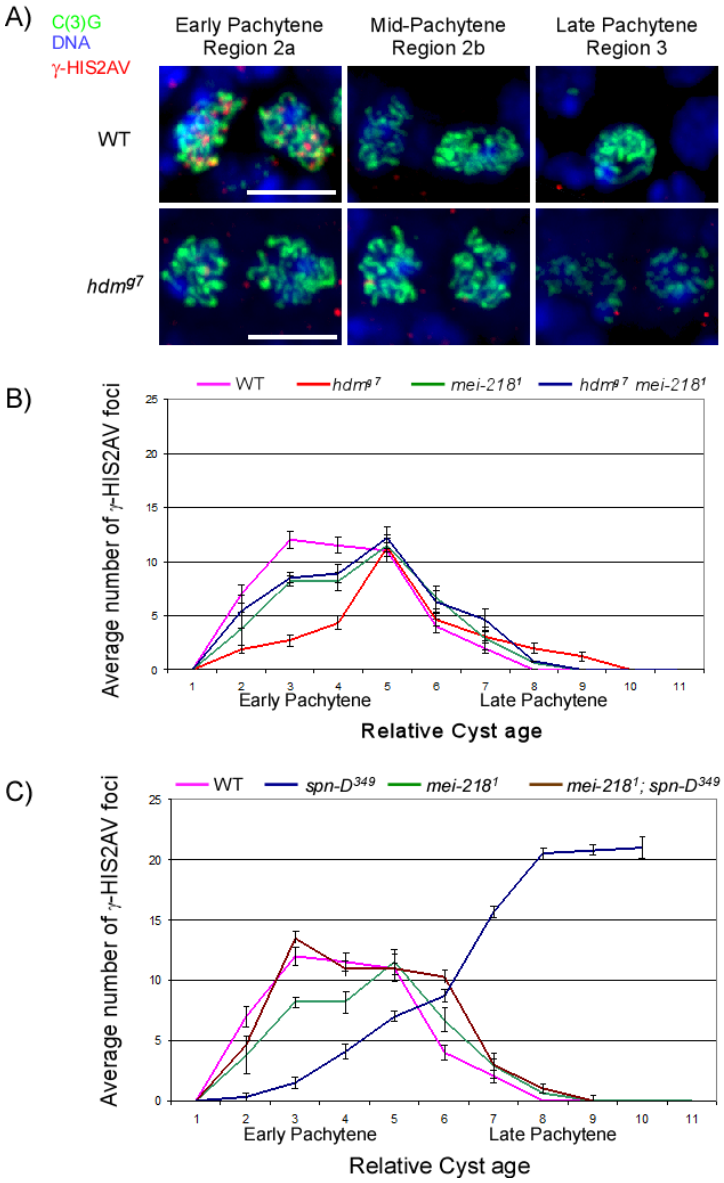

Figure 8: Pattern of γ-HIS2AV staining in wild-type and crossover-defective mutants.

A) Representative examples of γ-HIS2AV staining (red) at different stages of pachytene in wild-type and *hdm*^{g7} mutants, with SC staining (C(3)G) in green and DNA in blue. Each image shows a projection of all confocal sections through the oocyte nucleus. The three panels of each genotype were cropped from the same germarium and image stack. When two oocytes are observed, the C(3)G staining often had reduced intensity relative to other oocytes in the same cyst. The scale bar is 5 μM. B) The average number of γ-HIS2AV foci is plotted relative to cyst age in *hdm*^{g7} and *mei-218*^{1} mutants. Cyst 1 is the first to have complete SC, cyst 8 is in late pachytene (region 3) and cysts 9-11 are in later stage cysts (stages 2-4) which have left the germarium. The age difference between each cyst is approximately 12 hours (King 1970). Because the oocytes are arranged in temporal order in the ovary, the lower number of γ-HIS2AV foci in early stage oocytes (cysts 2-4) of *hdm*^{g7} mutants indicates there is a delay in their appearance. *mei-218*^{1} suppresses the delayed onset and persistence of γ-HIS2AV in *hdm*^{g7} mutants. C) Same graph as B) but for *spn-D*^{349} and *mei-218*^{1} mutants. *mei-218*^{1} suppresses the delayed onset of γ-HIS2AV in *spn-D*^{349} mutants. Because *spn-D*^{349} has a DSB repair defect, the γ-HIS2AV foci persist in high numbers into late stages of pachytene. Error bars denote the standard error of the mean.

Delayed oocyte selection in crossover mutants is DSB-independent

The delay in oocyte selection caused by mutations in exchange and DSB repair genes could be caused by the activation of a checkpoint sensitive to the accumulation of repair intermediates. This hypothesis was tested by eliminating meiotic DSBs using mutants defective in DSB formation. In Drosophila, the programmed DSBs that initiate meiotic recombination require the genes *mei-W68* (encoding a Spo11 ortholog) and *mei-P22* (McKim et al. 1998; Liu et al. 2002). A high frequency of the two-oocyte phenotype was still observed in *hdm; mei-W68* (51.5%, p = 0.420 compared to *hdm*) and *mei-P22 spn-A* (82.6%, p= 0.491 compared to *spn-A*) double mutants (Figure 7). A similar result was previously observed in a *mei-W68; mus301* double mutant (mus301 is also required for meiotic DSB repair, McCaffrey et al. 2006). These results demonstrate that the delay in oocyte selection does not depend on the induction of DSBs or persistent repair intermediates.

Exchange and DSB repair mutants exhibit a delay in the chromatin remodeling response to DSBs

To determine if exchange and DSB-repair mutations, which caused a delay in oocyte selection, delayed other aspects of meiotic progression, we examined the dynamics of DSB formation and repair by staining for γ-HIS2AV. In wild-type oocytes, γ-HIS2AV foci were most abundant at early pachytene (region 2a, cyst 3 in Figure 8) and absent by late pachytene (region 3, cyst 8 in Figure 8). Interestingly, in the exchange mutants, *hdm* (Figure 8B), *mei-9* (Figure S 1) and *mus312* (data not shown), γ-HIS2AV foci did not reach maximum numbers until cyst 5 (approximately the last cyst in region

2a). These mutants did not affect the total number of γ-HIS2AV foci (Joyce et al. 2009), only the timing of their appearance. Thus, exchange mutant females exhibited a delay in the appearance of γ-HIS2AV foci in region 2a.

Mehrotra and McKim (2006) previously reported a delay in the appearance of γ-HIS2AV staining in DSB repair mutants. To examine this in more detail and compare to the exchange mutants, we examined the effect on γ-HIS2AV staining of mutations in *spn-D* (Figure 8C) and *spn-B* (data not shown). These and other mutations in DSB repair genes, such as *spn-A* and *okr,* have two effects on γ-HIS2AV foci. First, they cause a delay in the appearance of γ-HIS2AV foci, much like that observed in exchange mutants. Second, they cause large numbers of γ-HIS2AV foci to accumulate into late stages of pachytene because DSBs are not repaired.

Exchange mutants only show the first phenotype observed in DSB repair mutants; the delay in the appearance of γ-HIS2AV foci. In contrast to what we observed in DSB repair mutants, only a few γ-HIS2AV foci (1.4 foci per region 3 oocyte, n=26) persisted into late pachytene (region 3) oocytes in *hdm* mutant cysts (Table 1). *mei-9* mutants also showed the persistence of only a few γ-HIS2AV foci (1.3 foci per region 3 oocyte, n=10). In wild-type, the persistence of γ-HIS2AV foci in region 3 oocytes was extremely rare (0.04 foci per region 3 oocyte, n=26). These observations are consistent with the conclusion that mutants like *spn-A* and *spn-B* have a block in DSB repair while exchange mutants like *hdm* and *mei-9* only have a delay in DSB repair.

Unlike the DSB repair and the exchange mutants, precondition mutants *mei-218* and *rec* did not exhibit a delay in either the appearance or disappearance of γ-HIS2AV

foci staining, with the exception of a reproducibly tighter curve from cyst 2 through 4 (Figure 8 and data not shown).

The delayed appearance of γ-HIS2AV foci in exchange and DSB repair mutants could represent either a delay in DSB formation or a delay in the response to DSBs. To test for a delayed response to DSB formation, we compared γ-HIS2AV staining in *hdm; mei-W68* double mutants to *mei-W68* single mutants following irradiation. Because *mei-W68* mutants do not generate meiotic DSBs, the only DSBs in this experiment were induced by irradiation. Furthermore, the X-ray treatment would induce the same average number of DSBs in early pachytene (region 2a) cells as late pachytene (region 3) cells of the germarium, allowing for a direct comparison of the γ-HIS2AV response to DSBs at different stages of meiotic prophase. Specifically, we examined the effects of exchange mutations on X-ray induced γ-HIS2AV foci in the first pachytene pro-oocytes (same as cyst 1 in Figure 8). *mei-W68* single mutant pro-oocytes in early pachytene (region 2a) showed a low number of γ-HIS2AV foci at one hour after irradiation and did not reach maximum numbers until approximately five hours after irradiation (Figure 9). This is in agreement with Mehrotra and McKim's observation (2006) that early pachytene oocytes respond to X-ray induced DSBs slower than late pachytene oocytes or somatic cells (Madigan et al. 2002).

If *hdm* mutations only delayed the formation of DSBs, we would have expected the response time to X-ray induced breaks to be the same in *hdm; mei-W68* and *mei-W68* single mutants at all time points. At one hour after irradiation, the *hdm; mei-W68* mutant had the same low number of γ-HIS2AV foci in early pachytene oocytes as the *mei-W68* mutant (Figure 9). At five hours after irradiation, however, the number of γ-HIS2AV foci

in *hdm; mei-W68* mutants was significantly reduced compared to *mei-W68* mutants. At 24 hours after irradiation, the number of γ-HIS2AV foci in both *mei-W68* and *hdm; mei-W68* mutants was again similar throughout the germarium, indicating that the same number of γ-HIS2AV foci develop in *hdm* mutants as wild-type, but take longer to appear. A strikingly similar delayed response time to X-ray induced DSBs was previously found in DSB repair mutants *spn-B* and *okr* (Mehrotra et al. 2006). Thus, along with the delay in oocyte selection, mutations in exchange genes like *hdm* and *mei-9*, and DSB repair genes such as *spn-B* and *spn-D*, cause a delay in the γ-HIS2AV response to DSBs. It remains possible that these mutations also cause delays in DSB formation, but this cannot currently be tested.

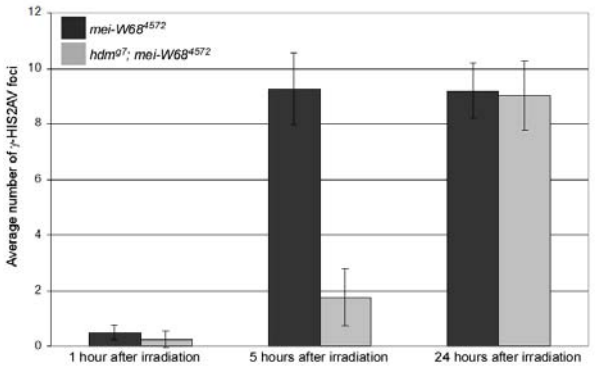

Figure 9: *hdm* delays the response to X-ray induced DSBs.

The average number of γ-HIS2AV foci in *mei-W68*^{4572} (black) and *hdm*^{97}; *mei-W68*^{4572} (grey) females at 1, 5 and 24 hours after irradiation. The data at the 1 and 5 hour time points are from the first cyst with pro-oocytes in pachytene (the first pair of region 2a pro-oocytes with SC staining). At 5 hours after irradiation, *hdm*^{97}; *mei-W68*^{4572} pro-oocytes had 18.9% of the γ-HIS2AV foci found in *mei-W68*^{4572}. The data at the 24 hour time point is from the third cyst with pro-oocytes in pachytene which, due to movement down the germarium, was approximately the first cyst at the time of irradiation. Error bars denote the standard error of the mean.

Delays in meiotic progression require the precondition class of crossover genes

Mutations in the precondition genes *mei-218* and *rec* did not lead to a significant increase in the frequency of the two-oocyte phenotype or delayed γ-HIS2AV response to DSBs. Therefore, we examined whether precondition mutations could suppress these

delays in DSB repair and exchange mutants. In all cases, *mei-218* and *rec* mutations suppressed the delay phenotypes of DSB repair or exchange mutants. For example, a *mei-218* mutation reduced the frequency of the two-oocyte phenotype in *mei-9* and *hdm* mutants to 15.0% (p= 0.0006 compared to *mei-9*) and 14.3% (P= 0.002 compared to *hdm*), respectively, which are not significantly different than wild-type (Figure 7). Similarly, we observed a reduced frequency of the two-oocyte phenotype in the *hdm; rec* mutant (18.8%, p=0.0097 compared to *hdm).* Furthermore, while *hdm; mei-W68* mutant females had a high frequency of the two-oocyte phenotype, *hdm mei-218; mei-W68* mutant females did not (Figure 7, 20.7%, p=0.033 compared to *hdm; mei-W68*), indicating that the suppression of the two-oocyte phenotype by a *mei-218* mutation did not depend on DSBs. Precondition mutations also reduced the frequency of the two-oocyte phenotype in DSB repair mutants, such as in *rec spn-A* (16.0%, P = 0.0003 compared to *spn-A*) and *mei-218; spn-B* double mutants (21.4%, p=0.039 compared to *spn-B*) (Figure 7). Similar results were observed using γ-HIS2AV staining. A *mei-218* mutation suppressed the delayed onset of γ-HIS2AV foci in *hdm* and *spn-D* mutants (Figure 8B, C). Interestingly, the high numbers of persistent foci typical of DSB repair mutants also disappear in the *mei-218; spn-D* double mutant (see Appendix 3).

Precondition mutations could suppress the delay phenotypes indirectly by accelerating progression through pachytene. This hypothesis was tested by ascertaining the frequency of region 2b (mid-pachytene) cysts with two-oocytes in *mei-218* mutants and wild-type. If progression through pachytene was accelerated in a *mei-218* mutant, we would expect a lower frequency of region 2b cysts with two-oocytes compared to wild-type. Instead, we found two-oocytes in 75% and 87.5% of the wild-type and *mei-*

218 mutant region 2b cysts, respectively, indicating no significant change in progression through pachytene in *mei-218* mutant females (P=0.63). Furthermore, the γ-HIS2AV response in these mutants was not faster than wild-type (Figure 8). Therefore, precondition genes are required for the mechanism which delays pachytene progression in exchange and DSB repair mutants.

pch2 is required for the pachytene delay observed in DSB repair and exchange mutants

Mutations in DSB repair but not the exchange genes activate a DSB repair checkpoint pathway that requires the Drosophila ATR homolog *mei-41* (Ghabrial et al. 1999). However, the *mei-41*-dependent DSB repair checkpoint pathway is not responsible for the delays we observed in pachytene progression because this phenotype occurs independently of DSBs. In support of this conclusion, *mei-41* mutants showed a high frequency of the two-oocyte phenotype (73% region 3 cysts with two-oocytes, Figure 7) and also showed a pattern of γ-HIS2AV staining in oocytes similar to that seen in DSB repair mutants, including delayed onset and persistence of foci into late pachytene (Figure S 3). These results suggest that MEI-41 is required for the repair of DSBs during meiosis in addition to its role in the DSB repair checkpoint (see also LaRocque et al. 2007).

A DSB-independent surveillance mechanism has been proposed to monitor pachytene events in *S. cerevisiae* and *C. elegans.* The conserved *pch2* gene, which encodes an AAA-adenosine triphosphatase (AAA-ATPase), is essential for a pachytene arrest in response to mutants with synapsis defects in *S. cerevisiae*, (Wu et al. 2006). In

C. elegans, pch-2 is required for a DSB-independent checkpoint pathway that induces apoptosis in response to mutations that cause synapsis defects (Bhalla et al. 2005). The Drosophila ortholog of *pch2* is CG31453, which encodes a predicted protein that is 22.4% identical and 35.2% similar to *S. cerevisiae* Pch2, and 34.4% identical and 48.3% similar to *C. elegans* PCH-2 (Figure S 4).

We determined whether a mutation in *pch2* could suppress the delay in oocyte selection and delayed γ-HIS2AV response in DSB repair and exchange mutants. Females homozygous for a *pch2* null allele (see Materials and Methods) were fully viable and fertile with a normal distribution and frequency of *X*-chromosome crossing over, showing that *pch2* is not required for meiotic recombination. Furthermore, the *pch2* mutant did not exhibit a delay in oocyte selection or the γ-HIS2AV response to DSBs (Figure 10). However, the frequency of the two-oocyte phenotype in the *hdm; pch2* double mutant was reduced to 23.3% (P= 0.003 compared to *hdm* and p=0.31 compared to wild-type) (Figure 10A). Consistent with this result, *hdm; pch2* mutants did not show the delayed onset of γ-HIS2AV staining observed in *hdm* single mutants (Figure 10B). Similar results were found with *mei-9; pch2* and *okr; pch2* double mutants in which the pachytene delay phenotypes observed in the *mei-9* and *okr* single mutants were suppressed (Figure 10A; Figure S 1). These results show that *pch2* is required for both of the pachytene delay phenotypes observed in *hdm, mei-9* and *okr* mutants. In the course of these experiments, we also found that *okr; pch2* mutants had the same number of γ-HIS2AV foci (23.3 +/- 6.9) in region 3 oocytes as *okr* mutants (22.0 +/- 2.2), suggesting that *pch2* mutations do not affect the number of DSBs.

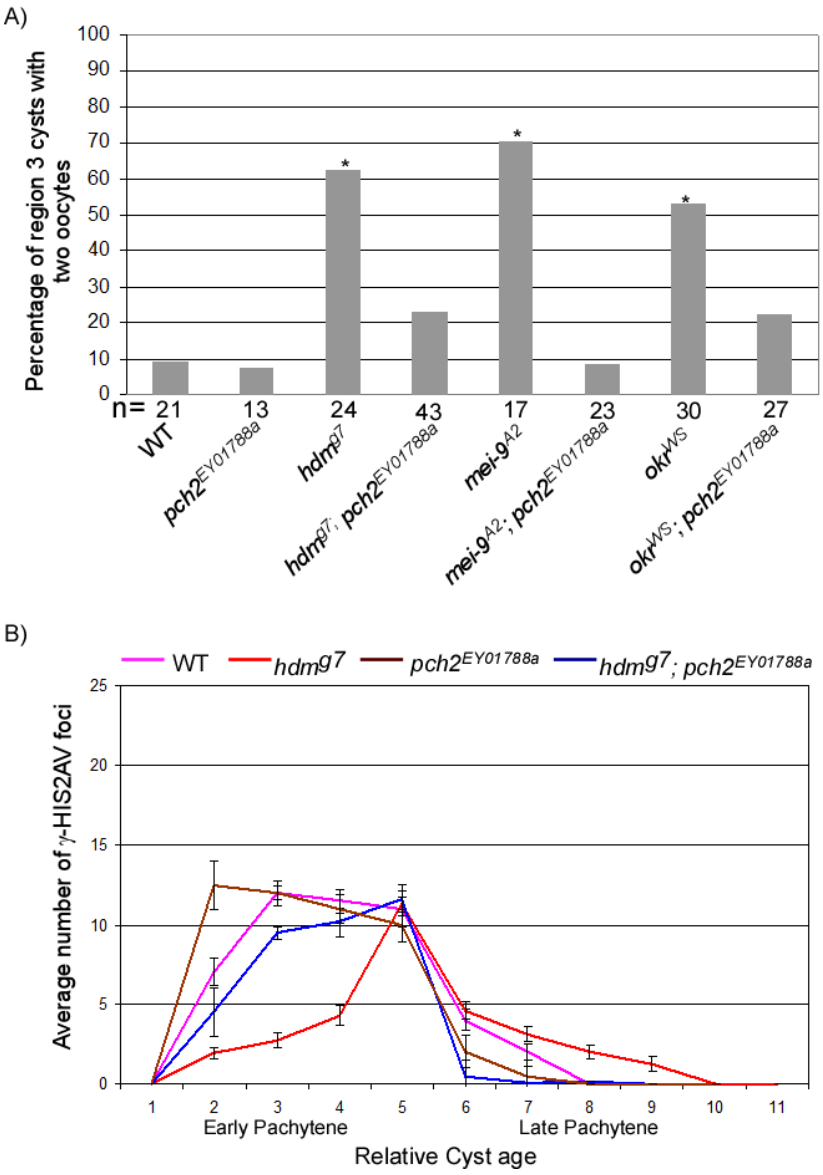

Figure 10: A *pch2* mutation suppresses the pachytene delay phenotypes in *hdm*, *mei-9* and *okr* mutants.

A) For each genotype, the percentage of region 3 cysts with two-oocytes is given based on C(3)G staining. $pch2^{EY01788a}$ mutations have no effect on the frequency of the two-oocyte phenotype and suppress the high frequency of two-oocytes observed in hdm^{g7}, $mei\text{-}9^{A2}$ and okr^{WS} mutants. Asterisks located above each bar correspond to a mutant giving a p-value less than 0.05 compared to wild-type and the number of cysts counted is shown at the bottom of each bar. B) The average number of γ-HIS2AV foci relative to oocyte age in hdm^{g7} and $pch2^{EY01788a}$ mutants (see Figure 8B for details). $pch2^{EY01788a}$ mutations do not alter the wild-type γ-HIS2AV staining pattern and suppress the delayed onset and persistence of γ-HIS2AV in hdm^{g7} mutants. $pch2^{EY01788a}$ also suppressed the delayed onset of γ-HIS2AV in mei-9^{A2} mutants (Figure S 1). Error bars denote the standard error of the mean.

The *pch2* mutation exacerbates the crossover recombination defect in *hdm* mutants

Checkpoints often function to slow progression through the cell cycle so that a problem can be corrected. Thus, a defective checkpoint can increase the severity of a mutation that would normally activate the checkpoint. This situation was observed in the *hdm; pch2* double mutant, in which *X*-chromosome nondisjunction was increased from 7.2% to 15.0% and crossing over was reduced a further 36% relative to the *hdm* single mutant. Although *pch2* is not required for crossing over in a wild-type background, this result demonstrates that it is required for some of the crossovers that occur in *hdm* mutants.

Asynapsis does not activate the *pch2*-dependent checkpoint

The *pch2*–dependent checkpoint in *C. elegans* and *S. cerevisiae* has been proposed to respond to defects in synapsis, (Bhalla et al. 2005; Wu et al. 2006). We tested whether asynapsis could cause delays in Drosophila meiotic prophase by examining a *c(3)G* mutant. *C(3)G* encodes a transverse filament protein that may be the functional homolog of *S. cerevisiae* Zip1 (Page et al. 2004). Because synapsis is abolished in $c(3)G^{68}$ mutant females, we used ORB staining to mark the oocytes (Lantz et al. 1994). The oocyte is identified by a concentration of cytoplasmic ORB protein around one cell in the 16-cell cyst. To confirm the efficacy of ORB staining at identifying the two-oocyte phenotype, we assayed how often ORB protein concentrated in the cytoplasm of two cells rather than one in late pachytene *hdm* mutant cysts. We found a two-oocyte phenotype in 20% (n=30) of region 3 cysts in *hdm* mutants, comparable to the frequencies previously reported in some DSB repair mutants (Gonzalez-Reyes et al. 1997; McCaffrey et al. 2006). In contrast, we did not observe any region 3 cysts with

two-oocytes in *c(3)G*^{68} mutant (0%, n=71) or wild-type control females (0%, n=43), indicating that asynapsis does not cause pachytene delay phenotypes in Drosophila.

VI. Discussion

Mutations in exchange class and DSB repair genes cause delays in pachytene progression

As in most other cell types, there is a checkpoint response to unrepaired DSBs in Drosophila female meiosis (Ghabrial et al. 1999). Our results define a second and distinct DSB-independent checkpoint that operates during pachytene. Mutations in exchange class (e.g. *hdm*, *mei-9* and *mus312*) and DSB repair genes (e.g. *okr, spn-A, spn-B, spn-D* and *mei-41*) cause delay in the timing of at least two events: the chromatin remodeling response to DSBs (phosphorylation of HIS2AV) and, through a process which is DSB-independent, the selection of a single oocyte. Both of the delay phenotypes we have observed can be explained if their timing is linked to the progression through pachytene (Figure 11). A delay in pachytene has also been proposed to explain why Rad51 foci, a DSB response marker, persist into late pachytene in synapsis-defective *C. elegans* mutants (Carlton et al. 2006).

pch2 is required for a pachytene checkpoint that is independent of DSBs

Our results show that the proposed pachytene checkpoint depends on the Drosophila *pch2* ortholog. In *C. elegans* and *S. cerevisiae, pch2* is required for a DSB-independent checkpoint pathway that responds to synapsis defects (Bhalla et al. 2005; Wu et al. 2006). In Drosophila, however, two sets of observations suggest that synapsis

defects may not be the trigger of the PCH2-dependent checkpoint. First, our immunofluorescent studies using SC components C(2)M (data not shown) and C(3)G suggest that exchange mutants (*e.g. hdm* and *mei-9*) and DSB repair mutants (*e.g. okr* and *spn-D*) are able to form SC. Indeed, complete reconstructions from electron micrographs have shown that *mei-9* mutants synapse their chromosomes normally (CARPENTER 1979). Second, *c(3)G* mutations, which abolish synapsis in Drosophila, do not trigger pachytene delays.

Because the exchange mutants have reduced crossover formation but no detectable synapsis defects, our results point to a defect in the pathway that leads to crossovers as the mechanism which triggers pachytene delays. Interestingly, the synapsis mutants analyzed in *C. elegans* and *S. cerevisiae* also have defects in crossover production, suggesting there may be a common mechanism to activate the PCH2-dependent checkpoint in all three species. In fact, a non-null crossover-defective *zip1* allele in budding yeast was reported to exhibit normal synapsis by immunofluorescence but still activated the PCH2-dependent checkpoint (Mitra et al. 2007). In *C. elegans* and *S. cerevisiae*, it could be a secondary consequence of the synapsis defects on the crossover pathway that triggers the *pch2*-dependent checkpoint pathway.

A model for the determination and monitoring of crossover formation

As with most checkpoints, there are two components to the PCH2-dependent checkpoint. First, activation of the checkpoint signal must depend on a specific substrate in the cell (such as a DSB in the canonical DNA repair checkpoint). Second, there must be a process that turns off the checkpoint signal. The first component of the PCH2-

dependent checkpoint depends on the precondition genes, but not DSB formation. This is based on the observation that mutations in precondition genes *mei-218* and *rec* suppress the pachytene delay phenotypes while mutations in DSB formation genes *mei-P22* and *mei-W68* do not (Table 3). Similar to the original proposal by Carpenter and Sandler (1974), precondition genes like *mei-218* and *rec* may be required for establishing the pattern of crossovers, such as their distribution and frequency. MEI-218 and REC both have homology to MCM proteins (Blanton et al. 2005) and recently a hypomorphic allele of the Drosophila *mcm5* gene has been found to have a precondition mutant phenotype (Lake et al. 2007). In addition to their role in DNA replication, MCM proteins affect chromosome structure in as yet poorly defined ways (Bailis et al. 2004) and may interact with checkpoint and recombination proteins (Bailis et al. 2008). Thus, the function of precondition gene products could include modifying the meiotic chromosome structure (see Zickler et al. 1999) which in turn interacts with and is required to activate the PCH2-dependent checkpoint signal.

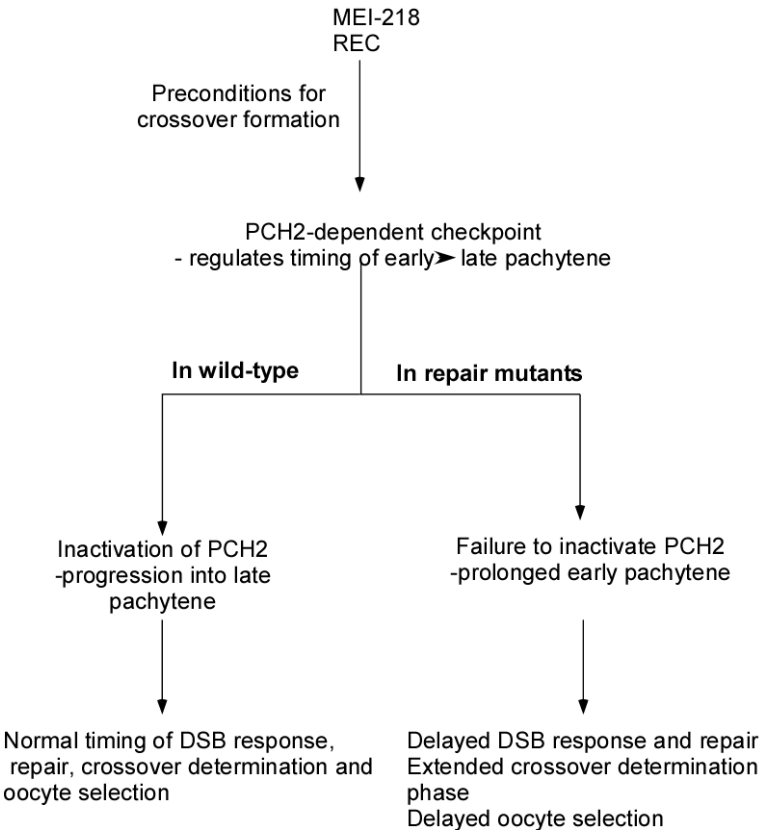

Figure 11: Model for how precondition genes, the PCH2-dependent checkpoint and the exchange genes interact to affect pachytene progression.

Crossover determination requires precondition gene products MEI-218 and REC. Crossover determination generates a substrate which activates the PCH2-dependent checkpoint and delays pachytene progression until the early functions of DSB repair and exchange proteins alleviates the activator of PCH2. This process, from crossover determination to the early function of the DSB repair and exchange genes, is DSB-independent, but the timing relative to DSB formation is not known. Since the consequence of a DSB repair or exchange mutant is observed in early pachytene (the γ-HIS2AV response to DSBs), their activity may turn off the checkpoint close to this time. In DSB repair and exchange mutants, the PCH2-dependent checkpoint remains active, which has several effects on prophase events. Activation of the PCH2-dependent checkpoint early in pachytene leads to the delayed appearance of γ-HIS2AV foci observed in DSB repair and exchange mutants. In the case of the two-oocyte phenotype, the transition into late pachytene could be required for one of the two pro-oocytes to convert to a nurse cell fate. When PCH2 remains active, the transition into late pachytene is delayed. Finally, the active PCH2-dependent checkpoint may prolong the "Crossover determination" phase, which in some cases can result in additional crossovers.

These data are also consistent with previous models that place *mei-218* function upstream of exchange genes in the generation of crossovers (Sekelsky et al. 1995; Bhagat et al. 2004). However, *mei-218* and *rec* also suppressed the pachytene delay phenotypes observed in the DSB repair mutants, *spn-A* and *spn-D*, which provides evidence for precondition gene products functioning early, during or prior to the first steps of DSB repair. While it is possible that the effects of precondition mutations on pachytene progression and crossover formation are not related, the simplest model is that precondition genes function early in the repair process, close to the time of DSB formation to commit a subset of DSBs to the crossover pathway (Figure 11). Such an early time for crossover decision has also been proposed in budding yeast (Bishop et al. 2004; Fung et al. 2004) and in *C. elegans* (Couteau et al. 2005).

The second component, which turns off the checkpoint signal, depends on a previously undescribed DSB-independent function of the DSB repair and exchange genes. If the initial activation of the checkpoint involves precondition gene-dependent changes in chromosome structure, then the DSB repair and exchange genes may function to reverse these changes or block how they interact with the checkpoint. Importantly, a defect in any one of the DSB repair or exchange proteins can trigger the checkpoint. One possibility is that all the proteins required for meiotic recombination preassemble for a "dry run" prior to the actual repair of DSBs. The absence of a functional DSB repair or exchange protein would result in a reduction or impairment of DSB repair complexes capable of generating crossovers and modifying the activity of the PCH2 checkpoint. In support of this hypothesis, exchange gene products are known to form a complex (Sekelsky et al. 1995; Yildiz et al. 2002, Joyce et al., this issue; Joyce et al. 2009).

Whether the exchange and DSB repair proteins form one or multiple complexes has yet to be determined. Preassembling repair complexes before programmed DSB formation occurs could suppress alternative repair pathways as well as provide a mechanism to ensure there is the proper number of crossovers.

Another implication of the delay phenotypes is that the exchange and DSB repair genes are required in early pachytene before the phosphorylation of HIS2AV. A function at this time is not surprising for the DSB repair proteins which are presumably recruited shortly after the break is formed. It is surprisingly early, however, for the exchange genes, considering they are thought to function in the resolution step, relatively late in the repair process (Yildiz et al. 2004; Joyce et al. 2009). However, if all the proteins required for crossover repair preassemble as proposed above, relatively early mutant phenotypes could be the result.

Although Drosophila *pch2* single mutants had no significant change in crossover distribution or frequency, the *hdm; pch2* double mutant had fewer crossovers than the *hdm* single mutant, establishing a functional link between the checkpoint and generating crossovers. The activated PCH2-dependent checkpoint may promote crossover formation in some situations, such as when crossover formation is compromised. Additional crossovers may form due to an extended "window of opportunity" to generate crossovers (Lucchesi et al. 1968; Carlton et al. 2006) (Figure 11) or the activation of additional crossover promoting gene products.

Despite the sequence conservation of PCH2 in many organisms, a conservation of function is not clear. For example, the PCH2-dependent checkpoint in flies and budding yeast (San-Segundo et al. 1999) has been associated with a pachytene delay while in

nematodes with apoptosis (Bhalla et al. 2005). Most surprising, the mouse PCH2 homolog is required to complete recombination events but may not have a checkpoint function (Li et al. 2007). One way to reconcile these differences may be that PCH2 has a role in regulating the timing of important transitions during pachytene. PCH2 may be constitutively active in early pachytene until turned off by activities of proteins involved in crossover formation. This is supported by the observation that mutations in budding yeast *pch2* cause delays in the progression of both the crossover and noncrossover pathways but do not affect the final frequency of these events (Borner et al. 2008). In the future, it will be important to identify what the PCH2-dependent checkpoint responds to. In Drosophila, for example, it will be interesting to know if the proposed interaction of the precondition or repair gene products with the PCH2-dependent checkpoint is restricted to DSB sites or more generally dispersed along the chromosome.

Table 3: Comparison of crossover-defective mutant phenotypes

Class	Mutant	SC formation	Crossover levels	Crossover distribution	Pachytene progression defects			Suppress pachytene delay phenotypes
					Delayed γ-HIS2AV	Persistence of γ-HIS2AV foci [a]	Two-oocytes	
Synapsis	*c(3)G*	no	none	none [b]	ND	0.0	no	ND
DSB formation	*mei-W68*	yes	none	none [b]	none [b]	none [b]	no	no
	mei-P22	yes	none	none [b]	none [b]	none [b]	no	no
Precondition	*mei-218*	yes	reduction	abnormal	no	0.0	no	yes
	rec	yes	reduction	abnormal	no	0.0	no	yes
DSB repair	*spn-A*	yes	ND [c]	ND [c]	yes	21.0	yes	n/a[d]
	spn-D [e]	yes	reduction	abnormal	yes	20.9	yes	n/a[d]
	okra	yes	reduction [c]	abnormal [c]	yes	22.0	yes	n/a[d]
Exchange	*mei-9* [e]	yes	reduction	normal	yes	1.3	yes	n/a[d]
	hdm	yes	reduction	normal	yes	1.4	yes	n/a[d]
Surveillance mechanisms	*mei-41*	yes	reduction [c]	abnormal [c]	yes	21.0	yes	n/a[d]
	pch2	yes	normal	normal	no	0.0	no	yes

ND = not determined

[a] Average number of foci which persist into late pachytene (region 3) oocytes.

[b] Crossing over is eliminated by null alleles but the crossover distribution is altered by hypomorphic alleles (Liu et al. 2002; Bhagat et al. 2004).

[c] Crossover distribution in null mutants is not known because they are sterile. However, *mei-41* and *okr* hypomorphs are fertile and have reduced crossing over with an altered distribution (Baker et al. 1972; Bhagat et al. 2004).

[d] These mutants exhibit delay phenotypes.

[e] Results with *spn-B* were similar to *spn-D* and *mus312* were similar to *mei-9*.

Table 4: Crossing over in *hdm* and *pch2* mutants

	Nondisjunction and crossing over on the *X*-Chromosome						
Genotype	% X-ND [a]	*pn-cv* [b]	*cv-m*	*m-f*	*f-y+*	Total *pn-y+*	Total ♂ progeny [a]
Wild-type	0.1 (2440)	15.3 (100)	21.6 (100)	19.1 (100)	6.9 (100)	62.9 (100)	1479
hdm^{g7} [c]	7.2 (3524)	3.9 (25.5)	15.0 (69.2)	6.8 (35.3)	4.2 (60.1)	29.9 (47.5)	1656
$pch2^{EY01788a}/Df$	0.3 (2098)	12.6 (82.4)	25.2 (116.7)	19.5 (102.1)	7.8 (113.0)	65.1 (103.5)	960
hdm^{g7}; $pch2^{EY01788a}/Df$	15.0 (2305)	0.7 (4.6)	9.6 (44.4)	5.1 (26.7)	3.6 (52.2)	19.0 (30.2)	1107

For wild-type or $pch2^{EY01788a}$*/Df: y/y pn cv m f •*y^+ females were crossed to *C(1:Y)1, v f B; C(4)RM, ci ey* males. For hdm and hdm^{g7}*; *$pch2^{EY01788a}$*/Df: y pn cv* hdm^{g7}*/ y* hdm^{g7} *m f* y^+ females were crossed to *C(1:Y)1, v f B; C(4)RM, ci ey* males. Only the male progeny counts were used to calculate the crossover frequency.

[a] Nondisjunction and crossing over measured in the same experiment. Total progeny for nondisjunction is shown in parentheses. Total progeny for crossing over is only the male progeny from this experiment (see Materials and Methods).

[b] Crossing over is expressed as map units across the intervals shown. Numbers in parentheses denote the percentage of wild-type crossover frequency.

[c] data on *hdm* single mutant from(Joyce et al. 2009).

CHAPTER 4: Disorganized chromosome axes induce a checkpoint-mediated delay and interchromosomal effect on crossing over

I. Preface

This chapter was submitted as an individual paper to *Plos Genetics* and is currently under review. My contributions to the project and paper were: writing of the paper and performing all the experiments.

II. Abstract

Crossovers mediate the accurate segregation of homologous chromosomes during meiosis. The widely conserved *pch2* gene of *Drosophila melanogaster* is required for a pachytene checkpoint that delays prophase progression when genes necessary for DSB repair and crossover formation are defective. However, the underlying process that the pachytene checkpoint is monitoring remains unclear. Here we have investigated the relationship between chromosome structure and the pachytene checkpoint and show that defects in chromosome axis components as well as chromosome rearrangements trigger a *pch2*-dependent delay. Accordingly, the global increase in crossovers caused by chromosome rearrangements, known as the 'interchromosomal effect of crossing over,' is also dependent on *pch2*. These findings suggest a model in which the pachytene checkpoint monitors the organization of chromosome axes. Checkpoint-mediated effects correlate with extended PCH2 expression into late pachytene, which requires the histone

deacetylase Sir2. We propose that the pachytene checkpoint may function to promote an optimal number of crossovers by regulating the timing of a crossover determination phase defined by PCH2 expression.

III. Introduction

Meiotic recombination occurs during meiotic prophase when homologous chromosomes are synapsed along their entire length. Synapsis is defined as the close and stable association of homologous chromosomes through a proteinaceous structure called the synaptonemal complex (SC). In most organisms this complex can be broken down into two main parts: lateral elements that attach along the axis of each homologous chromosome and transverse elements that span the central region of the SC and function to tether the homologs (Zickler et al. 1999; Page et al. 2004). At the leptotene/zygotene stages of meiotic prophase, these structural proteins begin to load onto the chromosome axes, and are completely assembled at pachytene, when homologous chromosomes are synapsed along their entire length.

Recombination between the homologous chromosomes initiates with DNA double-strand breaks (DSBs) that are repaired as either crossovers or noncrossovers (Dernburg et al. 1998; McKim et al. 1998; Keeney 2001). Crossovers establish chromatin linkages called chiasmata, which, along with sister chromatid cohesion, hold homologs together after recombination has been completed and chromosomes have dissociated their SC proteins. Chiasmata help orient the homologous chromosomes on the metaphase I spindle and ensure their proper segregation at anaphase I. The failure to establish a crossover/chiasma can result in the nondisjunction of homologs and lead to aneuploid gametes.

Crossover formation is a tightly regulated process. Mutational analysis has revealed evidence for several mechanisms that control the frequency and position of crossovers along the chromosome arms (Sturtevant 1915; Muller 1916; Hillers 2004; Kleckner et al. 2004). For example, in *Drosophila melanogaster*, the precondition class of mutants exhibit reduced crossover levels with an altered distribution pattern, suggesting these genes have a role in establishing crossover sites, including their distribution (Carpenter et al. 1974). Changes in chromosome structure can also affect crossover distribution. Heterozygous inversions suppress crossing over near the breakpoints, yet enhance the frequency of exchange on the remaining chromosome pairs, a phenomenon referred to as the "interchromosomal effect" (Lucchesi et al. 1968).

Crossing over may also be regulated by surveillance mechanisms that coordinate the sequence of critical events throughout prophase. In Drosophila, the process of repairing meiotic DSBs is monitored by at least two checkpoints: the canonical DSB repair checkpoint that responds to DNA damage (Ghabrial et al. 1999; Jang et al. 2003) and another that monitors DSB-independent events leading to crossover formation, hereafter referred to as the "pachytene checkpoint" (Joyce et al. 2009). The pachytene checkpoint induces a delay in response to defects in DSB repair genes required to repair all meiotic DSBs and genes encoding an endonuclease complex required for crossover formation (exchange class). Pachytene checkpoint activity requires a group of MCM-related genes that promote crossover formation (precondition class) and the Drosophila homolog of the widely conserved AAA+ ATPase PCH2.

In *Saccharomyces cerevisiae* and *Caenorhabditis elegans,* pachytene checkpoint activity has been detected in mutants with disrupted SC formation (San-Segundo et al.

1999; Bhalla et al. 2005); however, it remains unclear what the underlying process is that the pachytene checkpoint is monitoring. For instance, yeast carrying a non-null *zip1* allele appear to form SC normally, yet still exhibit a Pch2-dependent delay (Mitra et al. 2007). Mutations that impair SC initiation in *C. elegans* triggers a Pch2-dependent response (Bhalla et al. 2005), although it is unclear whether the defect being monitored is synapsis *per se,* a prerequisite to synapsis such as axis stability and/or DSB repair. Some mutations that exhibit *pch2*-dependent delays in Drosophila have no obvious defects in SC formation and abolishing synapsis does not elicit any delay phenotypes (Joyce et al. 2009). Therefore, at least in Drosophila and possibly in these other organisms, it may not be the SC that is being monitored by the pachytene checkpoint.

We have investigated the relationship between chromosome structure and the pachytene checkpoint and show that defects in chromosome axis components cause *pch2*-dependent delays. Unlike the delays observed in DSB repair mutants, these delays occur independently of MCM-related genes. These findings suggest a model in which the pachytene checkpoint monitors two genetically distinct events: an early function of DSB repair proteins and the organization of chromosome axes. In support of this model, heterozygous chromosome aberrations result in a pachytene delay and interchromosomal increase in crossovers that are both dependent on *pch2*. A positive correlation was found between checkpoint-mediated effects and prolonged PCH2 activity, which require the histone deacetlyase Sir2. We propose the pachytene checkpoint may function to promote an optimal number of crossovers by regulating the timing of a crossover determination phase defined by PCH2 expression.

IV. Materials and Methods

Drosophila strains*:* Drosophila stocks and crosses were maintained on a standard medium at 25°C. The following mutant alleles were used unless otherwise noted- *ord*^{10} (Bickel et al. 1997), *c(2)M*^{EP}, *pch2*^{EY01788a} *(pch2*^{EY}*)*, *c(3)G*^{68} (Page et al. 2001), *hdm*^{g7}, *mei-218*^{1}, *rec*^{1}*and rec*^{2} (Blanton et al. 2005), *Ercc1*^{X} (Radford et al. 2005), *mei-9*^{a}, *spn-A*^{1}, *spn-B*^{Bu}, *sir2*^{17} (Astrom et al. 2003), and *mei-W68*^{4572}. The deficiency *Df(2L)BSC245* deletes cytological bands 33F3-34A9, which includes the *sir2* locus. *T(2;3)DP*^{77} and *T(2;3)dp*^{D} translocations were obtained from the Bloomington Stock Center. *T(2;3)DP*^{77} breakpoints are at 26E-27A on the 2nd and 85C on the 3rd. *T(2;3)dp*^{D} breakpoints are at 25A on the 2nd and 95B-D on the 3rd. The *T(2;3)lt*^{X16} translocation has breakpoints at 40 (heterochromatin) on the 2nd and 95A3 on the 3rd and was obtained from B. Wakimoto (Wakimoto et al. 1990).

Genetic techniques*:* X-chromosome nondisjunction was assayed by crossing females to *yw/Y*^{BS} males. The frequency of X-chromosome nondisjunction is calculated as 2(Bar females + Bar^{+} males)/ [2(Bar females + Bar^{+} males) + Bar^{+} females + Bar males]. To estimate wild-type X chromosome crossing over frequency, *y/y pn cv m f • y*$^{+}$ female flies were crossed to *C(1:Y)1, v f B: [+]; C(4)RM, ci ey* males, and X chromosome recombinants were scored in males. Second chromosome crossing over was assayed by crossing *al dp b pr cn/+* females to *al dp b pr cn/ CyO* males and scoring for recombinants among the *Cy*$^{+}$ progeny. P-values were calculated using the Fisher's exact test.

Cytology and Immunofluorescence*:* For immunolocalization experiments, females were aged at room temperature for about 16 hours and ovaries were dissected and fixed using the "Buffer A" protocol (McKim et al. 2008). The antibody to γ-HIS2AV was described by Mehrotra et al. (2006) and used at a 1:500 dilution. Additional primary antibodies included mouse anti-C(3)G antibody used at 1:500 (Page et al. 2001), rabbit anti-C(2)M antibody used at 1:400 (Manheim et al. 2003), a combination of two mouse anti-Orb antibodies (4H8 and 6H4) used at 1:100 (Lantz et al. 1994), mouse anti-Lamin antibody developed by Fisher, P.A. used at 1:800, and a rat anti-HA antibody (Roche) used at 1:15.

The secondary antibodies were Cy3 labeled goat anti-rabbit (Jackson Labs) used at 1:250, Cy3 labeled goat anti-rat (Jackson Labs) used at 1:100 and Alexa fluor 488 goat anti-mouse (Invitrogen) used at 1:100. Chromosomes were stained with Hoechst at 1:50,000 (10mg/ml solution) for seven minutes at room temperature. Images were collected using a Leica TCS SP2 confocal microscope with a 63X, N.A. 1.3 lens. In most cases, whole germaria were imaged by collecting optical sections through the entire tissue. These data sets are shown as maximum projections. The analysis of the images, however, was performed by examining one section at a time.

Counting the frequency of the two-oocyte phenotype and calculating P-values: The oocytes were observed using an anti-C(3)G antibody. In some cases, such as when C(3)G staining was not visible, anti-ORB staining was used to identify the oocyte(s). A cell was scored as an oocyte if complete SC filaments were clear and distinct or by a concentration of ORB staining in the cytoplasm of a cell (Gonzalez-Reyes et al. 1997). P-values were calculated using the Fisher's exact test. The P-value from the test

compares the ratio of one-oocyte to two-oocyte cysts that were observed in two genotypes.

Counting γ-HIS2AV foci in repair-proficient and repair-defective backgrounds: The γ-HIS2AV foci were counted from germaria where the foci were clear and distinct. Foci numbers in wild-type were at a maximum in region 2a (early pachytene) and few foci were visible by region 2b (mid pachytene). Therefore, to compare foci numbers in different genotypes, we used a method that calculates all cysts with γ-HIS2AV foci, averaging the amount in each pair of pro-oocytes. We compared the average foci in all the pro-oocytes or oocytes of each germarium, starting with the youngest cysts at the anterior end, by examining a full series of optical sections.

For counting γ-HIS2AV foci in repair-defective backgrounds, ORB staining was used to identify oocytes in region 3 (late pachytene). The foci were counted from germaria where the foci were clear and distinct. The foci were counted manually by examining each section in a full series of optical sections containing complete pro-oocyte nucleus.

Plotting γ-HIS2AV foci as a function of relative cyst age: Since the position of a cyst in the germarium is only a rough estimate of its meiotic stage, the foci were first counted in all the pro-oocytes/ oocytes (identified by C(3)G staining) in the germarium. The meiotic stage of each pro-oocyte was then normalized according to the relative position of the entire cyst within the germarium since the relative position is more important than absolute position. The pro-oocytes from 13 wild-type germaria, 4 *FM7/+*, 4 *CyO/+*, 5 *FM7/+; CyO/+*, 5 *spn-B*^{Bu}, and 4 *sir2*^{17}*/Df; spn-B*^{Bu} were arranged according to their

relative age. The average number of γ-HIS2AV foci per pro-oocyte at each stage was then calculated and plotted as a function of relative cyst age.

Construction of PCH2 transgenes: The annotated coding region of *pch2* was obtained from Flybase and amplified off the *pch2* cDNA clone LD24646 (Stapleton et al. 2002) by PCR. The coding region of *pch2* was then cloned into the Gateway® pENTR™4 vector (Invitrogen). An LR 'clonase' reaction was then performed to recombine *pch2* into the ppHW destination vector (Invitrogen) that contains 3 copies of an N-terminus HA-tag under the control of an inducible UASP promoter. The construct was injected into fly embryos by Model System Genomics at Duke University. To express the transgenic lines, they were crossed to flies expressing Gal4 using either the NGT (*P[Gal4-nos.NGT]40*) (Tracey et al. 2000) or MVD1 (*P[Gal4::VP16-nos.UTR]MVD1*) drivers (Van Doren et al. 1998).

Counting PCH2 foci: The HA-PCH2 foci were counted from germaria where the foci were clear and distinct. We counted the average foci surrounding nuclei in all the cysts at region 2 and region 3 of each germarium by examining a full series of optical sections.

V. Results

Defects in chromosome axis components cause a *pch2*-dependent pachytene delay

In the Drosophila germarium, oocytes are born within cysts composed of 16 cells that are connected by ring canals. Two out of the sixteen cells, each with four ring canals, initially contain equivalent levels of SC proteins and are termed the pro-oocytes (Figure 12A). As the developing cysts travel from the anterior (region 2) toward the posterior (region 3) of the germarium, the pro-oocytes go through the pachytene stage of meiosis where synapsis is completed and DSB formation and recombination occurs. By late pachytene (region 3), one of the two pro-oocytes will exit meiosis and lose its SC while the other will continue through development and form the oocyte (Figure 12A).In DSB repair and exchange-defective mutants, the transition into late pachytene is delayed by pachytene checkpoint activity (Joyce et al. 2009). This results in both pro-oocytes persisting into region 3 cysts, referred to as the "two-oocyte phenotype," which can be identified by the persistence of the SC transverse filament C(3)G in both pro-oocytes (Joyce et al. 2009) or the concentration of ORB protein in the cytoplasm of two cells rather than one in region 3 cysts (Figure 12B) (McCaffrey et al. 2006).

Abolishing synapsis by mutation of *c(3)G* does not elicit the two-oocyte phenotype (Figure 12C), suggesting the pachytene checkpoint is not monitoring SC formation (Joyce et al. 2009). We further investigated the relationship between chromosome structure components and the pachytene checkpoint and determined the effects of mutations in two other genes, *ord* and *c(2)M,* which encode structural proteins.

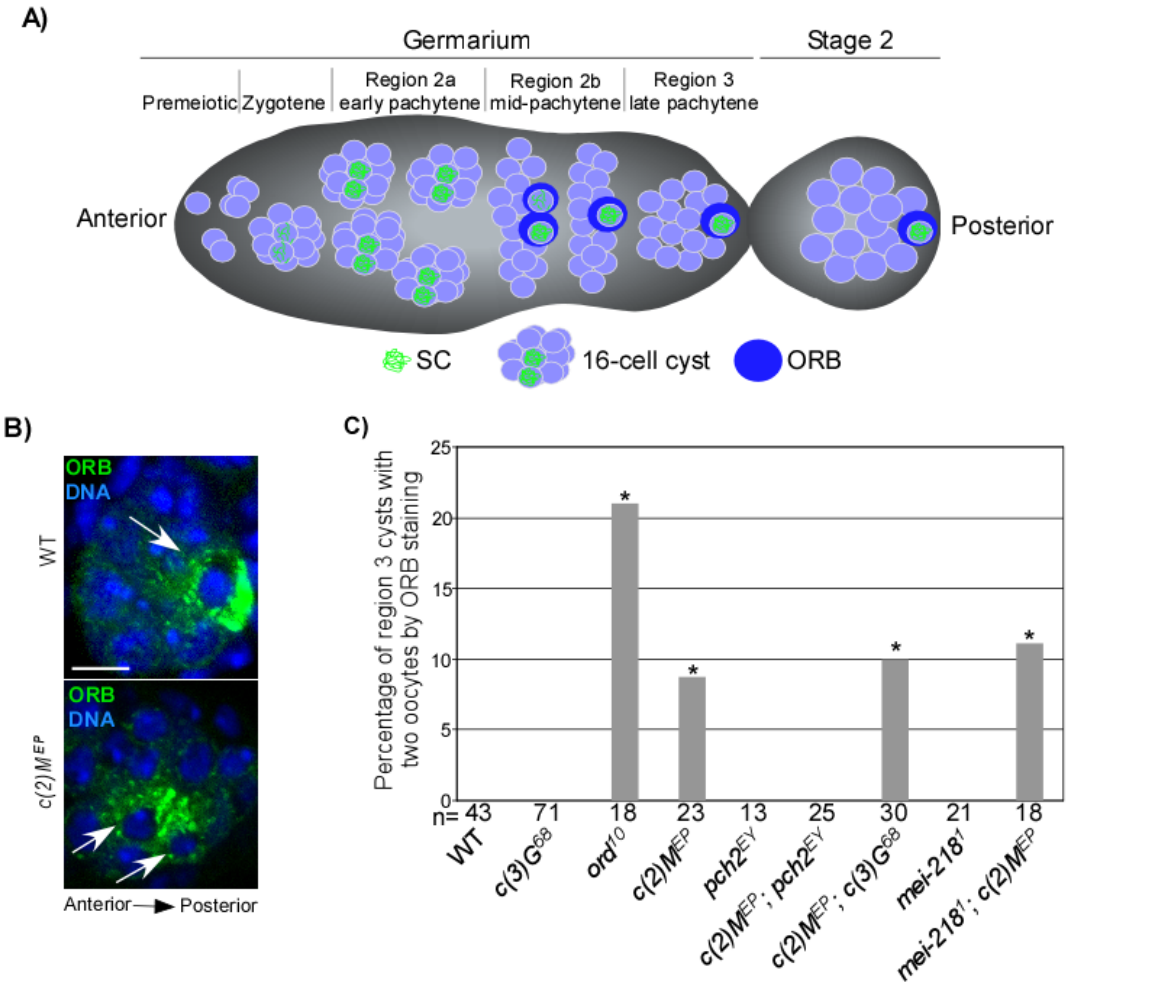

Figure 12: Pachytene delays in axis-defective mutants.

(A) Schematic depiction of germline cysts and oocyte markers in a wild-type germarium. Changes in cyst morphology differentiate regions 2a (small and round cysts), 2b (flat oblong cysts), and 3 (large and round cysts). Cysts travel anterior to posterior and the age difference between each cyst is ~12-24 hrs (our unpublished data and (King 1970)). (B) Maximum projections of region 3 cysts stained with DNA (blue) and ORB (green) in wild-type and *c(2)M* mutant females. In wild-type, the cytoplasmic ORB protein enriches around a single oocyte (white arrow) localized to the most posterior side of the cyst. In *c(2)M* mutants, the cytoplasm of two cells (the pro-oocytes) is enriched with ORB . Scale bar is 5µM. (C) A pachytene delay phenotype is defined as a significantly greater percentage of region 3 cysts with two-oocytes based on ORB staining when compared to wild-type (asterisks are located above each bar when P-value was <0.05). Note that the pachytene delay observed in a *c(2)M* mutant was suppressed by mutation of *pch2* but not by mutation of *c(3)G* or *mei-218*. The number of cysts/germaria counted is at the bottom of each bar.

ORD localizes to chromosome axes in oocytes independent of SC components and has roles in meiotic recombination and sister chromatid cohesion (Bickel et al. 1997; Webber et al. 2004). Although *ord* mutants initially display normal C(3)G and C(2)M localization, only rare structures resembling SC were observed by electron microscopy (EM), suggesting that the ultrastructure of chromosome axes was disorganized (Webber et al. 2004). Consistent with this interpretation, C(3)G and C(2)M staining precociously deteriorates in *ord* mutants as the oocytes progress through pachytene (Webber et al. 2004). We found that *ord* mutants displayed a high frequency of the two-oocyte phenotype (Figure 12C), indicative of a delay in meiotic progression and supporting the hypothesis that the pachytene checkpoint is sensitive to defects in axis components.

C(2)M is a component of the SC lateral element and localizes adjacent to the chromosome axes even in the absence of synapsis (in *c(3)G* mutants), suggesting it may interact with axis components (Anderson et al. 2005). In *c(2)M* mutant oocytes, C(3)G protein fails to develop into complete strands along the lengths of each chromosome, but instead appears as small patches (Figure 13A). The most likely explanation is that SC initiates in *c(2)M* mutants but polymerization is defective. Similar to *ord* mutants, *c(2)M* mutants exhibited a high frequency of the two-oocyte phenotype that was not observed in wild-type (Figure 12C). The two-oocyte phenotype was suppressed in *c(2)M; pch2* double mutants, indicating the delay was dependent on the pachytene checkpoint (Figure 12C). The high frequency of the two-oocyte phenotype observed in *c(2)M* mutants was not suppressed by mutation of *c(3)G* (Figure 12C), demonstrating the pachytene checkpoint can signal independently of SC formation. Together, these results suggest the

pachytene checkpoint may monitor the organization of axis components like ORD and C(2)M.

Chromosomal rearrangements disrupt axis integrity and cause a *pch2*-dependent pachytene delay

If the pachytene checkpoint monitors the organization of chromosome axes we reasoned that structural rearrangements would also exhibit pachytene delays. Balancers are multiply-inverted chromosomes that fail to cross over with a normal homolog, presumably due to the disruption of SC continuity (Novitski et al. 1954; Gong et al. 2005; Sherizen et al. 2005). We characterized the integrity of SC-associated proteins in balancer heterozygotes with antibodies recognizing the SC components C(3)G and C(2)M. Single balancer heterozygotes had thread-like C(3)G and C(2)M staining that was indistinguishable from wild-type (data not shown; see wild-type in Figure 13A) (Gong et al. 2005). Double balancer heterozygotes (*CyO/+; TM3/+*) also initially displayed normal C(3)G and C(2)M localization, but the staining became fragmented and sometimes undetectable in late pachytene oocytes (Figure 13A). This precocious deterioration of SC proteins during pachytene is similar to what is observed in *ord* mutant oocytes (Webber et al. 2004), suggesting that chromosome rearrangements might disrupt axis organization.

Using C(3)G staining to detect oocytes, we found that heterozygotes of the balancers *FM7, Bwinscy, TM2* and *TM3* each exhibited a high frequency of the two-oocyte phenotype (Figure 13B), suggestive of a pachytene delay. The high frequency of the two-oocyte phenotype was suppressed in *FM7/+; pch2* and *TM3/+; pch2*, confirming

the delays were dependent on the pachytene checkpoint (Figure 13B; $P<0.05$ compared to either balancer heterozygote alone).

Each balancer chromosome contains several inversions. For example, the *TM3* chromosome includes 10 breakpoints (Lindsley et al. 1992). To investigate the effects of a more subtle disruption in chromosome organization on the pachytene checkpoint, we tested whether a single aberration, or two breakpoints, would be enough to induce pachytene delays. Remarkably, heterozygotes of single translocations between the 2nd and 3rd chromosomes (*T(2;3)DP77/ +*, *T(2;3)dp^{D}/+*, and *T(2;3)lt^{X16}/+*) and a single inversion on the X chromosome (*In(1)dl49/+*) each exhibited a high frequency of the two-oocyte phenotype, suggesting the threshold to trigger the pachytene checkpoint is low and only requires as few as two local alterations (Figure 13B). Importantly, pachytene delays were not observed in *In(1)dl49* homozygotes. This suggests the pachytene delays were caused by a break in homology between homologs, and not the rearrangement itself.

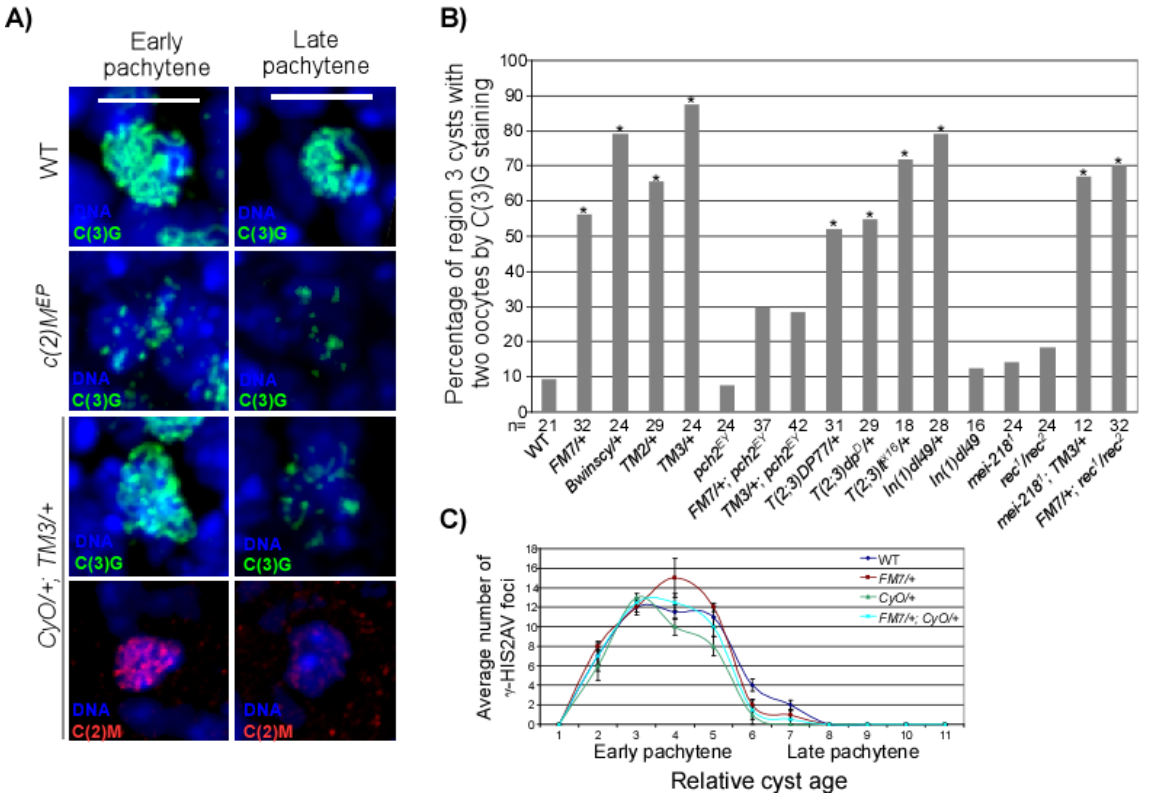

Figure 13: SC deterioration and pachytene delays in balancer heterozygotes.

(A) SC localization in a germarium from wild-type, *c(2)M,* and *CyO/+; TM3/+* females. Single oocyte nuclei from early pachytene and late pachytene cysts are enlarged next to their corresponding germarium. In wild-type germaria, extensive threadlike C(3)G is visible in oocytes at each stage. In early pachytene *CyO/+; TM3/+* germaria, threadlike C(3)G and C(2)M staining is detected, but deteriorates in the majority of late pachytene oocytes. Threadlike C(3)G staining is never observed in the germaria of *c(2)M* mutants (Manheim et al. 2003), which show fragments of C(3)G staining throughout pachytene, suggestive of an assembly defect. Scale bars for germaria and single-cell images are 10µM and 5µM, respectively. (B) Based on C(3)G staining, a high frequency of the two-oocyte phenotype was found in heterozygotes for single translocations, a single inversion (*In(1)d149*) and the balancer chromosomes *FM7, Bwinscy, TM2,* and *TM3*, which was suppressed by mutation of *pch2,* but not by *mei-218.* Asterisks are located above each bar when P-value was <0.05 compared to wild-type. The number of cysts counted is at the bottom of each bar. (C) The average number of γ-HIS2AV foci as a function of relative cyst age in wild-type and balancer heterozygotes. Cyst 1 is the first to have complete SC, cyst 8 is in region 3 and cysts 9-11 are in later-stage cysts (stages 2-4), which have left the germarium. Neither single nor double balancer heterozygotes significantly altered the appearance or disappearance of γ-HIS2AV foci throughout the germarium. Error bars denote the standard error of the mean.

Disorganized chromosome axes trigger the pachytene checkpoint independent of the MCM-related precondition genes

In addition to the delay in oocyte selection, DSB repair and exchange-defective mutants also exhibit a *pch2*-dependent delay in the response to DSBs (Joyce et al. 2009). To monitor DSB formation and repair in balancer heterozygotes, we stained ovaries with an antibody to γ-HIS2AV (Madigan et al. 2002; Mehrotra et al. 2006). In wild-type oocytes, γ-HIS2AV foci are most abundant in early pachytene nuclei (region 2a, cyst 3 in Figure 13C) and absent by late pachytene (region 3, cyst 8 in Figure 2C), indicating DSBs have been repaired. Likewise, both *FM7/+* and *CyO/+* heterozygotes exhibited maximum γ-HIS2AV foci in early pachytene oocytes at a similar cyst age to wild-type (Figure 13C). The same result was also observed in the double heterozygote *FM7/+; CyO/+*. Therefore, balancer heterozygotes do not cause a delay in the γ-HIS2AV response to DSBs, revealing a distinction between DSB repair mutants and chromosomal rearrangements. While mutations in DSB repair genes induce *pch2*-dependent delays in early pachytene (delayed response to DSBs) and late pachytene (delayed oocyte selection), chromosomal rearrangements only delay the latter.

If the pachytene checkpoint can cause delays through two distinct pathways, it should be possible to define them genetically. This was tested with mutations in the MCM-related precondition genes *mei-218* and *rec,* which are required for 90% of all crossovers and the pachytene delays caused by mutations in DSB repair and exchange genes (Joyce et al. 2009). Unexpectedly, the high frequency of the two-oocyte phenotype was still observed in *mei-218; TM3/+* and *FM7/+; rec* (Figure 13B, $P<0.05$ compared to *mei-218* and *rec* single mutants). Consistent with this finding, the pachytene delay in

c(2)M mutants was not suppressed in *mei-218; c(2)M* double mutants (Figure 12C). These results show that, unlike the DSB repair and exchange-defective mutants, disorganized chromosome axes interact with the pachytene checkpoint independent of precondition genes and possibly at a later step (*i.e.* after DSB response).

PCH2 can induce interchromosomal effects on crossing over

pch2 is required for some of the crossovers that occur in the exchange-defective mutant, *hdm* (Joyce et al. 2009). Consequently, *hdm; pch2* double mutants exhibit an elevated frequency of nondisjunction compared to *hdm* single mutants. These results suggest a functional link between the pachytene checkpoint and the production of crossovers. To determine if this is a general property of mutants that exhibit pachytene delays, we tested additional double mutants with *pch2.* Exchange class genes *Ercc1* and *mei-9* encode components of an endonuclease complex of proteins that includes HDM and is required for normal levels of meiotic recombination (Radford et al. 2005; Joyce et al. 2009). Loss of ERCC1 function results in 14% X-chromosome nondisjunction, which is elevated to 30% in a *pch2* mutant background, suggesting crossovers are further reduced (Table 7). In addition, the low level of crossovers that are generated along the 2nd chromosome in *mei-9* mutants are mostly suppressed in *mei-9*; *pch2* double mutants (Figure 14A). These results suggest the residual crossovers in recombination-defective mutants are generated by a secondary compensatory increase in crossing over facilitated by *pch2*.

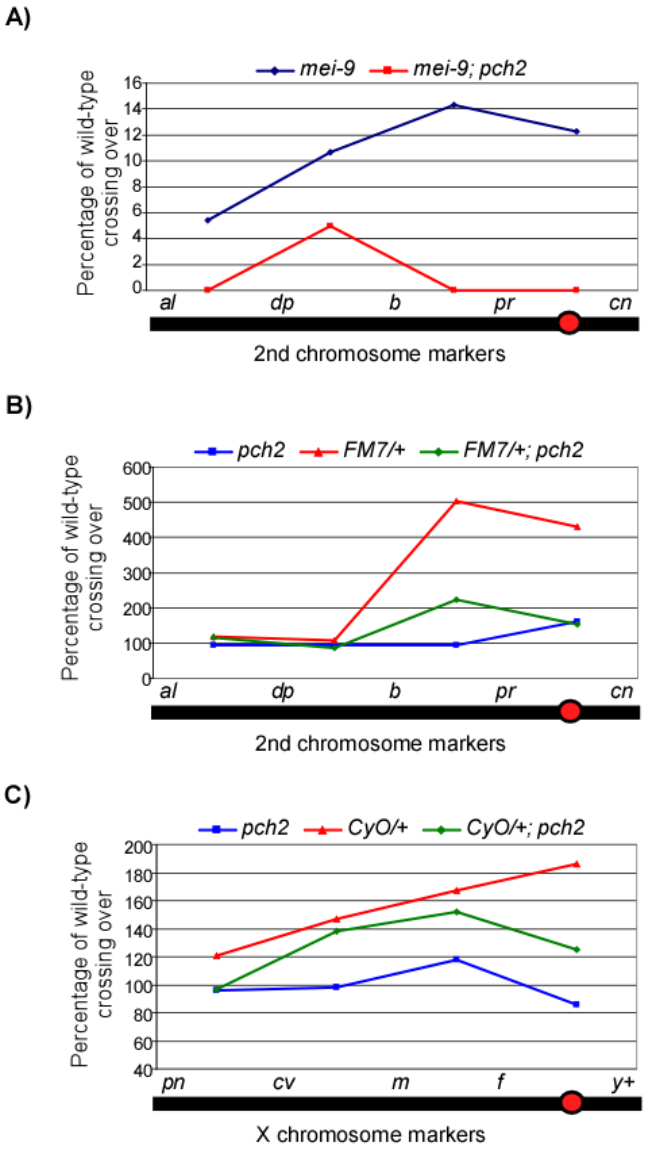

Figure 14: Percentage of wild-type crossing over in balancer heterozygotes, *mei-9* and *pch2* mutant females.

(A) Percentage of wild-type crossing over in *mei-9* (blue) and *mei-9; pch2* (red) mutant females along the 2nd chromosome. Most crossovers in a *mei-9* mutant are dependent on *pch2*. (B) Percentage of wild-type crossing over along the 2nd chromosome in *pch2* (pink), *FM7/+* (green), and *FM7/+; pch2* (orange) mutant females. *pch2* mutants have wild-type levels and distribution of exchange. The interchromosomal effect of the *FM7* balancer was mostly suppressed in *pch2* mutants. (C) Percentage of wild-type crossing over along the X-chromosome in *pch2* (pink), *CyO/+* (green), and *CyO/+; pch2* (orange) mutant females (note the scale is reduced). The interchromosomal effect elicited by the *CyO* balancer was reduced in *pch2* mutants, especially in the most proximal and distal intervals.

While suppressing crossing over along the rearranged chromosome, balancer heterozygotes cause an interchromosomal effect that increases crossing over on the remaining chromosome pairs (Lucchesi et al. 1968). Since the pachytene checkpoint can partially compensate for the decreased crossing over in recombination mutants, we asked if it was also responsible for the increase in crossovers observed in balancer heterozygotes. Consistent with previous work on interchromosomal effects (Szauter 1984; Carpenter 1988), we found that *FM7/+* heterozygotes exhibit 151% of wild-type crossing over along the 2nd chromosome with an altered distribution (Table 5). Although there was little deviation from wild-type controls in the distal regions of the chromosome (*al-b*), the genetic map distance was increased ~4-5 times that observed in wild-type centromere-proximal intervals (Table 5; Figure 14B). Remarkably, 2nd chromosome crossing over in *FM7/+* heterozygotes was reduced to 106% of wild-type in a *pch2* mutant background ($p<0.00005$; Table 5; Figure 14B). Similarly, introduction of the *CyO* chromosome increased crossing over along the X chromosome to 149% of wild-type, which was reduced to 129% in *pch2* mutants ($p<0.05$; Table 6; Figure 14C). Interestingly, the closer the interval being tested was to the centromere, the greater the interchromosomal effect and *pch2* dependence (Table 6; Figure 14C). Since *pch2* single mutants exhibited normal levels of crossing over on the X and 2nd chromosome (Table 5; Table 6; Figure 14), these data show that *pch2* is required for most of the interchromosomal increase in crossover levels in balancer heterozygotes.

The pachytene checkpoint regulates the chance of DSBs becoming crossovers

The increased crossing over observed in balancer heterozygotes could be explained by pachytene checkpoint activity increasing DSB levels. However, we failed to observe any significant change in the number of γ-HIS2AV foci in oocytes single or doubly heterozygous for *FM7* and *CyO* compared to wild-type (Figure 13C). Since asynchrony of DSB formation can complicate measuring the total number of γ-HIS2AV foci, we repeated the above experiment in a *spn-A* (Drosophila Rad51) mutant background, in which repair of DSBs is blocked (Jang et al. 2003). The number of γ-HIS2AV foci in late pachytene oocytes of these mutants is expected to be close to the total number of DSBs that occurred (McKim et al. 2002; Mehrotra et al. 2006). *spn-A* mutant late pachytene oocytes displayed an average of 21.0 (+/- 1.5) γ-HIS2AV foci. Similarly, *FM7/+; CyO/+; spn-A* late pachytene oocytes had an average of 24.0 (+/- 1.4) γ-HIS2AV foci.

These results indicate that the ability of the pachytene checkpoint to increase crossing over in the genome is not mediated by a substantial increase in the total number of DSBs. Instead, pachytene checkpoint activity most likely increases the chance of DSBs becoming crossovers, particularly those that occur near centromeres.

PCH2 localizes to the nuclear periphery and persists when pachytene is delayed

To investigate how PCH2 affects crossover frequency, we monitored the protein localization pattern during meiosis. A transgene was constructed containing a hemagluttin (HA) epitope at the N-terminus of the *pch2* transcript under the control of an inducible UASP promoter. We expressed PCH2 using the germline specific driver

P(Gal4-nos.NGT)40 (Tracey et al. 2000), abbreviated as *NGT,* known to express in pachytene at moderate levels. PCH2 staining formed foci that localized around the nucleus in zygotene and early pachytene (region 2) cells, when crossover determination and recombination occurs (Figure 15A-B). No PCH2 foci were detected in region 3 cells, suggesting the protein is rapidly degraded after early pachytene.

Surprisingly, PCH2 foci did not overlap with the DNA stain. To determine if PCH2 foci localized within the nucleus, we counterstained with the nuclear envelope component, Lamin. We found that 73% of PCH2 foci showed a close association with the cytoplasmic side of the Lamin staining (n=368; Figure 15C), indicating they localized adjacent to the nuclear envelope and outside the nucleus. The remaining 27% of PCH2 foci not closely associated with Lamin were found dispersed within the cytoplasm.

To determine if PCH2 localization pattern changes in mutant backgrounds that exhibit pachytene delays, we examined PCH2 expression in mutants that cause checkpoint delays: *hdm, mei-9* and in *TM3/+* heterozygotes. In *hdm* and *mei-9* mutants, the number of PCH2 foci per oocyte was increased ~2-fold compared to controls (Figure 15J). In addition, the foci persisted into region 3 oocytes, which was never observed in control germaria (Figure 15D and J). However, PCH2 localization was never detected past stage 2 of oogenesis (data not shown), indicating the mechanism to degrade PCH2 is only delayed in exchange-defective mutants. In *TM3/+* heterozygotes, the levels of PCH2 foci in region 2 cells was unchanged compared to controls, but were present in region 3 (Figure 15J), revealing a correlation between the prolonged expression of PCH2 and delayed pachytene.

The intracellular localization pattern of PCH2 did not change when pachytene was delayed since the foci remained juxtaposed to the nuclear envelope in *hdm* and *mei-9* mutants and in *TM3/+* heterozygotes at all stages (Figure 15E and data not shown). Furthermore, mutation of *mei-W68,* which eliminates DSB formation, showed a normal staining pattern of PCH2, and *hdm; mei-W68* double mutants showed the same PCH2 staining pattern as *hdm* single mutants (Figure 15D and data not shown), consistent with our previous conclusion that the pachytene checkpoint functions independently of DSB formation (Bhalla et al. 2005; Joyce et al. 2009). These observations provide a connection between the nuclear envelope and pachytene checkpoint activity and suggest that PCH2's role in nuclear events like crossing over is indirect and at a distance from the chromosomes.

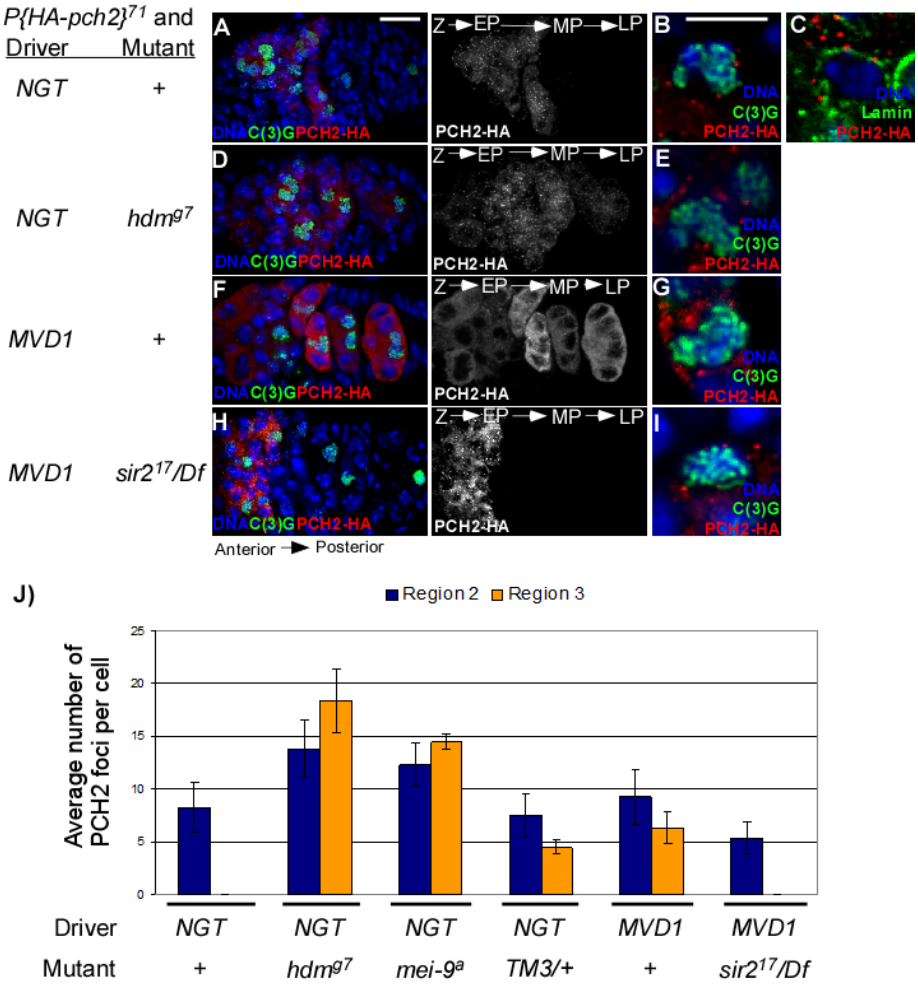

Figure 15: PCH2 localization during pachytene

(A-C) PCH2 localization in a wild-type germarium when the *UASP: pch2* transgene was driven by *P(Gal4-nos.NGT)40* (=*NGT*). (A) PCH2 expression is restricted to zygotene and early pachytene cells. Scale bar is 10µM. (B) A single section of an early pachytene oocyte with PCH2 foci localizing to distinct foci adjacent to the DNA stain. Scale bar is 5µM. (C) PCH2 foci localize to the cytoplasmic side of the nuclear envelope protein, Lamin. (D) PCH2 expression persists into mid- and late-pachytene cells of *hdm* mutants. (E) A single section of an early pachytene oocyte with PCH2 foci adjacent to the DNA stain, indicating the localization pattern within a cell does not change in *hdm* mutants. (F-G) PCH2 driven by *P(Gal4::VP16-nos.UTR)MVD1* (=*MVD1*). (F) PCH2 foci persist into mid- and late-pachytene cells. Also, two populations of PCH2 become present: unlocalized protein distributed evenly throughout the cytoplasm and distinct bright spots classified as foci. (G) A single section of an early pachytene oocyte with bright spots of PCH2 foci localizing adjacent to the nucleus. (H) PCH2 expression is no longer observed past early pachytene cells of *sir2* mutants. (I) A single section of an early pachytene oocyte with PCH2 localizing adjacent to the DNA stain, indicating that *sir2* has no effect on PCH2 localization pattern within a cell. (J) Quantification of PCH2 foci. The average number of PCH2 foci per cell was increased in both region 2 and region 3 cells of *hdm* and *mei-9* mutants. PCH2 foci levels did not increase in *TM3* heterozygotes or when PCH2 was overexpressed by the *MVD1* driver, but did persist into region 3 cells.

Prolonged PCH2 activity leads to a pachytene delay and altered crossover distribution

To test the significance of the correlation between pachytene delays and prolonged PCH2 expression, we manipulated the timing and expression levels of PCH2 in the germline. PCH2 levels were increased by driving the *UASP:pch2* transgene with *P(Gal4::VP16-nos.UTR)MVD1* (Van Doren et al. 1998), abbreviated as *MVD1*, known to drive high levels of expression in the germarium. *MVD1*-driven *pch2* caused the protein to persist into region 3 oocytes, which was never observed with the *NGT* driver in a wild-type background (Figure 15F and J). In addition to distinct foci, PCH2 was also distributed more evenly throughout the cytoplasm (Figure 15F-G). Thus, *MVD1*-driven *pch2* resulted in overproduction and prolonged expression of the protein throughout pachytene.

Pachytene delays were not observed when the *pch2* transgenes were expressed using the *NGT* driver (Figure 16A). In contrast, *MVD1*-driven *pch2* induced a pachytene delay that resulted in a high frequency of the two-oocyte phenotype (Figure 16A). In fact, 100% (n=10) of the germaria with PCH2 expression in region 3 cysts also contained two oocytes, as viewed by C(3)G staining, suggesting prolonged PCH2 expression is sufficient to induce a delayed transition into late pachytene.

Since overproducing PCH2 caused a pachytene delay, we determined if crossover frequency or distribution was also affected. We found that PCH2 expression driven by *MVD1* altered the distribution of exchange in all 3 transgenic lines tested (Table 5; Figure 16B). The most dramatic increase in crossover frequencies was observed in the centromere proximal interval of chromosome 2, *b-pr*. Although all the transgenic lines

that were tested showed the same change in crossover distribution, the magnitude was different, which probably reflects different transgenic protein levels. In support of this conclusion, the presence of two transgenic copies of *HA-pch2*^{71} driven by *MVD1* exacerbated the effect on both crossover levels and distribution (Table 5; Figure 16B). These data show that the frequency and distribution of crossing over is highly sensitive to the timing and level of PCH2 expression during pachytene.

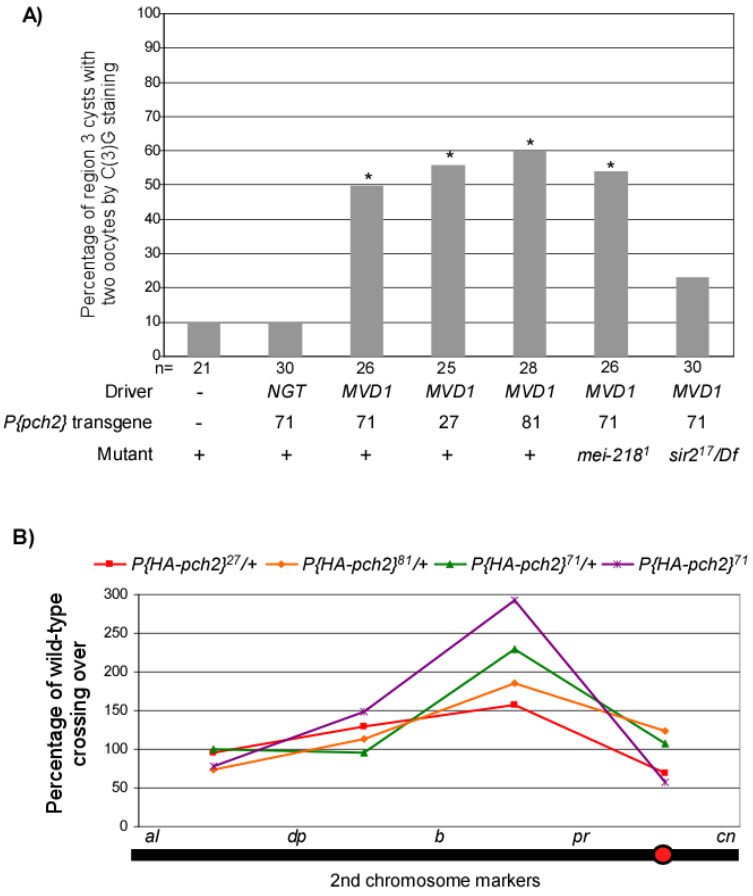

Figure 16: PCH2 overexpression leads to pachytene delays and altered crossover distribution

(A) Three different PCH2 transgenic lines driven by *MVD1* exhibit a high frequency of the two-oocyte phenotype whereas PCH2 driven by *NGT* does not. The pachytene delay in *MVD1*-driven PCH2 was suppressed by mutation of *sir2*, but not by *mei-218* (also see Supplementary Figure 1). Asterisks are located above each bar when P-value was <0.05 compared to wild-type. The number of cysts counted is at the bottom of each bar. (B) Percentage of wild-type crossing over along the 2nd chromosome in three different transgenic lines where PCH2 is overexpressed by the *MVD1* driver. All lines display a similar altered distribution pattern with elevated exchange in the *b-pr* interval, yet each exhibits a different level of effect on total crossover levels. Two copies of the transgene driven by *MVD1* have the greatest effect on both crossover distribution and levels.

sir2 is required for prolonged PCH2 activity and the pachytene checkpoint

We sought to identify factors that facilitate prolonged PCH2 expression and cause pachytene delays. The first candidate we tested was *mei-218* since it is required for the *pch2*-dependent pachytene delays observed in DSB repair and exchange-defective mutants. *mei-218* mutants, however, did not show an effect on the levels or distribution of *MVD1*-driven PCH2 (Figure S 5). Also, the two-oocyte phenotype caused by PCH2 overexpression was not suppressed in *mei-218* mutants (Figure 16A), suggesting that MEI-218 is not required for PCH2 localization.

The second candidate we tested was Sir2, which encodes a histone deacetylase that is required for the nucleolus localization of Pch2 and the pachytene checkpoint during *S. cerevisiae* meiosis (San-Segundo et al. 1999). Five Drosophila genes belong to the Sir2 family. Of these, Sir2 is the closest homolog of the *S. cerevisiae* Sir2 (Astrom et al. 2003). Drosophila *sir2* null alleles have no obvious effects on viability, but affect position effect variegation, heterochromatic silencing and fly life span (Newman et al. 2002; Rosenberg et al. 2002; Astrom et al. 2003). We analyzed the role of *sir2* in meiosis and found that mutants were fully fertile with wild-type levels of X-chromosome nondisjunction (Table 7), indicating Sir2 is dispensable for meiotic recombination.

Strikingly, the region 3 localization of *MVD1*-driven *pch2* was eliminated in a *sir2* mutant (Figure 15H-J). In contrast, loss of *sir2* did not change the level of PCH2 in region 2 cells and had no effect on the peri-nuclear localization of PCH2 driven by *NGT* (Figure 15H-J and data not shown). In addition, expression of a *c(2)M* transgene driven by *MVD1* was not affected, indicating the effect of *sir2* on PCH2 was not due to a reduction in the transcription of UAS-driven genes (Figure S 6).

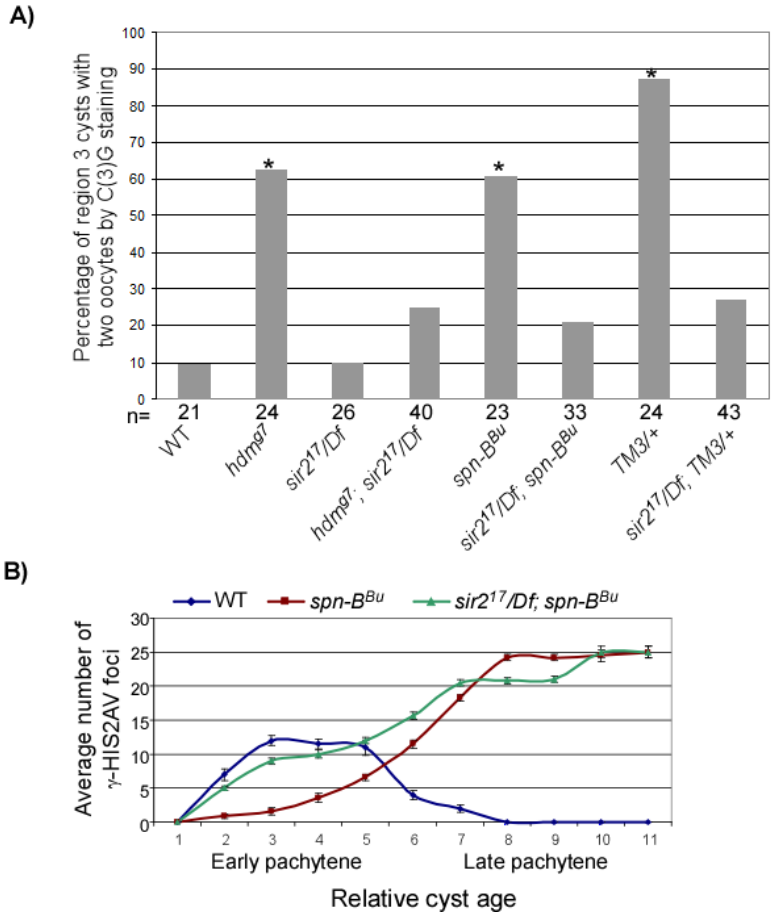

Figure 17: *sir2* is required for the pachytene delays.

(A) Mutation of *sir2* suppressed the high frequency of the two-oocyte phenotype observed in the exchange-defective mutant *hdm*, DSB repair mutant *spn-B* and in *TM3* heterozygotes. Asterisks are located above each bar when P-value was <0.05 compared to wild-type. The number of cysts counted is at the bottom of each bar. (B) The average number of γ-HIS2AV foci is plotted as a function of relative cyst age in wild-type, *spn-B* and *sir2; spn-B* mutants. Mutation of *sir2* suppressed the delayed onset of γ-HIS2AV (see cyst 2-5) in *spn-B* mutants. *spn-B* mutants also have a block in DSB repair that cause γ-HIS2AV to accumulate into late stages of oogenesis, which is not suppressed by *sir2*. Error bars denote the standard error of the mean.

Since *sir2* is required for prolonged PCH2 expression, we investigated whether Sir2 is also involved in the pachytene checkpoint. Indeed, mutation of *sir2* suppressed the high frequency of the two-oocyte phenotype observed when PCH2 is overexpressed with the *MVD1* driver (Figure 16A), supporting the hypothesis that high levels of PCH2 are dependent on Sir2 and essential for the pachytene delays. The high frequency of the two-

oocyte phenotype observed in the exchange-defective mutant *hdm* and DSB repair mutant *spn-B* was also suppressed by *sir2* (Figure 17A). Likewise, *sir2* was required for the pachytene delay observed in *TM3/+* heterozygotes (Figure 17A) and the delayed onset of γ-HIS2AV staining in *spn-B* mutants (cyst 2-5 in Figure 17B). Thus, like *pch2*, the *sir2* mutant is defective in the pachytene checkpoint, providing evidence for a connection between histone deacetylation and pachytene checkpoint activity.

VI. Discussion

The pachytene checkpoint is sensitive to chromosome axis organization

We have previously shown that removing the SC central element component C(3)G does not cause *pch2*-dependent delays in Drosophila meiotic prophase (Joyce et al. 2009). Therefore, the pachytene checkpoint is not monitoring the process of synapsis *per se*. Instead, two lines of evidence suggest the pachytene checkpoint is sensitive to the organization of homologous chromosome axes.

First, mutations in genes that encode structural components, C(2)M and ORD, cause *pch2*-dependent pachytene delays. Since these delays are observed independently of synapsis (in *c(3)G* mutants), they most likely reflect a defect in axis integrity. Second, heterozygous breakpoints also cause a *pch2*-dependent delay, suggesting the pachytene checkpoint is sensitive to the continuity of chromosome axes. Homozygous rearrangements do not cause delays; therefore, checkpoint monitoring of axes is dependent on homolog pairing but not SC formation. SC-independent changes in axis status includes the organization of chromosome structure components, such as ORD and C(2)M. The heterozygous aberrations might cause physical contortions and/or block a

change in axis status that occurs between homologous chromosomes. The result could destabilize the integrity of chromosome axes and expose substrates that trigger the pachytene checkpoint. Indeed, females doubly heterozygous for balancer chromosomes show deterioration of C(2)M staining in late pachytene oocytes similar to *ord* mutants (Webber et al. 2004), suggesting lateral elements are compromised by the heterozygous inversion breakpoints.

Two genetically distinct pathways can trigger the pachytene checkpoint

The delay in oocyte selection observed in *c(2)M* mutants and balancer heterozygotes is not dependent on the MCM-related precondition genes such as *mei-218,* which are required for the pachytene delays in DSB repair and exchange-defective mutants (Joyce et al. 2009). Also, balancer heterozygotes do not cause a delayed response to DSBs or increase in the number of PCH2 foci as observed in DSB repair and exchange-defective mutants. Therefore, two pathways lead into a *pch2*-dependent checkpoint: a *mei-218*-dependent pathway involving the early function of DSB repair proteins and a *mei-218*-independent pathway involving the structural organization of chromosome axes (Figure 18). Differences between meiotic mutants in budding yeast also suggests that more than one pathway can cause a Pch2-dependent delay (Roeder et al. 2000).

Intriguingly, the *mei-218*-independent pathway involving chromosome structure has similarities to the pachytene checkpoint in other organisms. Single heterozygous inversions and translocations in Drosophila induce a pachytene delay, suggesting a model in which the pachytene checkpoint can respond to one or two breaks in axis continuity

between paired homologs. *C. elegans* pachytene checkpoint also monitors meiotic chromosome structure since a local defect in a SC-nucleating "pairing center" triggers a Pch2-dependent response (Bhalla et al. 2005). Similarly, the budding yeast pachytene checkpoint has been proposed to monitor SC-dependent events that may involve the relationship between recombination complexes and chromosome axes (Borner et al. 2004; Borner et al. 2008; Joshi et al. 2009). Therefore, one commonality between the pachytene checkpoints in these organisms is their sensitivity to aberrant chromosome structure with the main difference being SC-dependent defects (yeast and worms) *versus* SC-independent axis defects (Drosophila). Interestingly, both yeast Pch2 and mouse Trip13/Pch2 have been proposed to have a checkpoint-independent role in the organization of chromosome axis proteins (Joshi et al. 2009),(Wojtasz et al. 2009). We do not know as of yet, however, if this is related to the axis sensitivity of the Drosophila pachytene checkpoint, although it is tempting to suggest such a model.

As in budding yeast, Drosophila *sir2* mutants are defective in the pachytene checkpoint. Therefore, Pch2 and Sir2 may be core components of a conserved regulatory surveillance mechanism that is sensitive to local changes in chromosome axes. Drosophila may have evolved an additional *mei-218*-dependent pachytene checkpoint, not shared with yeast and worms, which is sensitive to DSB repair complexes.

Disruption of axis organization induces *pch2*-dependent interchromosomal effects on crossing over

The effect of inversion heterozygosity on the frequency of crossing over has been known since the work of Sturtevant (1919). Most often these intrachromosomal

rearrangements cause an interchromosomal increase in recombination levels. Exhaustive work has been carried out investigating the interchromosomal effect and several models have been proposed in order to account for the increase in crossing over (Lucchesi et al. 1968). The most recent and generally accepted model was last described by Lucchesi and Suzuki in 1968 who proposed a timing model where pairing and crossover formation are coupled during the pachytene stage of prophase (Lucchesi et al. 1968). They suggested that when the pairing process between one set of homologs is perturbed or delayed by chromosome rearrangements, pachytene was lengthened and the opportunity to make crossovers was prolonged. We propose a modified version of the timing model where axis status is coupled to the crossover determination phase via the pachytene checkpoint (Figure 18).

The timing model proposed by Lucchesi and Suzuki predicts that a factor exists which controls the time clock of meiotic prophase and can affect the level of exchange (Lucchesi et al. 1968). The pachytene checkpoint may regulate this timing mechanism. Although *pch2* is dispensable for crossing over in a wild-type background, it is required for most of the residual crossovers that occur in recombination-defective mutants. *pch2* is also required for most of the interchromosomal effect and pachytene delays observed in inversion heterozygotes. To our knowledge, *pch2* is the first example of a gene in Drosophila required for the interchromosomal effect that is not required for crossing over in general. PCH2 may facilitate the formation of more crossovers by simply delaying a pachytene transition and extending the crossover determination phase, thereby allowing more crossover sites to be selected (Figure 18). Since the interchromosomal effect is not

mediated by an increase in DSBs, the extended crossover determination phase most likely increases the chance of DSBs becoming crossovers at the expense of noncrossovers.

PCH2 function, localization and mechanism of checkpoint activity

Drosophila PCH2 localizes to peri-nuclear foci in zygotene and early pachytene cells and is rapidly degraded prior to mid-pachytene. In mutants in which pachytene delays are observed, PCH2 expression persists into mid and late pachytene cells. The observation that overexpressing PCH2 induces effects on both timing and crossover levels indicates prolonged PCH2 expression is necessary and sufficient for the pachytene checkpoint's downstream effects. Since the duration of early pachytene correlates with the domain of PCH2 expression, we suggest that degradation of PCH2 turns off checkpoint activity and allows progression into late pachytene, which ends the crossover determination phase (Figure 18).

We observed PCH2 localization to the outside of the nuclear envelope. These results were surprising considering the effect a *pch2* mutation has on nuclear events like crossing over. While we cannot rule out the possibility that a small undetectable fraction of PCH2 protein enters the nucleus and interacts with the chromosomes, PCH2 may indirectly affect nuclear events by facilitating interactions between the chromosomes and the nuclear envelope. In budding yeast, the pachytene checkpoint requires the localization of Pch2 to the nucleolus and not the chromosomes (San-Segundo et al. 1999). The persistent association of PCH2 with the nucleolus in budding yeast and the nuclear envelope in Drosophila are Sir2-dependent. Therefore, like budding yeast, PCH2 in Drosophila may mediate the pachytene checkpoint at a distance from the chromosomes. Intriguingly, the

nuclear envelope has been linked to several cellular processes relevant to meiotic recombination, including homolog pairing and DSB repair (Phillips et al. 2006; Ding et al. 2007; Penkner et al. 2007; Nagai et al. 2008). In *C. elegans,* the pairing of homologous chromosomes first requires the relocation of chromosomal regions known as pairing centers to the nuclear envelope (Phillips et al. 2006). Chromosome deficiencies that remove the pairing center impair relocation and synapsis as well as trigger a *pch2*-dependent response (Bhalla et al. 2005). Therefore, it is possible that in other organisms, the nuclear envelope has a conserved role in transducing pachytene checkpoint effects.

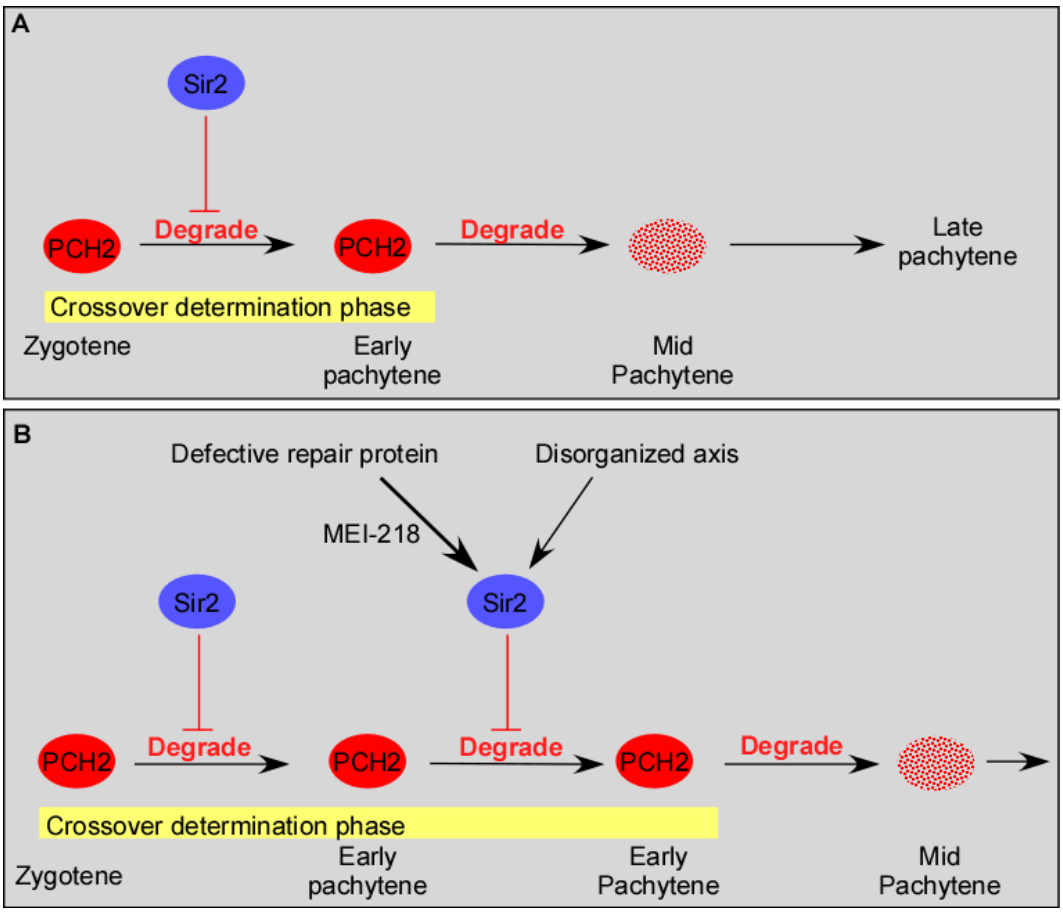

Figure 18: Model for pachytene checkpoint activity and crossover determination.

The pachytene checkpoint is coupled to a crossover determination phase that regulates the distribution and level of exchange per bivalent. PCH2 activity may regulate the crossover determination phase by restricting its time frame to the zygotene and early pachytene stages of prophase. (A) In wild-type early pachytene cells, Sir2 modulates PCH2 levels by inhibiting or slowing its degradation. Prior to mid-pachytene, however, PCH2 is normally degraded, which turns off the checkpoint signal and ends the crossover determination phase. (B) Two independent pathways can enhance Sir2 activity and mediate prolonged PCH2 expression: a *mei-218*-dependent pathway involving early functions of DSB repair proteins and a *mei-218*-independent pathway involving the organization of chromosome axes. These two pathways do not affect Sir2/PCH2 equally. Although a defect in either pathway results in the persistence of PCH2 into late pachytene, only defects in the DSB repair genes cause a significant increase in the number of PCH2 foci per cell and γ-HIS2AV delay, suggesting the *mei-218*-dependent pathway triggers a more robust response. Regardless, the persistence of PCH2 activity into late pachytene is sufficient to induce a delay in oocyte selection and increase in crossover levels.

Table 5: Effect of *pch2* on crossing over on the 2nd chromosome

	Crossing over on the Second Chromosome (cM)[a]					
Genotype[b]	*al-dp*	*dp-b*	*b-pr*	*pr-cn*	Total *al-cn*	N[c]
Wild-type	12.5	28.0	3.5	1.3	45.3	1008
pch2^{EY}	11.7 (94)	26.7 (95)	3.3 (94)	2.1 (162)	43.8 (97)	562
mei-9^{a}	0.67 (5.4)	3.0 (10.7)	0.5 (14.3)	0.2 (12.3)	4.3 (9.5)	993
mei-9^{a}; pch2^{EY}	0.0 (0.0)	1.4 (5.0)	0.0 (0.0)	0.0 (0.0)	1.4 (3.1)	360
FM7/+	14.8 (118)	30.3 (108)	17.6 (503)	5.6 (431)	68.3 (151)	568
FM7/+; pch2^{EY}	14.6 (117)	23.8 (85)	7.8 (223)	2.0 (154)	48.2 (106)	1176
MVD1 HA-pch2^{27}/+	12.0 (96)	36.0 (129)	5.5 (157)	0.9 (69)	54.4 (120)	1300
MVD1 HA-pch2^{71}/+	11.5 (92)	25.0 (89)	7.5 (214)	1.3 (100)	45.3 (100)	1404
MVD1 HA-pch2^{81}/+	9.3 (74)	31.5 (113)	6.5 (186)	1.6 (123)	48.9 (108)	992
MVD1 HA-pch2^{71}/MVD1 HA-pch2^{71}	9.8 (78)	41.7 (149)	10.3 (293)	0.8 (60)	62.6 (138)	1026

[a] Second chromosome crossing over was assayed by crossing al dp b pr cn/+ females to al dp b pr cn/ CyO males in the indicated backgrounds. The Cy+ progeny were scored for recombinants. Crossing over is expressed as cM across the intervals shown. Numbers in parentheses denote the percentage of wild-type recombination frequency.

[b] MVD1= P(Gal4::VP16-nos.UTR)MVD1

[c] N= total flies counted

Table 6: Effect of *pch2* on crossing over on the X-chromosome

	Crossing over on the X Chromosome (cM)[a]					
Genotype	*pn-cv*	*cv-m*	*m-f*	*f-y*$^+$	Total *pn-y*$^+$	N[b]
Wild-type	15.4	18.9	11.9	7.3	53.5	657
pch2^{EY}	14.8 (96)	18.5 (98)	14.1 (118)	6.3 (86)	53.7 (100)	569
CyO/+	18.6 (121)	27.7 (147)	19.9 (167)	13.6 (186)	79.8 (149)	1319
CyO/+; pch2^{EY}	15.0 (97)	26.1 (138)	18.1 (152)	9.1 (125)	68.3 (128)	1148

[a] X chromosome crossing over was assayed by crossing *y pn cv m f • y*$^+$*/y* females to wild-type males in the indicated backgrounds. The male progeny were scored for recombinants. Crossing over is expressed as cM across the intervals shown. Numbers in parentheses denote the percentage of wild-type recombination frequency.

[b] N= total flies counted

Table 7: X-Chromosome nondisjunction in *Ercc1*, *pch2* and *sir2* mutants

	X-chromosome nondisjunction	
Genotype	% X-ND	N[a]
Wild-type	0.1	2440
$pch2^{EY}$	0.3	2098
$Ercc1^{X}$	13.6	353
$Ercc1^{X}$; $pch2^{EY}$	30.0	300
$sir2^{17}/Df$	0.2	632

[a] N= total flies counted

CHAPTER 5: ATM and ATR analysis reveal two modes of HIS2AV regulation during Drosophila oogenesis

I. Preface

This chapter will soon be submitted as an individual paper. My contributions to the project were: writing of the paper and also performing all the experiments with the exception of the analysis of karyosome morphology and GRK localization (Figure 19).

II. Abstract

DNA double strand breaks (DSBs) are essential for meiotic recombination, yet are a potentially lethal form of DNA damage, associated with genome instability and cancer in humans. ATM and ATR-related kinases are conserved regulators of cellular responses to DSBs, including DSB repair mechanisms and cell cycle checkpoints that provide time for repair. During Drosophila meiosis, MEI-41 (ATR) function has been implicated in DSB repair and checkpoint activation; however, the role of ATM remains unclear due to an essential role in telomere maintenance. We addressed this question by analyzing oogenesis in a conditional *atm* mutant, where we observed profound defects in the repair of meiotic DSBs. We also present evidence that ATM and ATR are functionally redundant for HIS2AV phosphorylation, a conserved chromatin modification in response to DSBs. Furthermore, our analysis of ATM and ATR function during meiosis has led to

new insight into HIS2AV dynamics during Drosophila oogenesis, which may include two distinct mechanisms for γ-HIS2AV removal.

III. Introduction

DNA double strand breaks (DSBs) can cause aneuploidy or trigger apoptosis if they are not promptly repaired; consequently, a cell's ability to respond to chromosome DSBs is critical for survival (Wyman et al. 2006). In organisms as distantly related as fungi, insects and humans, conserved ATM and ATR-related kinases serve as master regulators of both DNA repair mechanisms and cell cycle checkpoints that provide time for repair (Shiloh 2006). Due to the apparent functional redundancies of ATM and ATR (Shiloh 2006; Matsuoka et al. 2007), the unique roles played by these genotoxic stress kinases remains elusive.

The gene encoding Drosophila ATM was originally named *tefu* due to its role in preventing spontaneous telomere fusions (Queiroz-Machado et al. 2001). As a result, *atm* mutant tissues exhibit high levels of chromosome aberrations and apoptosis (Queiroz-Machado et al. 2001; Bi et al. 2004; Silva et al. 2004; Song et al. 2004). Cell cycle checkpoint functions have also been reported for ATM (Bi et al. 2004; Song et al. 2004), although these are not as critical as the checkpoint functions of the ATR homolog, MEI-41 (Sibon et al. 1999; Laurencon et al. 2003; Jaklevic et al. 2004). Many checkpoint signaling proteins, including MEI-41/ATR, Brca2, and Hus1 have also been reported to serve an additional function in meiotic DSB repair (LaRocque et al. 2007; Klovstad et al. 2008; Joyce et al. 2009; Peretz et al. 2009); however, it remains unclear if ATM shares this role. Evidence for a mitotic DNA repair function came from studies of conditional *atm* mutants, which were found to be sensitive to ionizing radiation, characteristic

features of Drosophila DSB repair mutants (Silva et al. 2004). ATM also interacts with the Drosophila MRN (Mrell-Rad50-Nbs1) complex (Bi et al. 2004; Ciapponi et al. 2004; Gorski et al. 2004; Bi et al. 2005; Ciapponi et al. 2006; Oikemus et al. 2006; Slijepcevic 2006). Although MRN has been implicated in DSB repair and telomere maintenance in Drosophila and other eukaryotic organisms (Ciapponi et al. 2006; Lee et al. 2006; Lavin 2007), conclusive evidence that ATM is also involved in DSB repair during meiosis has been lacking.

IV. Materials and Methods

Drosophila genetics: The genotype of the temperature-sensitive atm^{8} mutants referred to in this report was p^{p} atm^{8} *e* (Silva et al. 2004). atm^{8} mutant progeny were raised at 18°C (which is the permissive temperature for the atm^{8} allele). Once the flies reached adulthood, the atm^{8} mutants were shifted to 25°C (restrictive temperature for atm^{8}). This regimen was based on temperature-shift experiments that had previously defined temperature-sensitive phases for specific developmental defects (including lethality or female sterility) in atm^{8} mutants (Silva et al. 2004). After 4 days at the restrictive temperature, atm^{8} mutant germaria failed to produce new cysts, indicating cell death from a premeiotic defect. References for the specific mutant alleles of other genes that were analyzed in this study are as follows: $mei\text{-}41^{D3}$ (Laurencon et al. 2003), mnk^{P6} (Abdu et al. 2002), $mei\text{-}W68^{4572}$ (Baker et al. 1978), $spn\text{-}A^{1}$ (Staeva-Vieira et al. 2003) and the HIS2AV:GFP fusion protein was obtained from (Kanda et al. 1998).

Cytology and Immunofluorescence*:* For immunolocalization experiments, females were aged at room temperature for about 16 hours (unless otherwise noted as in atm^{8} mutants) and ovaries were dissected and fixed using the "Buffer A" protocol (McKim et al. 2008). The antibody to γ-HIS2AV was described by Mehrotra et al. (Mehrotra et al. 2006) and used at a 1:500 dilution. An unpurified version of the antibody that recognized all HIS2AV was used at 1:500. Additional primary antibodies included mouse anti-C(3)G antibody used at 1:500 (Page et al. 2001), a combination of two mouse anti-Orb antibodies (4H8 and 6H4) used at 1:100 (Lantz et al. 1994), a mouse anti-GRK used at 1:10 (Queenan et al. 1999), a Rabbit anti-RPA70 used at (Mitsis 1995), and a sheep acetylK4-H2A.Z used at 1:500 (Abcam).

The secondary antibodies were Cy3 labeled goat anti-rabbit (Jackson Labs) used at 1:250, Cy3 labeled anti-sheep (Abcam) used at 1:100, and Alexa fluor 488 goat anti-mouse (Invitrogen) used at 1:100. Chromosomes were stained with Hoechst at 1:50,000 (10mg/ml solution) for seven minutes at room temperature. Images were collected using a Leica TCS SP2 confocal microscope with a 63X, N.A. 1.3 lens. In most cases, whole germaria were imaged by collecting optical sections through the entire tissue. These data sets are shown as maximum projections. The analysis of the images, however, was performed by examining one section at a time.

Counting γ-HIS2AV foci in repair-proficient and repair-defective backgrounds: The γ-HIS2AV foci were counted from germaria where the foci were clear and distinct. Foci numbers in wild-type were at a maximum in region 2a (early pachytene) and few foci were visible by region 2b (mid pachytene).

For counting γ-HIS2AV foci in repair-defective backgrounds, C(3)G staining was used to identify oocytes in region 3 (late pachytene). The foci were counted from germaria where the foci were clear and distinct. The foci were counted manually by examining each section in a full series of optical sections containing complete pro-oocyte nucleus.

V. Results and Discussion

Loss of ATM activates the meiotic DSB repair checkpoint

During Drosophila oogenesis, germline stem cells produce oogonia that proceed through four mitotic cell cycles to form 16-cell germline cysts (Spradling 1993). Although all 16 cells undergo developmentally regulated induction and repair of DNA double strand breaks (DSBs) associated with meiotic recombination, only one of these 16 cells ultimately becomes an oocyte and completes meiosis (von Wettstein et al. 1984; Walker et al. 2000; Page et al. 2001).

During normal development, a TGF (transforming growth-factor)-related protein called Gurken (GRK) interacts with growth factor receptors in somatic follicle cells that are adjacent to the oocyte, inducing a dynamic reorganization of the microtubule network to localize cell fate determinants properly for establishing correct dorsal-ventral and anterior-posterior polarity (Neuman-Silberberg et al. 1993; Ray et al. 1996; Sapir et al. 1998; Riechmann et al. 2001; Barbosa et al. 2007). When meiotic DSB repair fails because of mutations in DNA repair genes, activation of a meiotic checkpoint disrupts

this GRK localization mechanism, causing development to proceed abnormally (Ghabrial et al. 1999; Abdu et al. 2002).

To address the uncertainties regarding the role of ATM in meiosis, we undertook a functional analysis of DSB repair during Drosophila oogenesis. We used the temperature-sensitive allele of *tefu/atm* (*atm*^{8}) that was isolated previously (Silva et al. 2004), allowing us to bypass the developmental lethality associated with *atm* null mutants. The completely restrictive temperature for *atm*^{8} lethality is 25^{o} (Silva et al. 2004). We raised *atm*^{8} mutants at a permissive temperature (18^{o}), shifted them to the restrictive temperature, and examined whether the meiotic DSB repair checkpoint that disrupts GRK localization was activated (see Experimental Procedures). GRK is normally concentrated in the cytoplasm of control oocytes (Figure 19A). In ~87% of similarly staged *atm*^{8} mutant ovarioles, GRK expression appeared absent or much weaker than normal as well as mis-localized (Figure 19A; Table 8). Another characteristic feature of oocyte development is the assembly of the chromosomes into a distinctive structure, the karyosome (Spradling 1993). In control oocytes, the karyosome appeared compact and spherical (Figure 19B). However, in ~80% of the *atm*^{8} mutant ovarioles, karyosome morphology appeared abnormally flattened or fragmented (Figure 19B; Table 8). Similar karyosome defects were previously reported for a number of Drosophila DSB repair mutants (Ghabrial et al. 1998; Ghabrial et al. 1999; Abdu et al. 2002; Staeva-Vieira et al. 2003; McCaffrey et al. 2006).

MEI-W68 is the Drosophila homolog of Spo-11, a conserved endonuclease that catalyzes meiotic DSB induction in eukaryotes (McKim et al. 1998). We observed suppression of the GRK localization and karyosome morphology defects in the *mei-*

W86^{4572}*; atm*^{8} double mutants (Table 8), indicating the defects were due to unrepaired meiotic DSBs. These results suggest that ATM is required for repair but not the checkpoint response.

We also tested double mutant genotype combinations with *mei-41* and *mnk*, which encode the Drosophila ATR and Chk2 homologs, respectively, shown to be integral components of the meiotic checkpoint mechanism (Xu et al. 2001; Abdu et al. 2002). As expected, the checkpoint-mediated GRK localization and karyosome defects in *atm*^{8} mutants were suppressed in *mei-41*^{D3}*; atm*^{8} double mutants and reduced in *mnk*^{P6}*; atm*^{8} (Figure 19C; Table 8). These results show that loss of ATM function leads to activation of the MEI-41-dependent checkpoint response to unrepaired meiotic DSBs.

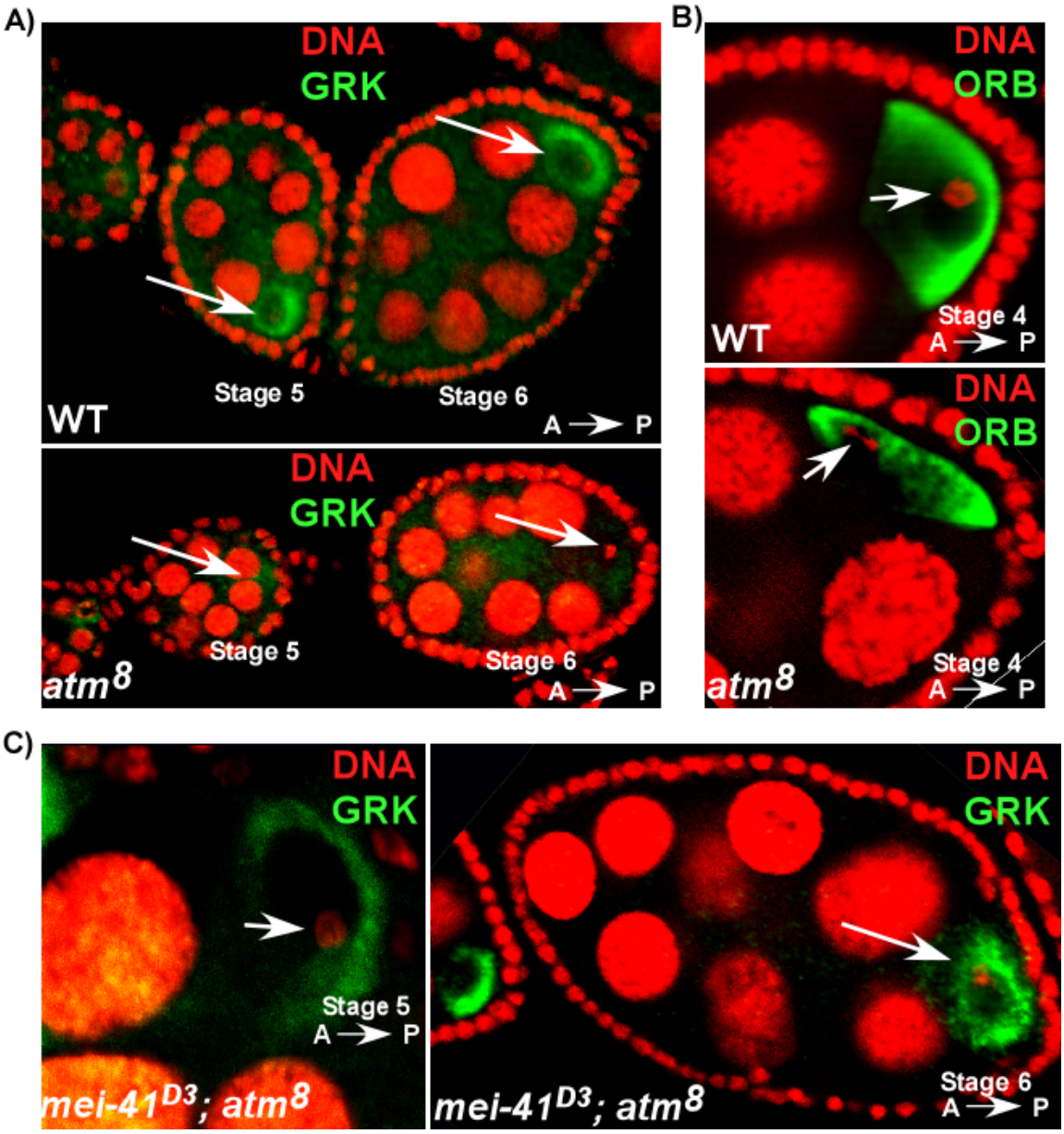

Figure 19: Loss of ATM activates the *mei-41*-dependent meiotic DSB repair checkpoint.

Drosophila ovaries of the indicated genotypes are shown. (A) In control ovarioles, GRK protein (green) localizes in a ring around the oocyte nucleus (arrows) in stage 5 and 6 egg chambers. In stage 6 atm^{8} mutant egg chambers, GRK staining is much weaker or absent altogether. (B) In control oocytes, chromatin becomes hyper-condensed during stage 4 of oogenesis into a spherical structure called the karyosome (arrow). Antibodies to ORB (green), a protein that localizes to the oocyte cytoplasm, were used to identify the oocyte nucleus. In similarly aged ORB-labeled atm^{8} mutant egg chambers, misshapen or fragmented karyosomes were observed (arrow). (C) The GRK localization and karyosome morphology defects were suppressed in $mei\text{-}41^{D3}$; atm^{8} mutants. Arrows denote the oocytes and DNA was stained with Hoescht (red).

atm and *mei-41* are required for DSB repair in the oocyte

The H2A variant, HIS2AV is phosphorylated at the sites of DNA breaks (Madigan et al. 2002). This phosphorylated protein is called γ-HIS2AV and forms distinctive foci in the nucleus that are observable by immunofluorescence (Madigan et al. 2002; Jang et al. 2003; Mehrotra et al. 2006). To directly assay for DSB repair defects in atm^{8} mutants, we examined γ-HIS2AV in oocytes, which were labeled with an antibody against the synaptonemal complex component C(3)G (Page et al. 2001). During normal oogenesis, meiotic DSBs are induced in regions 2a and repaired before region 3 of the germarium (Madigan et al. 2002; Jang et al. 2003; Staeva-Vieira et al. 2003; Gorski et al. 2004). As expected, γ-HIS2AV foci were found in region 2a oocytes of control germarium (Figure 20A; Table 9). Importantly, γ-HIS2AV foci were absent in region 3 cells, confirming that this chromatin modification is removed after the developmental stage when meiotic DSB repair is normally completed (Figure 20B).

In DSB repair mutants including the Rad51 homolog *spn-A*, γ-HIS2AV foci accumulate and persist throughout meiotic prophase (Figure 20C-D; (Mehrotra et al. 2006)). An average of 20.5 γ-HIS2AV foci was present in $spn\text{-}A^{1}$ region 3 oocytes, which is similar to previous estimates for the total number of DSBs per nucleus (Table 9; (McKim et al. 2002; Mehrotra et al. 2006)). Drosophila ATR (MEI-41) has also been implicated in homologous repair of somatic and meiotic DSBs (LaRocque et al. 2007; Joyce et al. 2009). Consistent with these observations, we found a level of γ-HIS2AV foci in $mei\text{-}41^{D3}$ region 3 oocytes that was similar to $spn\text{-}A^{1}$ mutants (Figure 20E-F; Table 9). In contrast to $spn\text{-}A^{1}$ mutants, the repair defect in $mei\text{-}41^{D3}$ was specific to the oocyte and

showed wild-type γ-HIS2AV kinetics in nurse cells (Figure S 7). Thus, Drosophila ATR is required for repair of meiotic DSBs specifically in oocytes.

In *atm*^{8} mutant germaria, we observed an increased level of γ-HIS2AV staining in regions 2a and 3 of the germarium, relative to controls (Figure 20G-H). Similar to *mei-41*^{D3}, the repair defect in *atm*^{8} mutants was specific to the oocytes (Figure S 7). Interestingly, oocyte-specific repair defects have also been reported for checkpoint-defective *hus1* and *brca2* mutants (Peretz et al. 2009). Thus, these proteins may not represent core components of the repair machinery, but rather regulatory factors with an indirect role in repair.

In contrast to other repair mutants like *spn-A*^{1} and *mei-41*^{D3}, the γ-HIS2AV staining in *atm*^{8} mutants exhibited more robust labeling and localized to threads that covered a large fraction of the chromosomes (Figure 20G-H). As a result, we were unable to quantify the staining; however, the presence of γ-HIS2AV in region 3 oocytes is consistent with a meiotic DSB repair defect in the *atm*^{8} mutants. The thread-like γ-HIS2AV labeling in *atm*^{8} mutant oocytes could be due to the induction of more DSBs, possibly arising from errors in DNA replication, or alternatively, to a loss of regulation on HIS2AV phosphorylation. To distinguish between these alternatives, we analyzed γ-HIS2AV staining in a *mei-W68* mutant background, where meiotic DSB formation was blocked. All γ-HIS2AV staining was eliminated in *mei-W86*^{4572}*; atm*^{8} double mutants (Figure 20I-J), indicating that ATM is a required for meiotic DSB repair and additional sources of DSBs are not generated in the absence of ATM. In addition, the thread-like γ-HIS2AV labeling in *atm*^{8} mutants provides evidence for a surprising role for ATM on the restriction of HIS2AV phosphorylation to break sites.

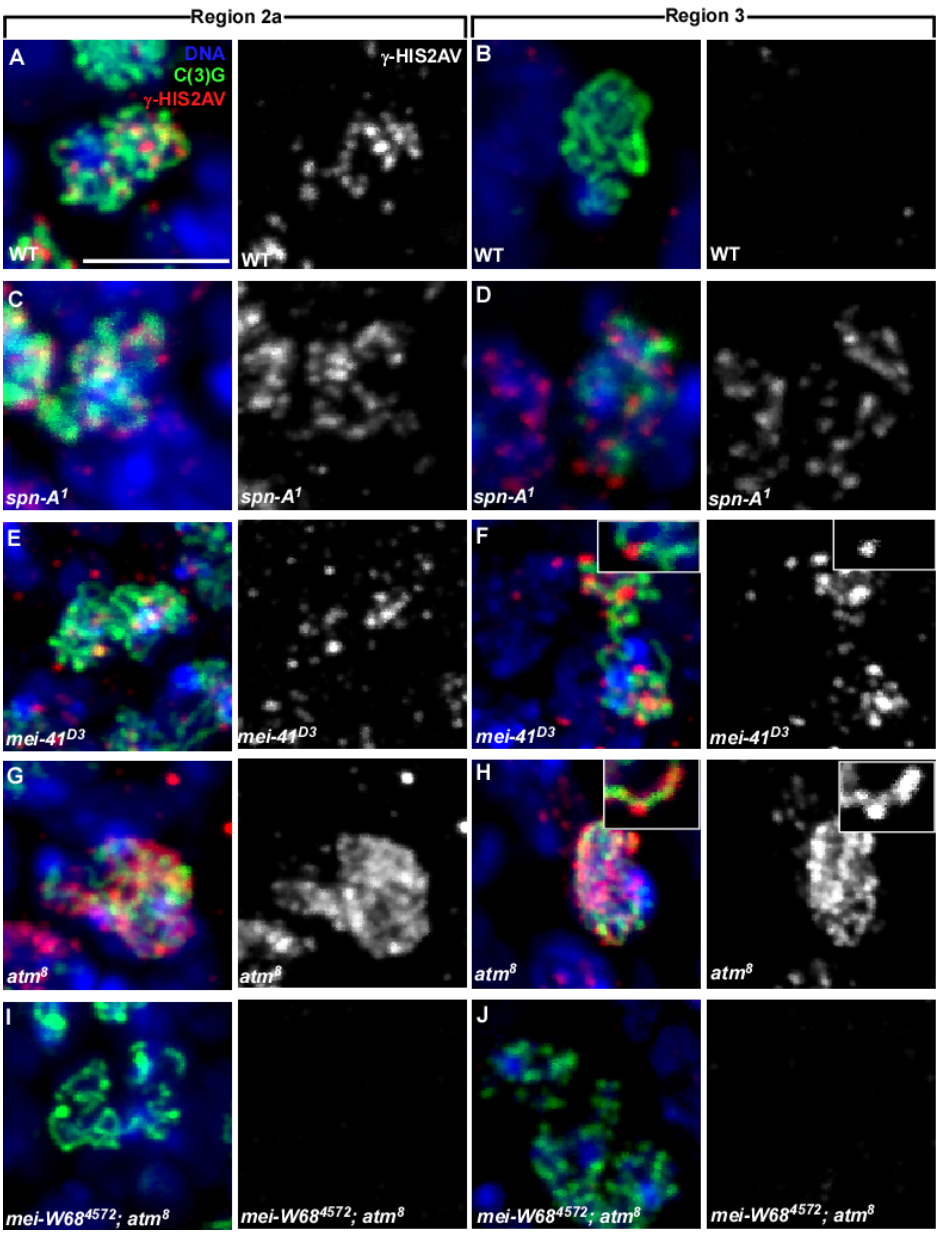

Figure 20: *atm* and *mei-41* are required for DSB repair in the oocyte.

C(3)G (green) is observed in region 2a pro-oocytes and region 3 oocytes as homologous chromosomes undergo meiotic recombination. (A) γ-HIS2AV labeling from a control germarium, showing foci in region 2a cells, where meiotic DSBs are induced by the MEI-W68 endonuclease, initiating meiotic recombination. (B) In region 3 oocytes, γ-HIS2AV labeling is absent from control germaria, indicating DSBs have been repaired. (C-D) γ-HIS2AV staining in region 3 cells in repair-defective mutant $spn\text{-}A^{1}$. (E-F) Persistence of γ-HIS2AV labeling in a $mei\text{-}41^{D3}$ germarium. Similar to controls, γ-HIS2AV staining formed distinct foci along chromosomes (inset). (G-H) Stronger γ-HIS2AV labeling (relative to controls, $spn\text{-}A^{1}$, *and* $mei\text{-}41^{D3}$) in region 3 was observed in atm^{8} mutant germarium. γ-HIS2AV localized to threads spread out along the chromatin instead of distinct foci (inset). (I-J) All γ-HIS2AV was eliminated in $mei\text{-}W68^{4572}$; atm^{8} double mutants. Scale bar is 5μM.

ATM and MEI-41/ATR are functionally redundant for HIS2AV phosphorylation

ATM and ATR-related kinases have been implicated in the phosphorylation of H2AX at sites of chromosomal DSBs in somatic cells of other experimental systems (Burma et al. 2001; Ward et al. 2001). To investigate whether ATM and MEI-41 might serve redundant roles in HIS2AV phosphorylation in response to meiotic DSBs, we examined *mei-41^{D3}; atm^{8}* double mutant germaria. At the permissive temperature (18^{o}), *mei-41^{D3}; atm^{8}* displayed a γ-HIS2AV staining pattern similar in severity to *mei-41^{D3}* single mutants with an average of 18.2 foci in region 3 oocytes (Figure 21A-B; Table 9). When shifted to the restrictive temperature (25^{o}) for 24 hours, however, no γ-HIS2AV staining was observed in the *mei-41^{D3}; atm^{8}* double mutant region 2a cysts (Figure 21C), indicating these mutants lost the ability to phosphorylate HIS2AV near newly generated DSBs. We therefore concluded from these results that, similar to their homologs in other organisms (Stucki et al. 2006), ATM and ATR are functionally redundant for the γ-HIS2AV response to meiotic DSBs.

We were surprised to find that γ-HIS2AV staining was also absent from region 3 oocytes in *mei-41^{D3}; atm^{8}* double mutants (Figure 21D), which presumably had already been phosphorylated prior to the shift to the restrictive temperature. Based on previous estimates for the timing of cyst progression (King 1970; Spradling 1993) and our unpublished data, region 3 cysts would have been in region 2b (after DSB formation) and, thus, would have had γ-HIS2AV at the time of shift to restrictive temperature (Figure 21G). To confirm that HIS2AV and DSBs were still present in region 3 nuclei, we transferred the *mei-41^{D3}; atm^{8}* double mutants from the restrictive temperature back to the permissive temperature and analyzed γ-HIS2AV staining. After only 24 hours at the

permissive temperature, γ-HIS2AV staining returned to the oocytes, albeit not as strong as in wild-type (Figure 21E-F; Table 9). Nonetheless, this result shows that unrepaired DSBs were present and suggests that there is a rapid turnover of the HIS2AV phosphorylation mark near meiotic DSBs, which must be maintained by ATM or MEI-41 activity.

Ubiquitous localization of RPA

The functional redundancy of MEI-41 and ATM in the γ-HIS2AV response to DSBs coupled with the thread-like γ-HIS2AV labeling in *atm*^{8} mutants (Figure 20) suggests that in the absence of ATM, MEI-41/ATR-mediated γ-HIS2AV is no longer spatially restricted.

Replication protein A (RPA) is a ssDNA-binding protein complex that appears at sites of DNA damage. ATR localizes to sites of DNA damage by interacting with the RPA-coated ssDNA substrates (Zou et al. 2003; Dart et al. 2004; Ball et al. 2005; Namiki et al. 2006). To determine the mechanism behind MEI-41's unrestricted kinase activity in *atm*^{8} mutants, we stained ovaries with an antibody against the 70-kDA subunit of Drosophila RPA (Mitsis 1995). We found labeling of RPA throughout both oocyte and nurse cell nuclei (Figure 21H). Suprisingly, RPA exhibited a thread-like staining pattern that colocalized with a large fraction of the DNA. Within oocytes, RPA staining was excluded from regions containing the synaptonemal complex central element C(3)G, suggesting the localization of RPA was restricted to chromatin loops rather than the axial core of chromosomes (Figure 21H). Accordingly, in *atm*^{8} mutants, γ-HIS2AV showed a similar staining pattern (Figure 21H), suggesting RPA is facilitating the ubiquitous activity of MEI-41 on HIS2AV phosphorylation in *atm*^{8} mutants. In addition, these

results provide evidence that suggest RPA has strong affinity for intact chromatin *in vivo*, which is in contrast to many *in vitro* assays where RPA showed binding preference for ssDNA substrates created at sites of DSBs (Bastin-Shanower et al. 2001; Zou et al. 2006).

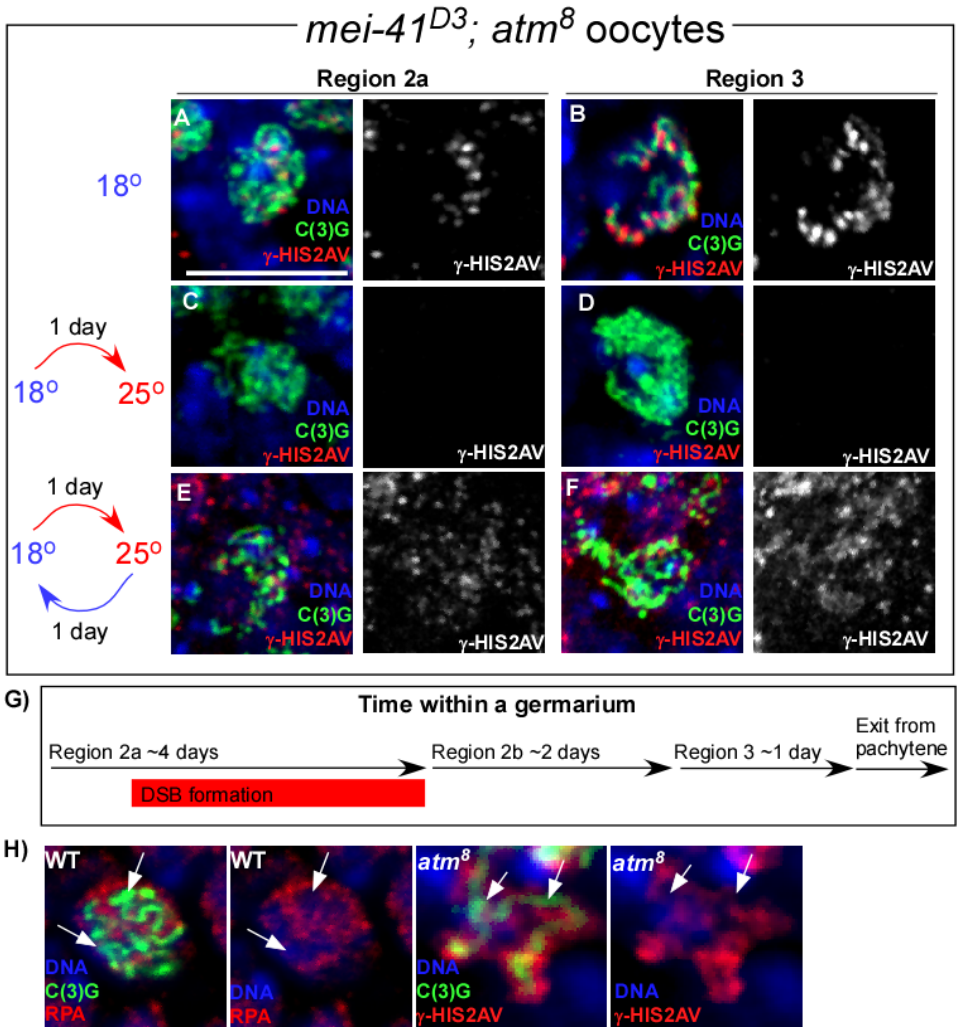

Figure 21: ATM and MEI-41 are functionally redundant for the γ-HIS2AV response to meiotic DSBs.

(A-B) At the permissive temperature (18°), *mei-41*^{D3}*; atm*^{8} displayed γ-HIS2AV foci (red) in region 2a and region 3 oocytes, similar to *mei-41*^{D3} single mutants. Scale bar is 5μM. (C-D) At the restrictive temperature (25°) for 1 day, no γ-HIS2AV staining was observed in *mei-41*^{D3}*; atm*^{8} double mutant oocytes in either region 2a or 3. (E-F) When the *mei-41*^{D3}*; atm*^{8} double mutants were transferred from restrictive temperature back to permissive temperature, γ-HIS2AV staining returned to both region 2a and region 3 oocytes. (G) Estimated timing of cyst progression and DSB formation within a wild-type germarium ((King 1970; Spradling 1993) and our unpublished data). (H) In wild-type oocytes, RPA staining colocalizes with a large fraction of the DNA (more than just DSB sites), but not C(3)G. This localization is similar to the thread-like γ-HIS2AV labeling in *atm*^{8} mutant oocytes, which is also shown flanking the C(3)G stain.

HIS2AV is removed from oocytes by stage 5 of oogenesis

The developmental delay in the disappearance of γ-HIS2AV foci observed in *spn-A*^{1}, *mei-41*^{D3} and *atm*^{8} mutant germaria suggested that meiotic DSB repair was defective in these mutants. However, we failed to observe γ-HIS2AV labeling in any mutant oocytes past stage 5 of oogenesis (*spn-A*^{1} shown in Figure 22A; (Mehrotra et al. 2006)). One possibility is that the DSBs are repaired at this stage by alternative repair pathways not active at earlier stages (Mehrotra et al. 2006). However, another explanation is that HIS2AV is removed from the nucleosomes independent of repair by stage 5-6 of oogenesis.

H2AX, the human homolog of the Drosophila histone variant HIS2AV, is present in chromatin at levels that vary between 2 and 25% of the H2A pool (Kinner et al. 2008). To evaluate the levels of HIS2AV during Drosophila oogenesis, we stained ovaries with an unpurified HIS2AV antibody that recognizes both modified and unmodified versions of the histone. As expected, HIS2AV labeling was abundant throughout the nucleus of all oocytes and nurse cells as well as the mitotically-dividing follicle cells from the germarium to stage 3 of oogenesis (Figure 22B). Strikingly, at stage 4-5 of oogenesis in wild-type, HIS2AV staining was drastically reduced in nurse cells and oocytes but not in follicle cells (Figure 22B). We repeated the experiment using a GFP tagged version of HIS2AV (Kanda et al. 1998) and again, we observed that the HIS2AV signal is nearly eliminated from the oocyte nucleus by stage 5 (Figure 22C). In contrast to the HIS2AV antibody, HIS2AV:GFP labeling was abundant within nurse cells of stage 5 egg chambers. The differing results probably reflect the inability of the antibody to penetrate

the polyploidy nuclei. However, the absence of the HIS2AV:GFP signal suggests an oocyte-specific mechanism for HIS2AV removal.

In somatic cells, the removal of γ-HIS2AV from the nucleosomes has been associated with its prior acetylation by the acetyltransferase dTip60 (Kusch et al. 2004). To determine if this chromatin modification correlates with the removal of HIS2AV in meiosis, we stained with an antibody that recognizes acetylK4-H2A.Z (Ac-HIS2AV). Although we observed no significant staining in cells within egg chambers at or prior to stage 3 of oogenesis, we found labeling in stage 4 oocyte nuclei (Figure 22D). These results indicate that HIS2AV is acetylated at stage 4 and removed from the nucleosomes between stages 5 and 6 of oogenesis. Furthermore, the absence of HIS2AV at stage 5 was also found in *spn-A*^{1}, *mei-41*^{D3} and *atm*^{8} mutant ovarioles (data not shown), suggesting this exchange most likely occurs independently of efficient repair.

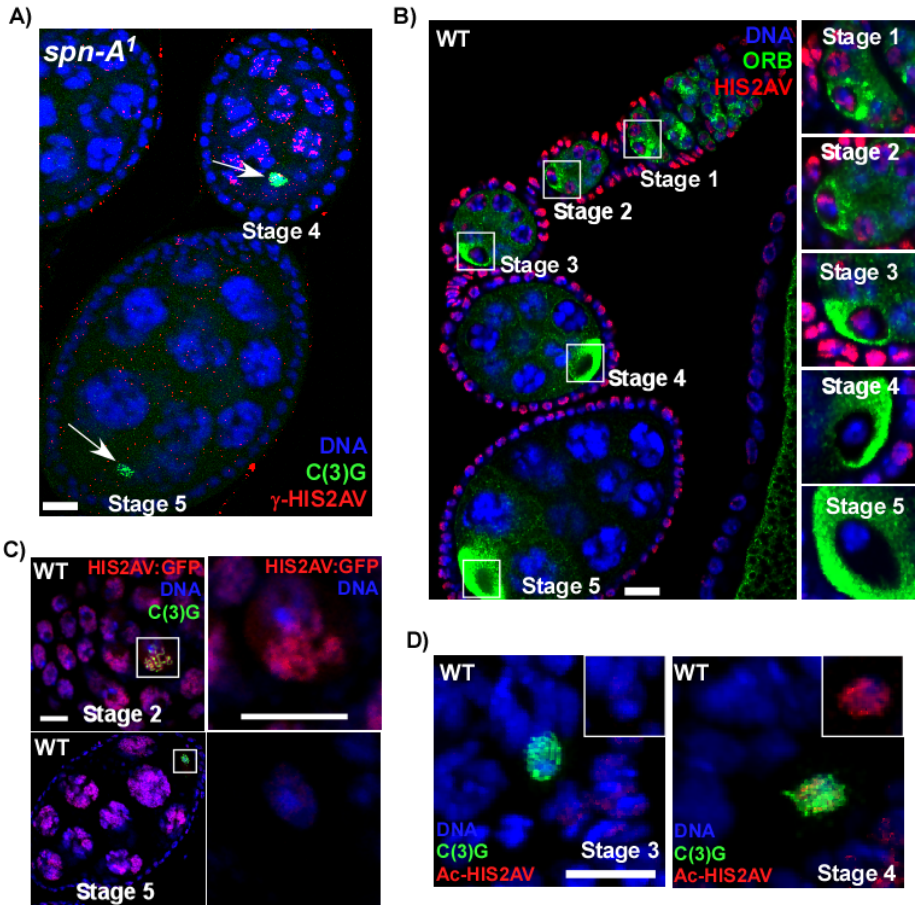

Figure 22: HIS2AV removed by stage 5 of oogenesis.

(A) In *spn-A*^{1} mutants, γ-HIS2AV foci (red) are not observed past stage 4 of oogenesis. (B) In wild-type, an antibody that recognizes both modified and unmodified versions of HIS2AV (red) showed abundant staining in cells from the germarium to stage 3 of oogenesis and is drastically reduced within egg chambers at stages 4 and 5. The mitotically-dividing follicle cells that surround the egg chambers also showed abundant HIS2AV labeling at all stages. (C) A similar result was found using HIS2AV:GFP (red). In stage 2 egg chambers, HIS2AV:GFP labels most of the oocyte nucleus, but is absent from stage 5 oocytes. (D) Although no Ac-HIS2AV staining (red) was observed in oocytes from stage 3 of oogenesis, we found robust labeling in stage 4 oocyte nuclei. Insets show nuclei with C(3)G staining removed. Scale bars are 5μM in all images.

Conclusion

We have shown that the Drosophila ATM and ATR kinases have unique roles in meiotic DSB repair as well as a functional redundancy in HIS2AV phosphorylation (Figure 23B). After completion of DNA repair, γ-HIS2AV is restored to an unmodified

HIS2AV. In Drosophila somatic cells, histone acetylation by dTip60 promotes the selective exchange of nucleosomal γ-HIS2AV with an unmodified HIS2AV (Kusch et al. 2004). Our analysis of Drosophila ATM and ATR in meiosis has revealed surprising features of HIS2AV dynamics which may include two distinct mechanisms for γ-HIS2AV removal.

First, γ-HIS2AV at meiotic DSB sites exhibits rapid turnover and requires maintenance by continuous ATM or ATR activity. Furthermore, acetylation of HIS2AV, the prerequisite to HIS2AV exchange in somatic cells (Kusch et al. 2004), is not observed in wild-type when γ-HIS2AV is removed in mid-pachytene (region 2b-3). Therefore, γ-HIS2AV removal in pachytene may be occurring through a dTip60-independent mechanism, either by acetylation-independent exchange or a direct modification at the nucleosome (*in situ* dephosphorylation). Similarly, studies in budding yeast argue that γ-H2AX turnover is a highly dynamic process near break sites, which may function to control the DNA damage response (Papamichos-Chronakis et al. 2006).

Second, we have shown that HIS2AV is removed from oocyte nuclei between stages 5 and 6 of oogenesis (after pachytene), which is preceded by acetylation at stage 4. In contrast to the rapid turnover of γ-HIS2AV in pachytene cells and the selective histone exchange of γ-HIS2AV by dTip60 in somatic cells, this exchange occurs to most, if not all, of the HIS2AV and independently of repair. This result also has important implications for the analysis of DSB repair in Drosophila, as γ-HIS2AV staining can not be used as a marker for DNA damage past stage 4 of oogenesis.

Finally, we showed that atm^{8} mutants exhibit thread-like γ-HIS2AV labeling in response to meiotic DSBs, suggesting ATM may have a function in the spatial restriction

of this chromatin modification to break sites. One explanation is that ATM is responsible to trigger a feedback signal to remove γ-HIS2AV at the end of repair. However, this does not explain why *atm*^{8} mutants exhibit more γ-HIS2AV than other repair mutants, such as *spn-A*^{1}. Alternatively, ATM could regulate the timed deactivation of MEI-41 (Figure 23B). If MEI-41 is a more active kinase compared to ATM, the accumulation of γ-HIS2AV in *atm*^{8} mutants would be an indirect consequence of overactive MEI-41. In fact, our examination of the DNA repair and ATR-recruiting protein RPA during meiosis supports this theory. In the absence of regulation by ATM, RPA-coated chromatin provides a nearly ubiquitous substrate for MEI-41-mediated phosphorylation of HIS2AV in meiotic cells. In wild-type, ATM may be important to spatially restrict the DNA damage response to ensure the recruitment of repair proteins to the correct site.

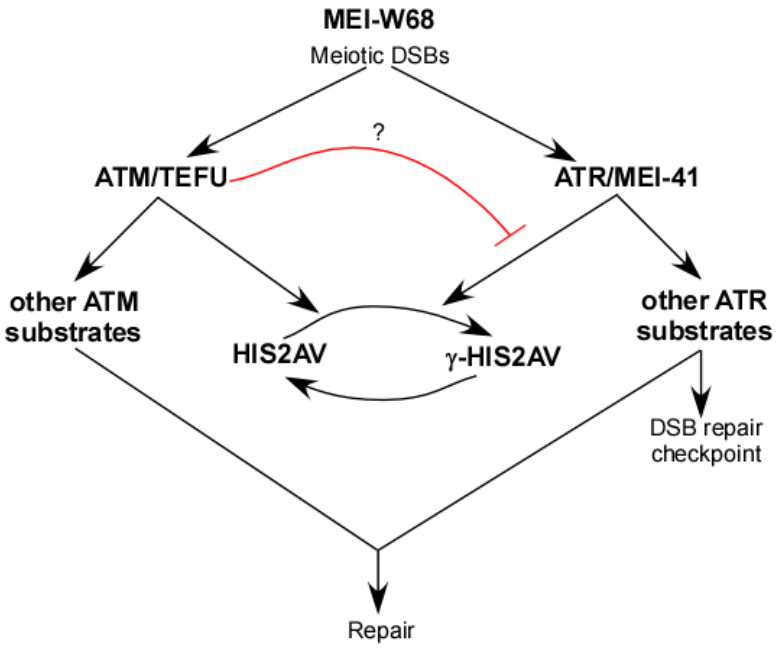

Figure 23: Model for the role of ATM and MEI-41 in the meiotic DSB response.

During female oogenesis, the MEI-W68 endonuclease induces DSBs to initiate meiotic recombination. Our results demonstrate that Drosophila ATM and ATR activity are essential for meiotic DSB repair, presumably because they facilitate recruitment of protein complexes required for repair. ATR/MEI-41 has an additional role in the DSB repair checkpoint that ATM is dispensable for. Our results also show that ATM and MEI-41 are functionally redundant for the γ-HIS2AV response to meiotic DSBs. The maintenance of γ-HIS2AV near DSB sites also requires ATM or MEI-41 activity, even after phosphorylation has occurred, providing evidence for a highly dynamic process. *atm*^{8} mutants lose the spatial restriction of γ-HIS2AV labeling to DSB foci, suggesting ATM may modulate MEI-41's role in this chromatin modification (question mark).

Table 8: *atm*^{8} activates DSB repair checkpoint

	WT	*atm*^{8}	*mei-W68*^{4572}; *atm*^{8}	*mei-41*^{D3}; *atm*^{8}	*mnk*^{P6}; *atm*^{8}
GRK defects[a]	0%	87%	0%	0%	40%
Karyosome defects[b]	0%	80%	0%	0%	12%
Total ovaries	38	40	30	30	40

[a] GRK defects include absent or much weaker expression than normal as well as mis-localized staining.
[b] Karyosome defects include abnormally flattened or fragmented morphology.

Table 9: DSB repair defects in *atm* and *mei-41* mutants

	Average γ-HIS2AV foci per oocyte	
Genotype	**Region 2a**	**Region 3**
Wild-type	6.2 +/- 1.1[b]	0.1 +/- 0.3
spn-A^{1}	3.7 +/- 1.4	20.5 +/- 1.5
atm^{8}	No foci[a]	No foci[a]
mei-41^{D3}	4.2 +/- 0.8	21.0 +/- 1.3
mei-W68^{4572}*; atm*^{8}	0.0	0.0
mei-41^{D3}*; atm*^{8} 18^{o}	7.5 +/- 1.7	18.2 +/- 2.1
mei-41^{D3}*; atm*^{8} 25^{o}	0.0	0.0
mei-41^{D3}*; atm*^{8} 25^{o} – 18^{o}	7.3 +/- 2.6	17.5 +/- 3.3

[a] could not count foci in *atm*^{8}

[b] "+/-" = standard deviation

CONCLUSION

My research focus was directed at understanding how homologous chromosomes exchange genetic material during meiosis and how this leads to the orderly segregation of the homologs at the first meiotic division. Specifically, the emphasis of my research was on the regulation and mechanisms of crossover formation using *Drosophila melanogaster* as a model system.

An endonuclease complex consisting of MEI-9, ERCC1, and MUS312 is required to cut repair intermediates during meiosis to generate crossovers, yet how this complex recognizes and binds to its single-strand-DNA (ssDNA) substrates remains unclear. In a screen for ethyl-methanesulfonate-induced mutations that increase X-chromosome nondisjunction, we recovered three alleles of *hdm*, which I mapped and characterized. Mutations in *hdm* result in phenotypes reminiscent of those found in endonuclease complex mutants. These include a reduction in meiotic crossover formation and sensitivity to DNA-damaging agents. I also found that HDM physically interacts with both MEI-9 and ERCC1 in a yeast two-hybrid assay, providing strong support that HDM joins the endonuclease complex that resolves meiotic recombination intermediates into crossovers. Intriguingly, bioinformatics programs predict *hdm*'s protein product contains three OB-folds and a zinc finger motif similar to that of RPA, suggesting it may bind ssDNA and act as a bridge between endonuclease activity and substrate specificity.

My analysis of HDM and other members of the endonuclease complex unexpectedly provided evidence for a novel meiotic checkpoint in Drosophila females. I found that crossover repair mutants cause delays in meiotic progression. Consistent with the hypothesis that a checkpoint has been activated, the delays require the Drosophila

homolog of PCH2, a highly conserved meiosis-specific checkpoint protein identified in budding yeast and nematodes. The PCH2-dependent delays also require proteins thought to regulate the number and distribution of crossovers, suggesting that this checkpoint monitors events leading to crossover formation.

Surprisingly, two lines of evidence suggest that the PCH2-dependent checkpoint does not reflect the accumulation of unprocessed recombination intermediates: the delays in meiotic progression do not depend on DSB formation or on *mei-41*, the Drosophila ATR homolog, which is required for the checkpoint response to unrepaired DSBs. In fact, my analysis of Drosophila ATR as well as the related kinase ATM during meiosis implicates these highly conserved proteins in DSB repair. I also found that ATM and ATR are functionally redundant for HIS2AV phosphorylation, a conserved chromatin modification in response to DSBs.

Thus, my results provided the first evidence of a DSB-independent checkpoint that functions during Drosophila meiosis. This analysis also led us to propose that the sites and/or conditions required to promote crossovers are established independently of DSB formation early in meiotic prophase, an idea now shared among several groups working on various model organisms.

The PCH2-dependent pachytene checkpoint has also been characterized in budding yeast and more recently in *C. elegans*. While a tremendous amount of progress has been made in identifying the factors involved in the checkpoint as well as the downstream effects of checkpoint activity, very little is actually known about the specific defect that the pachytene checkpoint responds to. Further characterization of the pachytene checkpoint in Drosophila has led us to several lines of evidence that suggest

the checkpoint monitors changes in chromosome structure that may be a prerequisite to the process of crossing over. In addition to mutations in structural components, heterozygous chromosomal rearrangements result in a checkpoint-mediated delay and global increase in crossovers that are both dependent on *pch2*. Thus, we have found a mechanism for the interchromosomal effect on crossing over; a phenomenon first observed over a hundred years ago by A.H. Sturtevant. Together, the data suggests the pachytene checkpoint may function to regulate the timing of critical events early in meiosis to generate an optimal number of crossovers.

While my work, in conjunction with studies in other labs over the past several years, has both clarified and altered our view of the mechanisms that produce and control crossover formation, many questions remain. What is the mechanism behind the pachytene checkpoint's effects on crossing over? Are crossover levels regulated simply by the length of pachytene or through more direct means such as modulating recombination proteins? Does the pachytene checkpoint transduce signals through the nuclear envelope and if so how? Are there specialized sites that promote a direct connection between chromosomes and the nuclear envelope or do protein-protein interactions indirectly facilitiate communication? Further studies aimed at answering these and related questions will help detmerine the exact mechanism behind this conserved surveillance mechanism and how it relates to crossover control.

APPENDIX 1: Supplementary figures

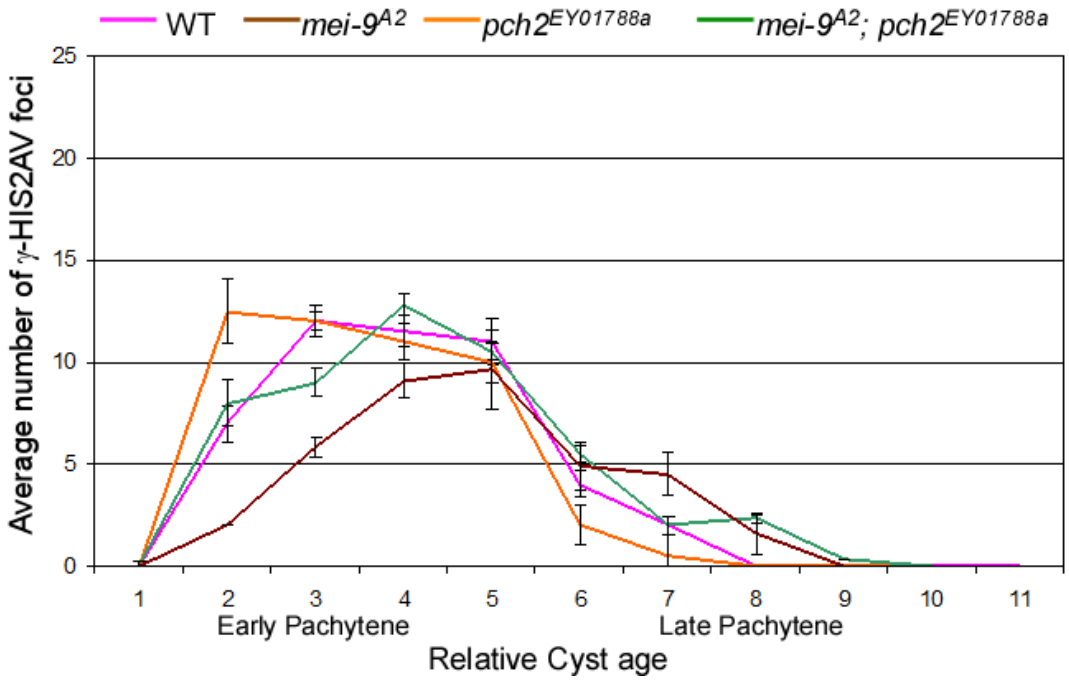

Figure S 1: Pattern of γ-HIS2AV staining in wild-type, *pch2* and *mei-9* mutants.

The average number of γ-HIS2AV foci relative to oocyte age (see Figure 8B for details). *pch2*^{EY01788a} mutations do not alter the wild-type γ-HIS2AV staining pattern and suppress the delayed onset of γ-HIS2AV in *mei-9*^{A2} mutants. Error bars denote the standard error of the mean.

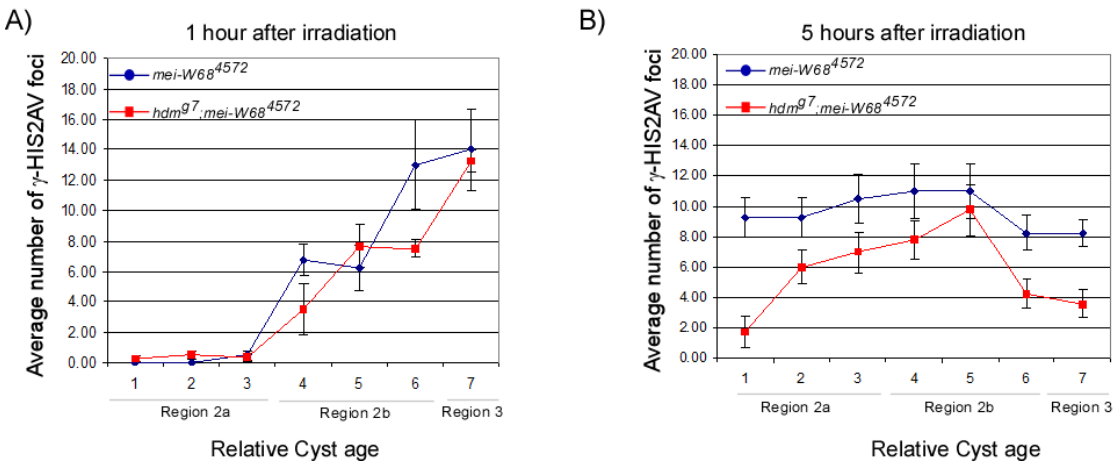

Figure S 2: *hdm* delays the response to X-ray induced DSBs.

The average number of γ-HIS2AV foci observed in pro-oocytes and oocytes of *mei-W68*^{4572} (blue) and *hdm*^{g7}*; mei-W68*^{4572} (red) females at (A) 1 hour and (B) 5 hours after irradiation. This graph shows how the response time to DSBs decreases as the pro-oocytes progress from early (region 2a) to late (region 3) pachytene. At one hour after irradiation, the number of γ-HIS2AV foci gradually increases between region 2a and 3, indicating the response time to X-ray induced DSBs gradually decreased from early to late pachytene oocytes. In region 3, the maximum number of γ-HIS2AV foci was observed within one hour after irradiation, which is similar to the response in somatic cells (Madigan et al. 2002). At five hours after irradiation, all pro-oocytes showed a uniform level of γ-HIS2AV foci throughout the germarium. The data in Figure 9 corresponds to cyst 1 in this Figure. Error bars denote the standard error of the mean.

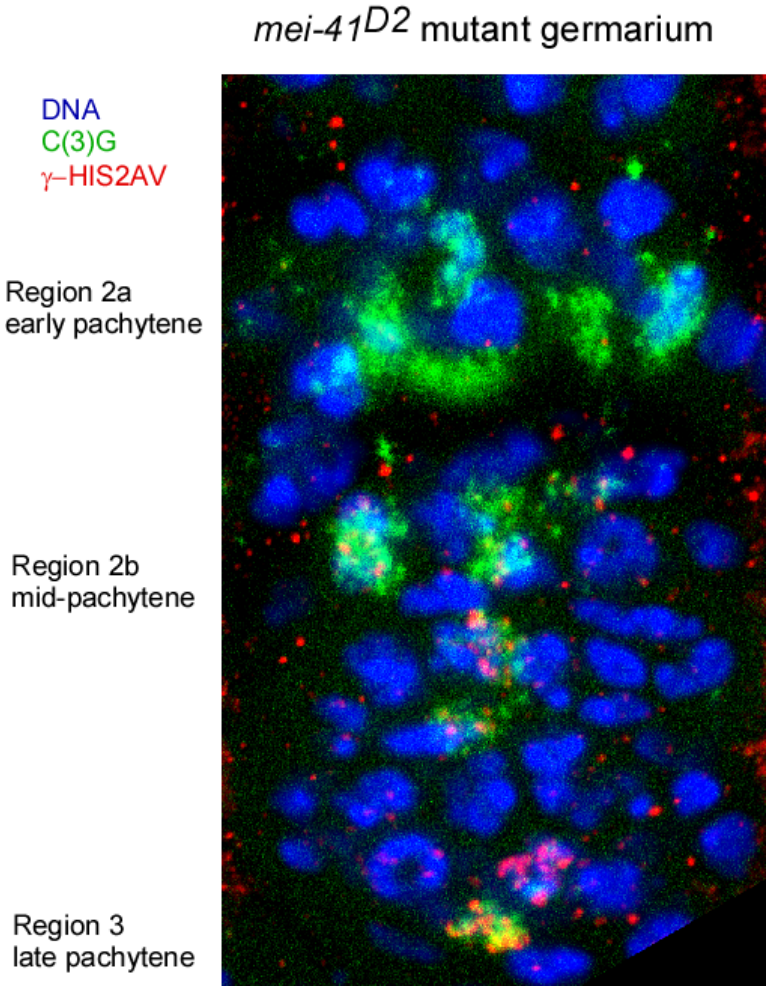

Figure S 3: Effect of *mei-41* on DSB repair.

A *mei-41*^{D3} mutant germarium stained for γ-HIS2AV shows a delay in the onset and a persistence of γ-HIS2AV phenotype similar to DSB repair mutants. Unlike most other DSB repair mutants, however, mutation in *mei-41* did not cause a persistence of γ-HIS2AV foci in nurse cells, suggesting these cells repair their DSBs with wild-type kinetics.

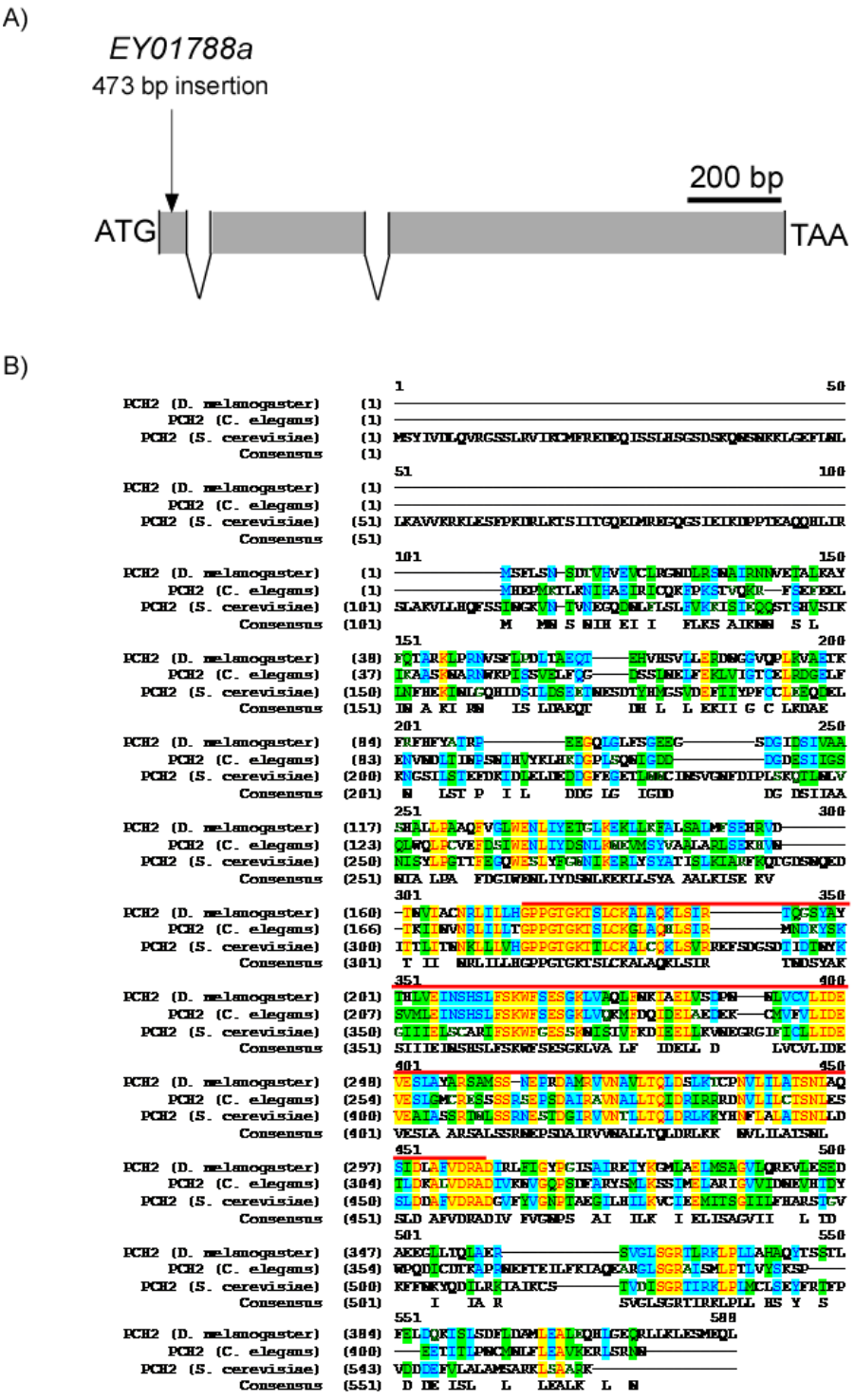

Figure S 4: Alignment of PCH2 orthologs.

A) Schematic of the Drosophila *pch2* transcript (CG31453) showing the splicing pattern and the location of the P-element insertion *EY01788a*. The coding region is shown in grey and the untranslated regions in black. B) Full-length protein sequence alignment of PCH2 homologs from *Drosophila*, *C. elegans* and *S. cerevisiae.* The location of the conserved AAA-ATPase domain is shown with an orange line.

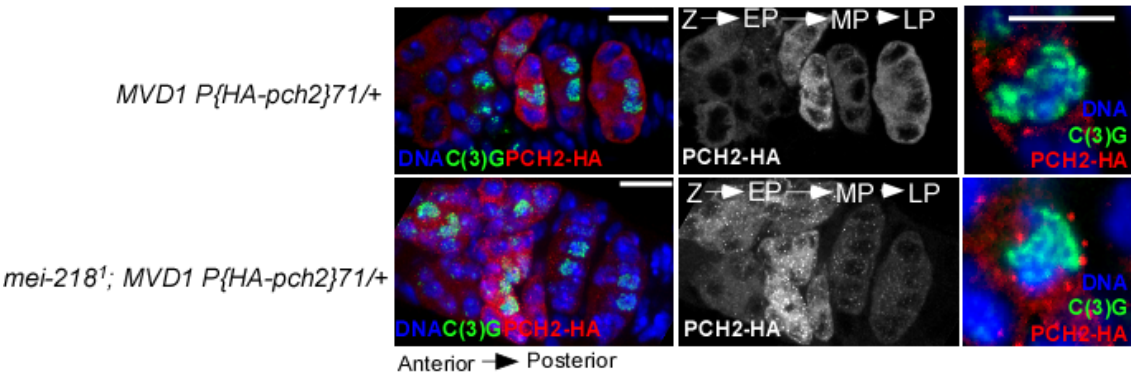

Figure S 5: PCH2 localization in *mei-218* mutants.

MVD1-driven PCH2 expression persists into region 2 and region 3 in a *mei-218* mutant. Single section of an early pachytene oocyte with PCH2 foci adjacent to the DNA stain, indicating that *mei-218* has no effect on the localization pattern of PCH2 within a cell.

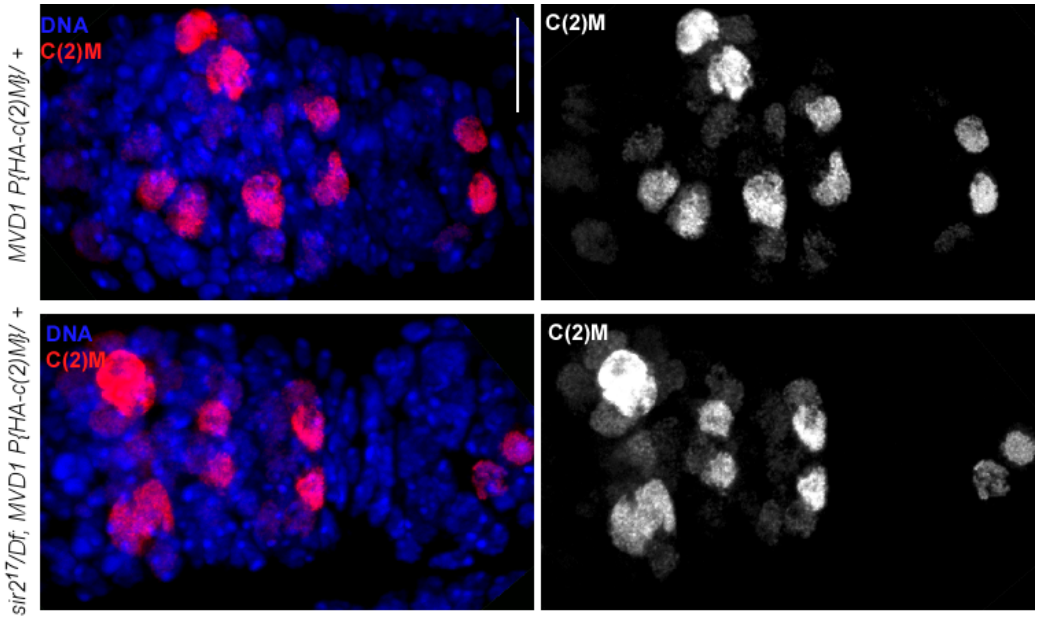

Figure S 6: C(2)M Expression by the *P(UAS:c(2)M3XHA)* transgene in wild-type and *sir2* mutants.

Germaria are stained with anti-HA to detect transgenic *MVD1*-driven *UASP:c(2)M*. In wild-type (*MVD1 UASP:c(2)M/+*), transgenic C(2)M staining is present in the pro-oocytes throughout the germarium. In *sir2* mutants, transgenic C(2)M staining is as robust as in wild-type, indicating the transcription of *UASP*-driven genes is not affected in this background. The images are a maximum projection of all sections through the germaria. Scale bar is 10μM.

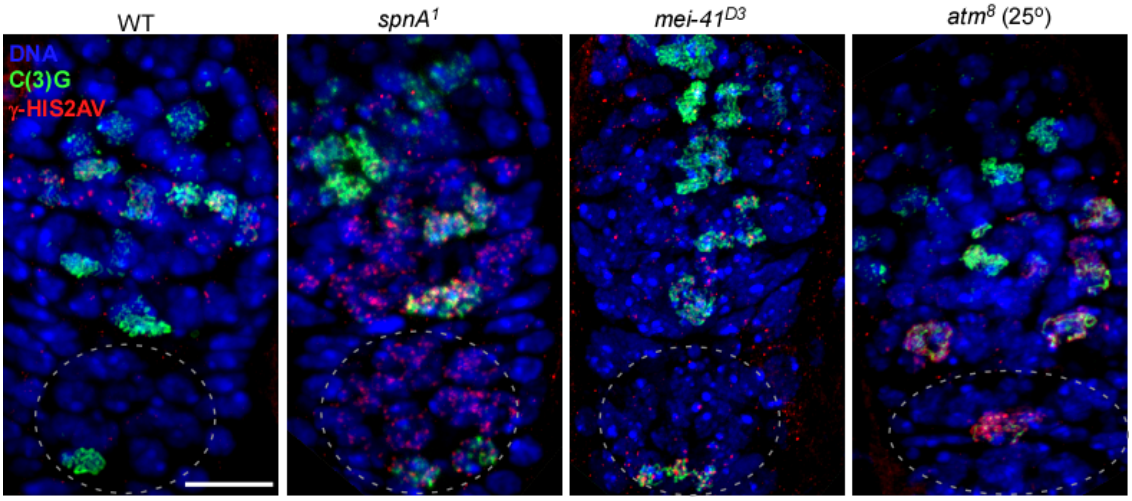

Figure S 7: Oocyte-specific DSB repair defects in *mei-41* and *atm* mutants.

Wild-type, *spn-A*^{1}, *mei-41*^{D3}, and *atm*^{8} mutant germaria with antibodies labeling γ-HIS2AV (red), DNA (blue), and C(3)G (green). In comparison to the repair-defective *spn-A*^{1} mutant, the persistence of γ-HIS2AV foci into region 3 cysts (dotted circle) in *mei-41*^{D3} and *atm*^{8} are restricted to the oocytes (C(3)G-staining cells).

APPENDIX 2: Localization of HDM during oogenesis

To analyze the HDM protein expression patterns during meiosis, a transgene was constructed containing a hemagluttin (HA) epitope at the N-terminus of the *hdm* transcript under the control of an inducible UASP promoter. We expressed HDM using the germline specific driver *P(Gal4::VP16-nos.UTR)MVD1* (Van Doren et al. 1998), abbreviated as *MVD1,* known to drive high levels of expression in the germarium.

We were able to detect the ~50kDa epitope-tagged HDM protein from all transgenic lines expressed with the *MVD1* driver by Western blotting using an anti-HA antibody (Figure 24). Genetic experiments assaying nondisjunction frequencies were performed to test whether the *HA-hdm* constructs produced functional protein. While only one transgenic line tested completely rescued the *hdm* nondisjunction phoenotype (*HA-hdm[60]*), three others reduced it and one failed to rescue at all (Table 10). These results probably reflect different transgenic protein levels or the timing of expression.

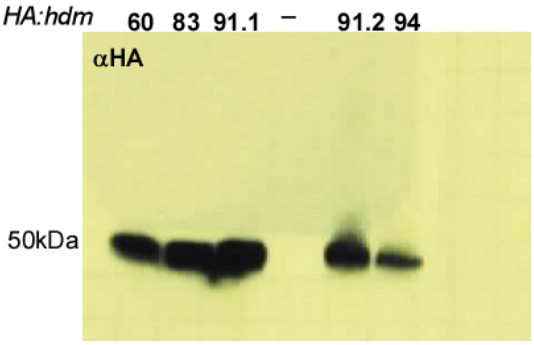

Figure 24: Western blotting from ovaries expressing transgenic *hdm*
HDM detected using anti-HA antibody. Western blot conducted by Shree Tanneti.

The most striking feature of HDM staining was that is was found between pachytene cells in the fusome, a germline specific organelle, which colocalized with a fusome-specific protein Hts (Figure 25). This, however, could be due to overproduction of the protein. HDM staining also formed foci that localized on the DNA in early pachytene (region 2) cells, when DSB formation and recombination occurs (Figure 25).

No HDM foci were detected in region 3 cells. Consistent with a role in DNA repair, HDM colocalized with γ-HIS2AV foci suggesting it is present at DSB sites (Figure 25). Suprisingly, HDM colocalized with ~80% (n=67) of the γ-HIS2AV foci, which is more than the expected number of crossovers (~5 or 25% of breaks); this suggests the protein is present at noncrossover sites as well. HDM may fail to colocalize with all recombination sites if its localization is short-lived and or becomes undetectable at a certain stage when γ-HIS2AV is still present. Although the fusome staining of HDM remained, no HDM foci were observed when DSB formation was blocked by a mutation in *mei-W68*, suggesting HDM localization was dependent on break formation.

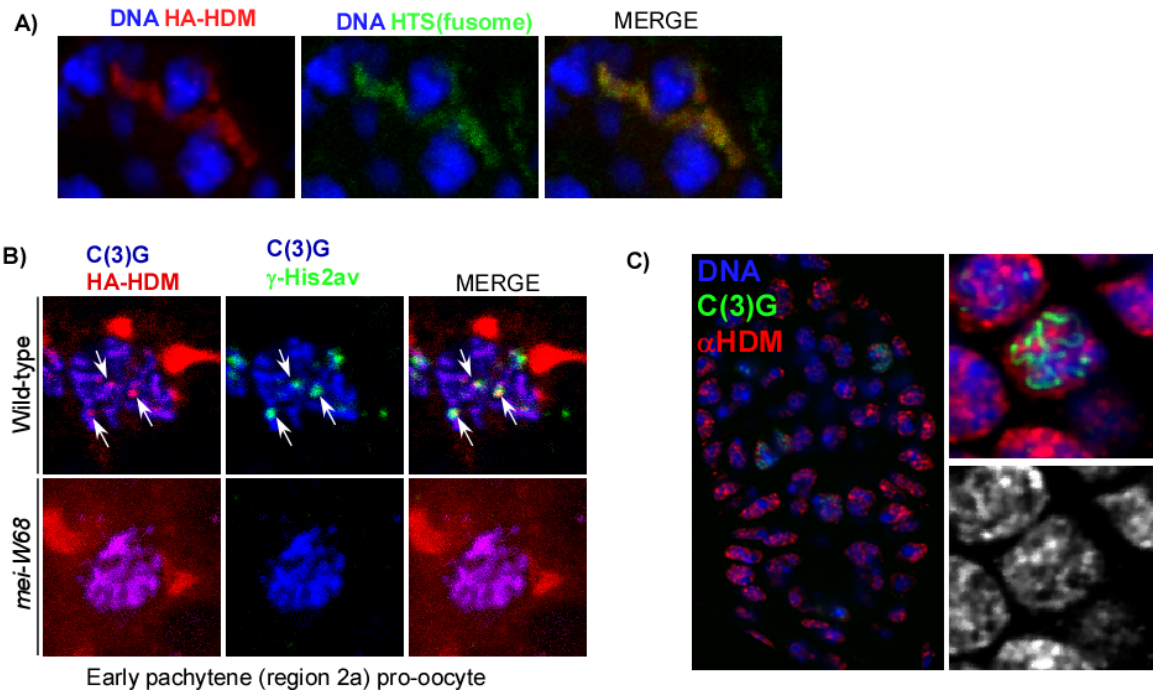

Figure 25: HDM localization during meiosis.

A) Meiotic nuclei showing colocalization between anti-HA staining to detect transgenic HDM protein and anti-Hts (fusome). B) Wild-type and *mei-W68* mutant oocytes stained with anti-HA to detect transgenic HDM and γ-HIS2AV to mark DSBs. In wild-type, the HDM foci colocalized with the majority of γ-HIS2AV foci. In *mei-W68* mutants, both γ-HIS2AV and nuclear HDM staining were eliminated. C) Wild-type germarium stained with anti-HDM antibody (αHDM) and C(3)G to mark the oocytes. αHDM staining shows thread-like nuclear staining in both oocytes and nurse cells.

To further investigate the localization pattern of HDM during oogenesis, we raised antibodies against a peptide corresponding to part of the protein (Figure 27). Antibodies were made using Genomic Antibody Technology™ by SDIX, which were then affinity purified. In wild-type, we found that αHDM localized throughout both oocyte and nurse cell nuclei. In contrast to our results with transgenic HDM, the αHDM produced a thread-like staining pattern that colocalized with a large fraction of the DNA.

To test the specificity of the antibody, we repeated αHDM staining in *hdm*^{g6} *hdm*^{g8}, and *hdm*^{g7} mutants (see Chapter 2 for mutant characterization). *hdm*^{g7} mutants contain a 161-bp deletion towards the end of exon 1 (Joyce et al. 2009). Since this causes a frame-shift prior to the peptide sequence used for antibody production, we expected to observe only non-specific background signal. To our dismay, the staining pattern was identical to that of wild-type in all mutants tested (data not shown), suggesting the αHDM antibody was recognizing a different protein. In support of this conclusion, we failed to observe any fusome staining with the αHDM antibody in ovaries expressing transgenic *hdm* (data not shown). These results indicate that the antibody raised against HDM most likely recognizes an unknown protein that binds ubiquitously to chromsomes. Furthermore, while we were able to detect a 50kDa band using the αHDM antibody by western blotting (Figure 24), we failed to detect a larger band that represented transgenic HDM containing multiple HA tags. We also detected numerous bands of various sizes in a wild-type background as well as from

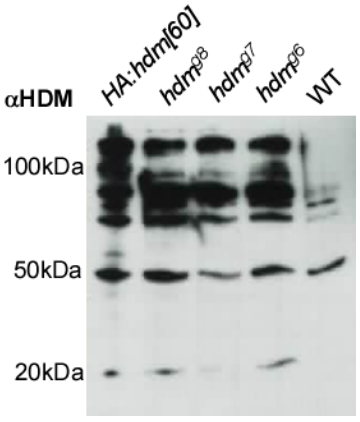

Figure 26: Western blotting from wild-type and *hdm* mutant ovaries. HDM detected using αHDM antibody. Western blot conducted by Shree Tanneti.

ovaries expressing transgenic HDM (Figure 26). The same result was observed using the αHDM antibody in *hdm* mutants (Figure 26). Together, these results indicate that the αHDM antibody is non-specific and most likely fails to recognize HDM protein.

My results with the anti-HA antibody and transgenic HDM suggests that HDM is localizing to all DSB sites and is dependent on break formation. These are somewhat suprising results considering *hdm* mutants exhibit crossover-specific recombination defects as well as DSB-independent phenotypes (see Chapters 1 and 2). However, HDM localization may be transient and only stabilized in the presence of DNA damage. That is, an undetectable amount of HDM may first associate with the chromosomes independent of DSBs, which then accumulates once the breaks are induced. Further analysis using the endogenous promoter or a different driver that is constitutively expressed may help determine the exact expression pattern and dependence of the HDM protein.

Although highly speculative, one possibility is that the αHDM antibody is recognizing RPA since the protein contains similar OB-folds to that of HDM. Indeed, the staining pattern of the αHDM antibody and RPA antibody show nearly identical localization (Figure 28). It is also worth noting that an antibody raised against the repair protein SPN-B, made by Trudi Schupbach's lab, showed a similar ubiquitous localization pattern to that of HDM and RPA. I repeated this experiment and found the same result (Figure 28), which was still observed in *spn-B* null mutants (data not shown). While it is possible that the sequence similarity between repair proteins limits the specificity of these antibodies, future studies directed at identifying the specific substrates recognized by these antibodies will help elucidate these confusing results and determine the localization of other repair proteins during meiosis.

HDM sequence

MARRIKFQRLAEMRPTMTRFSTVALIVSKSSPNIFYDKMSGTERGVLSLT

IRDSPNHLTNCKCWGQRDCVDEYAAMLQIGHVVDIVGAKVMSIPFAAPGE

QRYQPQATVSCALVVNEGSGYVVRHDNDDFGQITILQQLLHQPIRPLGAV

LKLADVRSGLGFPDKIITTNVNLLVVVAAVRPVRQIKRKLQGPLSEVQEL

LQCLEVIVIDASYPEGMLLSVWQPDWIQRAQQWQPRRTVLHLIDVRVSYS

NFHRSLVLSHSNCTLICENPQAAGDDCRLLLAFAATVPLTTFSGCDQAEL

DNMPAVASIQAQMTVRQIYSRAEGELQDPSIHQFTAVLYGMVTKFDLDGL

TSHVNRKCIACQQHIPRNLQDCASDACQQYFSLDNDEPRSISYFNINIHL

SDQTGTLVEARLAGHPAERILGLRAEDFERLAEREKSELKWRFLLKYFEV

RLMIKKPVGVRNHLVIVVVDMQAIPLEKLVANMVVF

Figure 27: HDM amino acid sequence.

Full-length HDM amino acid sequence. Black background with white font denotes sequence deleted in *hdm*^{g7} mutants. As this deletion causes a frame-shift mutation grey background with white font denotes wild-type sequence not predicted to be present in the mutant. Red font denotes peptide sequence that antibodies were raised against.

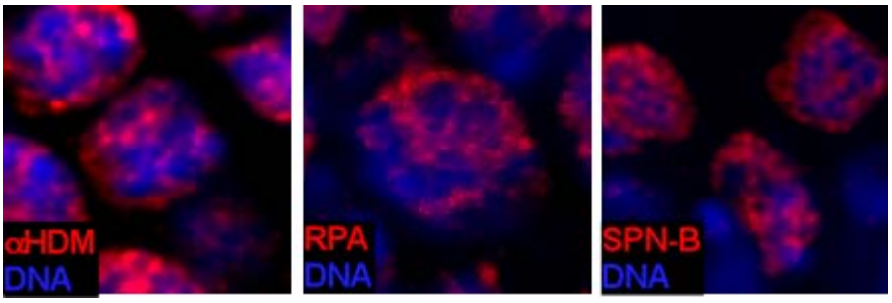

Figure 28: Comparison of αHDM, RPA and SPN-B staining in pachytene oocytes.

Table 10: Transgenic rescue of *hdm* mutants

Genotype[a]	**Transgenic Chromosome position**	**NDJ**	**N**[c]
hdm^{g7} [d]	n/a[b]	7.2%	1615
hdm^{g7}*; MVD1/ HA-hdm[83]*	3rd	2.5%	158
hdm^{g7}*; MVD1/ HA-hdm[91-1]*	3rd	11.2%	197
hdm^{g7}*; HA-hdm[91-2]/+; MVD1*	2nd	3.0	165
hdm^{g7}*; HA-hdm[60]/+; MVD1*	2nd	0%	215
hdm^{g7}*; HA-hdm[94]/+; MVD1*	2nd	3.4%	119

[a] MVD1= P(Gal4::VP16-nos.UTR)MVD1

[b] No transgene present

[c] N= total flies counted

[d] *hdm*^{g7} nondisjunction data from Table 2

APPENDIX 3: Two genetically distinct pathways inhibit *lig4*-dependent repair during meiotic recombination

Meiotic DNA double-strand breaks (DSBs) are repaired as either crossovers or noncrossovers , usually involving recombination with homologous sequences on a nonsister chromatid (Dernburg et al. 1998; McKim et al. 1998; Keeney 2001). Mutation of DSB repair genes such as *spn-A* (Drosophila Rad51) and its paralogs like *spn-D* (Drosophila Rad51C) and *spn-B* (Drosophila Xrcc3), block both repair pathways and, as a result, γ-HIS2AV foci accumulate into late stages of pachytene (Figure 8) (Abdu et al. 2003; Mehrotra et al. 2006). Unlike the DSB repair mutants, precondition mutants *mei-218* and *rec* do not exhibit a delay in the disappearance of γ-HIS2AV foci staining (Figure 8). Instead, these mutants exhibit severely reduced levels of crossover recombination, indicating a more specific defect in the ability to repair DSBs as crossovers (Manheim et al. 2002; Blanton et al. 2005; Joyce et al. 2009).

Surprisingly, in the *mei-218; spn-D* double mutant, both the levels of γ-HIS2AV foci throughout pachytene and the kinetics of foci formation and disappearance closely paralleled those observed in wild-type (Figure 8). Furthermore, since we observed γ-HIS2AV foci levels upon entrance into early pachytene (region 2a) with wild-type levels, MEI-218 and SPN-D are not required for the initiation of meiotic recombination (Figure 8). Together, these results suggest that DSBs are being repaired in the *mei-218; spn-D* double mutant with near-wild-type efficiency, even though repair is not resulting in crossovers.

We set out to determine why the high numbers of persistent γ-HIS2AV foci typical of DSB repair mutants disappear in the *mei-218; spn-D* double mutant. We first tested for a similar effect with a mutation in the Rad51 paralog *spn-B* and found an identical result. Persistent γ-HIS2AV foci were again suppressed in *mei-218; spn-B* double mutants (Figure 29). In contrast, *mei-218; spn-A* double mutants exhibited similar levels of persistent γ-HIS2AV foci to *spn-A* single mutants (Figure 29). Likewise, mutations in another precondition gene, *rec,* had no effect on the γ-HIS2AV persistence observed in *spn-D* mutants (Figure 29). To our knowledge, this is the first phenotypic difference found between precondition mutants *rec* and *mei-218*. Therefore, we reasoned that the precocious disappearance of γ-HIS2AV foci in *mei-218; spn-D* and *mei-218; spn-B* reflects an alternative repair mechanism that might be operating specifically in these double mutant combinations.

Consistent with the conclusion that DSB repair is occurring, the meiotic DSB repair checkpoint that disrupts the dorsal-ventral polarity in developing embryos (Ghabrial et al. 1999; Abdu et al. 2002), was suppressed in these double mutants. We observed a dramatic reduction in the levels of abnormal embryos from *mei-218; spn-D* and *mei-218; spn-B* females compared to the *spn-D* and *spn-B* single mutants (Figure 30). However, the double mutants still exhibit reduced fertility compared to *mei-218* single mutants (Liu et al. 2000; Liu et al. 2002), suggesting the alternative repair might be error-prone.

During meiotic recombination, several mechanisms are in place to inhibit alternative DSB repair pathways and promote homolog bias. For instance, DSB repair via sister chromatid exchange (SCE) is normally suppressed during meiotic recombination by

the cohesion-associated protein ORD (Webber et al. 2004). To test whether *mei-218* is required to inhibit exchange between sisters, we monitored the transmission of a Ring X-chromosome during meiosis. A single crossover between two Ring sister chromatids will create a dicentric Ring chromosome that will not be transmitted efficiently (Webber et al. 2004). In contrast, recombination between two normal "Rod" sister chromatids will not impair their transmission. Therefore, if lack of MEI-218 activity causes significant elevation of SCE in females that contain one Ring X and one normal X chromosome, progeny containing the normal X chromosome should greatly outnumber those that inherit the Ring chromosome.

We monitored meiotic transmission of the Ring X-chromosome *R(1)2* in wild-type, $mei\text{-}218^{1}$, and $mei\text{-}218^{1}; spn\text{-}D^{150}$ mutant females as well as in two other precondition mutants rec^{1}/rec^{2} and $mcm5^{A7}$. As shown in Table 11, the recovery of the *R(1)2* chromosome in all mutants was similar to wild-type. These data argue that SCE is not elevated and thus not responsible for the repair of DSBs in these mutants.

Alternatively, the DSBs may be repaired by non-homologous end-joining (NHEJ), where the broken chromosome ends are sealed together by LIG4 activity without the use of external homologies (Lieber et al. 2003). To examine the contribution of NHEJ to repair in the *mei-218; spn-D* and *mei-218; spn-B* females, we constructed triple mutants with a *lig4* allele and observed γ-HIS2AV foci. The levels of γ-HIS2AV foci in $mei\text{-}218^{1}\ lig4^{57}$ followed a similar trend to that observed in either a $lig4^{57}$ single mutant or wild-type background, indicating that NHEJ does not play a primary role in meiotic DSB repair in Drosophila (Figure 29). The contribution of NHEJ becomes evident, however, when homologous repair is blocked by mutations in either *spn-D* or

spn-B. Thus, *mei-218*^{1} *lig4*^{57}*; spn-D*^{150} late pachytene oocytes exhibited robust γ-HIS2AV labeling, with similar levels as *spn-D*^{150} single mutants (Figure 29). An analogous result was found in *mei-218*^{1} *lig4*^{57}*; spn-B*^{BU} females (Figure 29). These results suggest that LIG4-dependent NHEJ is responsible for meiotic DSB repair when both MEI-218 and either SPN-B or SPN-D activity is lacking.

Interestingly, the *mei-218*^{1} *lig4*^{57}*; spn-D*^{150} triple mutant did not produce abnormal embryos, suggesting the DNA damage checkpoint is inactive despite the persistence of unrepaired DSBs (Figure 30). Perhaps, in the *mei-218*^{1} *lig4*^{57}*; spn-D*^{150} mutant background, the initiation of the end-joining repair pathway is sufficient to block signaling to the DNA damage checkpoint. Indeed, the current model of DSB repair by NHEJ assumes that a heterodimer of Ku70 and Ku80 binds to DNA ends and recruits DNA-PKs and Lig4 to the site of the break, which results in stimulation of DNA end ligation (Critchlow et al. 1997; Doherty et al. 2001). Binding of Ku to the DNA ends may block or compete for resected DNA ends with the checkpoint signaling protein MEI-41 (Laurencon et al. 2003; Ball et al. 2005).

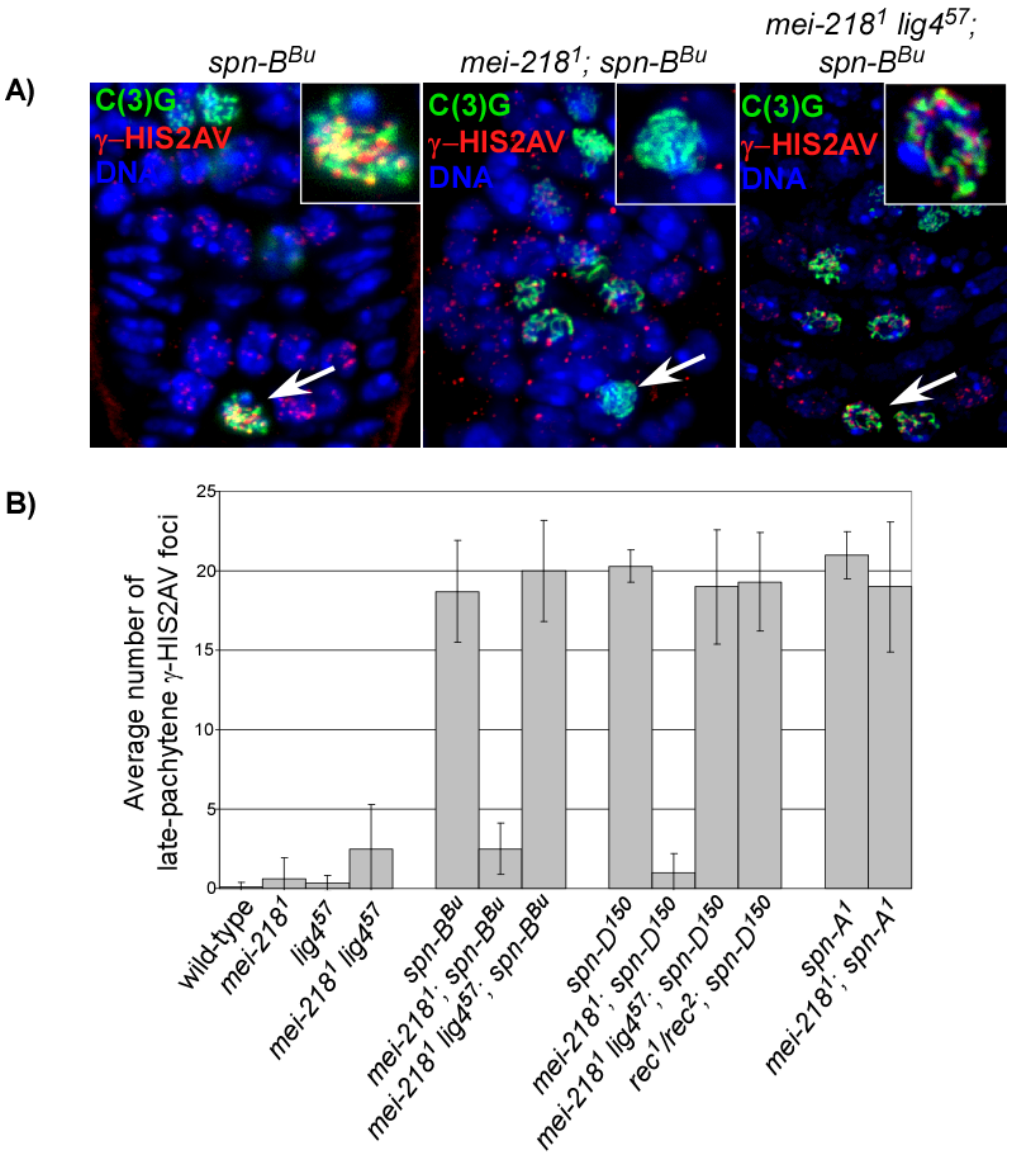

Figure 29: γ-HIS2AV foci in germaria from *spn-B*, *mei-218*; *spn-B* and *mei-218 lig4; spn-B* females. A) Insets are late pachytene oocytes. Note that the persisting γ-HIS2AV foci of *spn-B* mutants are suppressed by mutation of *mei-218* in a *lig4*-dependent manner. B) Average number of late-pachytene γ-HIS2AV foci in repair-defective backgrounds. Error bars denote the standard deviation.

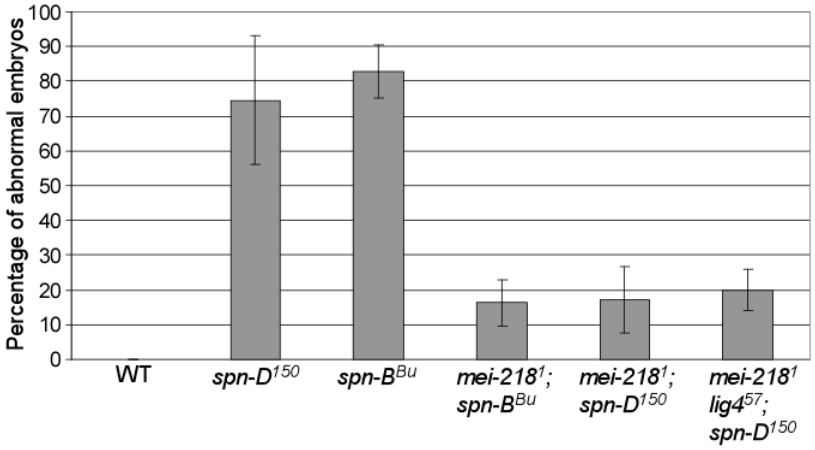

Figure 30: Percentage of abnormal embryos in repair-defective mutants.
Embryos were scored as abnormal if dorsal appendages exhibited ventralized phenotypes (Ghabrial et al. 1999; Staeva-Vieira et al. 2003). Error bars denote the standard deviation.

Table 11: Ring chromosome transmission assay.

Genotype	**Ring/Rod[a]**	**Total progeny**
R(1)2/+	0.90	4698
R(1)2 mei-218^{1}/mei-218^{1}	0.92	424
R(1)2 mei-218^{1}/mei-218^{1}; spn-D^{150}	0.96	450
R(1)2/+; rec^{1}/rec^{2}	0.92	655
R(1)2/+; mcm5^{A7}	0.86	227

[a] Number of Ring X-chromosomes recovered relative to normal Rod X-chromosomes

APPENDIX 4: The relationship between Sir2, acetyl-H3K9, and Synaptonemal complex formation

Sir2 regulates the level of SC: During wild-type oogenesis, oocytes differentiate within 16-cell germline cysts that are arranged temporally within a germarium. In early pachytene cysts, two pro-oocytes initially appear equivalent as both enter meiosis and form complete filaments of C(3)G and C(2)M staining in each pair of pro-oocytes. In late pachytene cysts, located in the most posterior position of the germarium, oocyte selection has occurred, which is characterized by the presence of only a single oocyte with SC staining (Figure 31). When *sir2* mutant ovaries were stained with antibodies recognizing SC components C(3)G and C(2)M to observe synapsis, we found that all 16 nuclei enter meiosis, as viewed by the attainment of SC components of at least mid-zygotene levels (Figure 31). We, therefore, concluded that Sir2 performs an active role in reducing the levels of SC in early pachytene (region 2). At late pachytene (region 3), however, all but the oocyte exit meiosis and become morphologically indistinguishable from nurse cells in 90% of the germaria, indicating *sir2* mutants do not exhibit the

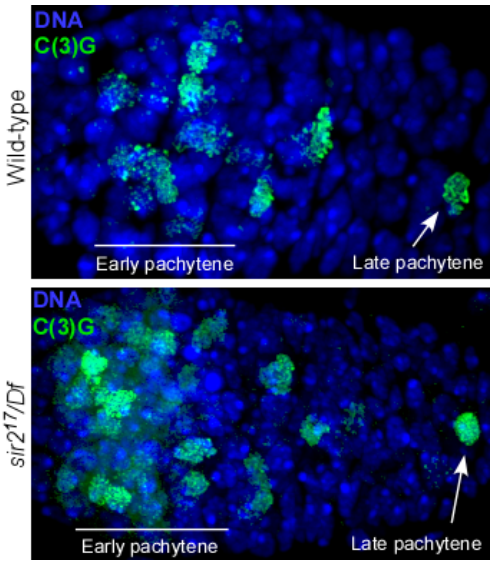

Figure 31: More SC in early pachytene *sir2* mutants.

Shown are maximum projections through wild-type and *sir2* mutant germaria.

progression delays associated with pachytene checkpoint activity (Figure 31).

Acetyl-H3K9 correlates with synapsis initiation during meiotic pachytene: Drosophila Sir2 is an active deacetylase *in vitro*, capable of deacetylating histone H4 (Barlow et al. 2001; Newman et al. 2002; Rosenberg et al. 2002; Astrom et al. 2003). To identify the specific target(s) of Sir2 during meiotic prophase, we analyzed the status of a panel of histone modifications in control and *sir2* mutant oocytes. Recently, H3K56 has been reported to be a direct target of Sir2 deacetylase function *in vivo* (Das et al. 2009). We tested whether H3K56 was a substrate of Sir2 in meiosis and found no acetyl-H3K56 labeling in nuclei during the zygotene and pachytene stages of control germaria. We did, however, find high expression during karyosome formation at stage 2 of oogenesis; although, this pattern of expression did not change in *sir2* mutants (data not shown). Therefore, the ability of Sir2 to deacetlyate H3K56 in somatic cells may not reflect the function of Sir2 or is not detectable during meiosis.

We next stained ovaries with antibodies recognizing other acetylated lysine residues on H3 as well as on H2A and H4. Antibodies against acetyl-H3K14 and acetyl-H4pan failed to stain the control ovaries within the germarium, indicating that either the modifications are absent from the pachytene stage of Drosophila meiosis or at low levels and difficult to detect in this tissue. Using an antibody against the acetylation of various residues on H2A (acetyl-H2Apan), we again found no staining during the zygotene or pachytene stages of meiosis. However, there was strong H2A acetylation staining in stage 2 oocytes during karyosome formation (Figure 32), which may be part of the mechanism that disassembles the SC and promotes karyosome formation (Lancaster et al. 2007). *sir2*

mutants did not differ in the timing or intensity of H2A acetylation during karyosome formation (data not shown).

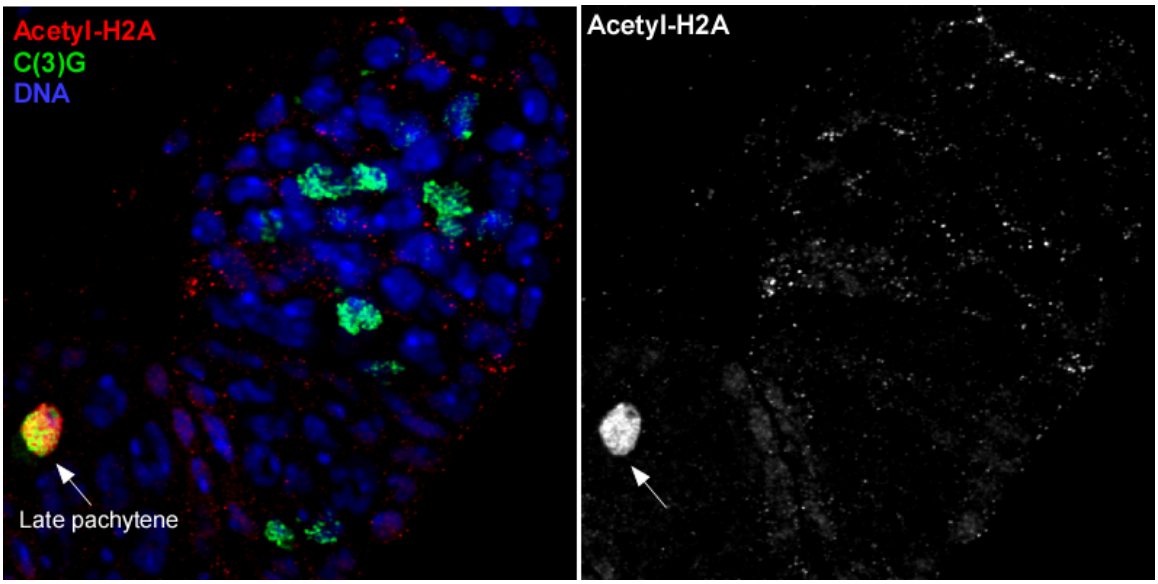

Figure 32: Acetyl-H2Apan staining in a wild-type germarium.

Acetylation staining was abundant in karyosome when SC disassembly begins. Arrow denotes stage 2 oocyte.

Our most striking results were found with acetyl-H3K9 staining, which showed robust labeling in nuclei at the zygotene stage of meiosis, when SC is partially formed (Figure 33). This hyperacetylation appeared to be uniform throughout most of the nucleus; however, there existed a small area of low to no acetylation corresponding to the heterochromatic cluster of centromeres known as the chromocenter (Figure 33). Moreover, within zygotene cells, C(2)M and C(3)G patches always colocalized with these deacetylated areas (Figure 33). Consistent with data from budding yeast (Tsubouchi et al. 2008), these results suggest synapsis initiates in regions at or near the centromeres.

At pachytene, when chromosomes are fully synapsed, acetyl-H3K9 staining becomes much lower compared to zygotene cells (Figure 33). Careful examination of cells at this stage showed an exclusion of C(2)M and C(3)G labeling from chromosome regions of high acetyl-H3K9 staining. This low acetylation state remained in the oocyte until karyosome formation at stage 2 of oogeneisis when desynapsis begins. Thus, we reasoned the SC either polymerizes in deacetylated regions and/or has a direct role in the deacetylation of H3K9.

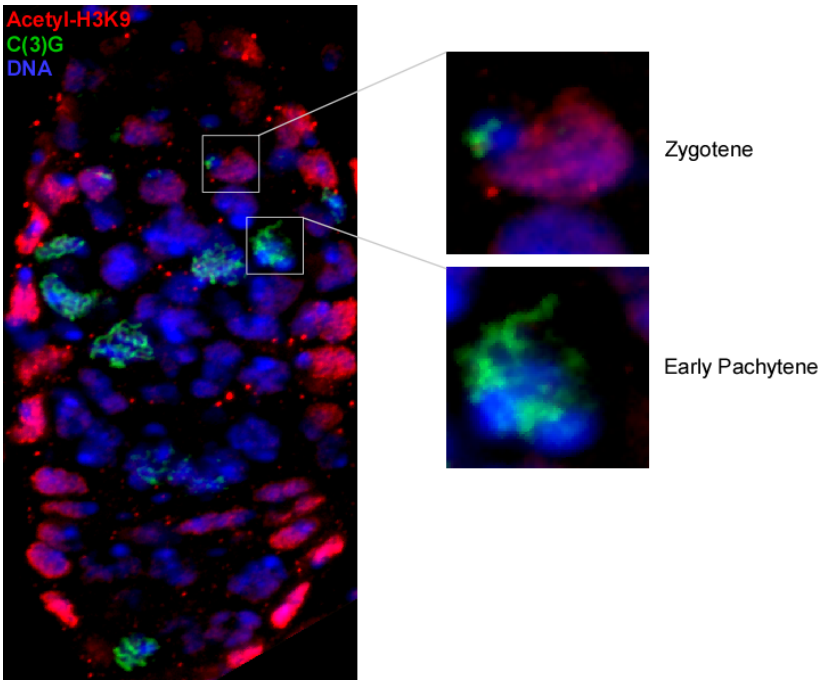

Figure 33: Acetyl-H3K9 staining in a wild-type germarium.

Acetylation levels are high in zygotene when synapsis initiates and becomes low at pachytene when synapsis is complete.

Sir2 is required for H3K9 deacetylation during meiotic pachytene: To determine if Sir2 plays a role in the deacetlyation of H3K9, *sir2* mutant ovaries were stained for acetyl-H3K9. In *sir2* mutants, the robust acetyl-H3K9 staining within

zygotene cells was not affected, but persisted within pachytene cells, which was never observed in wild-type (Figure 34). Also, in the absence of *sir2*, C(3)G was no longer excluded from chromosome regions with the acetyl-H3K9 staining. Therefore, Sir2 may have a role in preventing SC from polymerizing in acetylated regions of the chromosome.

Interestingly, mutation of *c(3)G* also suppressed the deacetylation of pachytene cells, suggesting synapsis formation is indirectly affecting H3K9 deacetylation (Figure 34). Taken together, these results suggest that synapsis initiates in zygotene at or near heterochromatic regions corresponding to the centromeres. As C(3)G polymerizes, it may rapidly promote Sir2 to deacetylate H3K9 during the pachytene stage of meiosis. During pachytene H3K9 remains in a low acetlyated state throughout the entire nucleus until karyosome formation and desynapsis at stage 2 of oogeneisis.

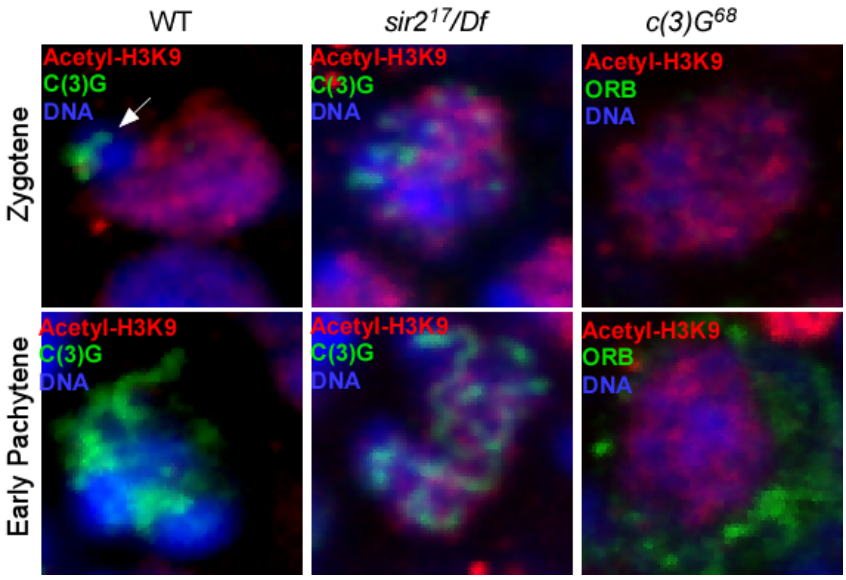

Figure 34: Acetyl-H3K9 staining in wild-type, *sir2* and *c(3)G* mutants.

Oocytes were labeled with an antibody against C(3)G or, in the case of *c(3)G* mutants, the cytoplasmic ORB protein. Arrow in wild-type denotes patch of C(3)G in deacetylated region of the nucleus (SC initiation site).

As of yet, the relationship between Sir2-mediated H3K9 deacetylation and the pachytene checkpoint remains unclear. No diffence in H3K9 acetylation levels was observed between wild-type and mutants that exhbit pachytene delays (data not shown). However, prolonged Sir2 activity may deacetlyate H3K9 to lower levels than wild-type, which may not be detectable. This low acetylated state of chromosomes may limit how much SC is incorporated and create an environment more suitable for crossover formation. Indeed, *c(3)G* heterozygotes, which presumably make half the wild-type levels of protein, exhibit increased levels of crossing over (Gowen et al. 1922). Therefore, H3K9 acetylation may modulate the levels of SC, which subsequently can affect the level of crossovers.

Table 12: Comparison of chromatin modifications in prophase I.

Modification[a]	**Localization in control**	**Localization in *sir2* mutant**
H2Aac	Karyosome formation[b]	same as WT
H3K56ac	Karyosome formation	same as WT
H3K14	No staining	No staining
H3K9ac	Zygotene cells, follicle cells and karyosome formation	Zygotene cells, Pachytene cells, follicle cells, and karyosome formation
H4ac	Follicle cells and karyosome formation	same as WT

[a] Ovaries from control and $sir2^{17}/Df$ mutant females were stained with antibodies specific to the the histone modification listed in the first column.

[b] Karyosome formation occurs at stage 2 of oogenesis. None of the listed modifications where observed past stage 3 of oogenesis.

REFERENCES

Abdu, U., M. Brodsky, et al. (2002). "Activation of a Meiotic Checkpoint during Drosophila Oogenesis Regulates the Translation of Gurken through Chk2/Mnk." Curr Biol **12**(19): 1645.

Abdu, U., A. Gonzalez-Reyes, et al. (2003). "The Drosophila spn-D gene encodes a RAD51C-like protein that is required exclusively during meiosis." Genetics **165**(1): 197-204.

Albertson, D. G. and J. N. Thomson (1993). "Segregation of holocentric chromosomes at meiosis in the nematode, Caenorhabditis elegans." Chromosome Res **1**(1): 15-26.

Anderson, L. K., K. D. Hooker, et al. (2001). "The distribution of early recombination nodules on zygotene bivalents from plants." Genetics **159**(3): 1259-69.

Anderson, L. K., S. M. Royer, et al. (2005). "Juxtaposition of C(2)M and the transverse filament protein C(3)G within the central region of Drosophila synaptonemal complex." Proc Natl Acad Sci U S A **102**(12): 4482-7.

Astrom, S. U., T. W. Cline, et al. (2003). "The Drosophila melanogaster sir2+ gene is nonessential and has only minor effects on position-effect variegation." Genetics **163**(3): 931-7.

Bailis, J. M. and S. L. Forsburg (2004). "MCM proteins: DNA damage, mutagenesis and repair." Curr Opin Genet Dev **14**(1): 17-21.

Bailis, J. M., D. D. Luche, et al. (2008). "Minichromosome maintenance proteins interact with checkpoint and recombination proteins to promote s-phase genome stability." Mol Cell Biol **28**(5): 1724-38.

Baker, B. S. and A. T. C. Carpenter (1972). "Genetic analysis of sex chromosomal meiotic mutants in *Drosophila melanogaster*." Genetics **71**: 255-286.

Baker, B. S., A. T. C. Carpenter, et al. (1978). "The utilization during mitotic cell division of loci controlling meiotic recombination in *Drosophila melanogaster*." Genetics **90**: 531-578.

Baker, B. S. and J. C. Hall (1976). Meiotic mutants: genetic control of meiotic recombination and chromosome segregation. The Genetics and Biology of *Drosophila*. M. Ashburner and E. Novitski. New York, Academic Press. **1a:** 351-434.

Ball, H. L., J. S. Myers, et al. (2005). "ATRIP binding to replication protein A-single-stranded DNA promotes ATR-ATRIP localization but is dispensable for Chk1 phosphorylation." Mol Biol Cell **16**(5): 2372-81.

Barbosa, V., N. Kimm, et al. (2007). "A maternal screen for genes regulating Drosophila oocyte polarity uncovers new steps in meiotic progression." Genetics **176**(4): 1967-77.

Barlow, A. L., C. M. van Drunen, et al. (2001). "dSIR2 and dHDAC6: two novel, inhibitor-resistant deacetylases in Drosophila melanogaster." Exp Cell Res **265**(1): 90-103.

Bass, H. W. (2003). "Telomere dynamics unique to meiotic prophase: formation and significance of the bouquet." Cell Mol Life Sci **60**(11): 2319-24.

Bastin-Shanower, S. A. and S. J. Brill (2001). "Functional analysis of the four DNA binding domains of replication protein A. The role of RPA2 in ssDNA binding." J Biol Chem **276**(39): 36446-53.

Bellen, H. J., R. W. Levis, et al. (2004). "The BDGP gene disruption project: single transposon insertions associated with 40% of Drosophila genes." Genetics **167**(2): 761-81.

Belmont, A. S., M. B. Braunfeld, et al. (1989). "Large-scale chromatin structural domains within mitotic and interphase chromosomes in vivo and in vitro." Chromosoma **98**(2): 129-43.

Bennett-Lovsey, R. M., A. D. Herbert, et al. (2008). "Exploring the extremes of sequence/structure space with ensemble fold recognition in the program Phyre." Proteins **70**(3): 611-25.

Bhagat, R., E. A. Manheim, et al. (2004). "Studies on crossover specific mutants and the distribution of crossing over in Drosophila females." Cytogenetic and Genome Res. **107**: 160-71.

Bhalla, N. and A. F. Dernburg (2005). "A conserved checkpoint monitors meiotic chromosome synapsis in Caenorhabditis elegans." Science **310**(5754): 1683-6.

Bhuiyan, H. and K. Schmekel (2004). "Meiotic chromosome synapsis in yeast can occur without spo11-induced DNA double-strand breaks." Genetics **168**(2): 775-83.

Bi, X., M. Gong, et al. (2005). "Drosophila ATM and Mre11 are essential for the G2/M checkpoint induced by low-dose irradiation." Genetics **171**(2): 845-7.

Bi, X., S. C. Wei, et al. (2004). "Telomere protection without a telomerase; the role of ATM and Mre11 in Drosophila telomere maintenance." Curr Biol **14**(15): 1348-53.

Bickel, S. E., D. W. Wyman, et al. (1997). "Mutational analysis of the Drosophila sister-chromatid cohesion protein ORD and its role in the maintenance of centromeric cohesion." Genetics **146**: 1319-1331.

Bishop, D. K. and D. Zickler (2004). "Early decision; meiotic crossover interference prior to stable strand exchange and synapsis." Cell **117**(1): 9-15.

Blanton, H. L., S. J. Radford, et al. (2005). "REC, Drosophila MCM8, Drives Formation of Meiotic Crossovers." PLoS Genet **1**(3): e40.

Borner, G. V., A. Barot, et al. (2008). "Yeast Pch2 promotes domainal axis organization, timely recombination progression, and arrest of defective recombinosomes during meiosis." Proc Natl Acad Sci U S A **105**(9): 3327-32.

Borner, G. V., N. Kleckner, et al. (2004). "Crossover/noncrossover differentiation, synaptonemal complex formation, and regulatory surveillance at the leptotene/zygotene transition of meiosis." Cell **117**(1): 29-45.

Boyd, J. B., M. D. Golino, et al. (1976). "The *mei-9*^{a} mutant of *Drosophila melanogaster* increases mutagen sensitivity and decreases excision repair." Genetics **84**: 527-544.

Brown, P. W., L. Judis, et al. (2005). "Meiotic synapsis proceeds from a limited number of subtelomeric sites in the human male." Am J Hum Genet **77**(4): 556-66.

Burma, S., B. P. Chen, et al. (2001). "ATM phosphorylates histone H2AX in response to DNA double-strand breaks." J Biol Chem **276**(45): 42462-7.

Burnham, C. R., J. T. Stout, et al. (1972). "Chromosome pairing in maize." Genetics **71**: 111-126.

Carlton, P. M., A. P. Farruggio, et al. (2006). "A link between meiotic prophase progression and crossover control." PLoS Genet **2**(2): e12.

Carpenter, A. T. C. (1975). "Electron microscopy of meiosis in *Drosophila melanogaster* females. I. Structure, arrangement, and temporal change of the synaptonemal complex in wild-type." Chromosoma **51**: 157-182.

Carpenter, A. T. C. (1979). "Recombination nodules and synaptonemal complex in recombination-defective females of *Drosophila melanogaster*." Chromosoma **75**: 259-292.

Carpenter, A. T. C. (1979). "Synaptonemal complex and recombination nodules in wild-type *Drosophila melanogaster* females." Genetics **92**: 511-541.

Carpenter, A. T. C. (1987). "Gene conversion, recombination nodules, and the initiation of meiotic synapsis." Bioessays **6**: 232-236.

Carpenter, A. T. C. (1988). Thoughts on Recombination nodules, meiotic recombination, and chiasmata. Genetic recombination. R. Kucherlapati and G. Smith. Washington, D.C., American Society of Microbiology**:** 529-548.

Carpenter, A. T. C. and B. S. Baker (1982). "On the control of the distribution of meiotic exchange in *Drosophila melanogaster*." Genetics **101**: 81-89.

Carpenter, A. T. C. and L. Sandler (1974). "On recombination-defective meiotic mutants in *Drosophila melanogaster*." Genetics **76**: 453-475.

Ciapponi, L., G. Cenci, et al. (2004). "The Drosophila Mre11/Rad50 complex is required to prevent both telomeric fusion and chromosome breakage." Curr Biol **14**(15): 1360-6.

Ciapponi, L., G. Cenci, et al. (2006). "The Drosophila Nbs protein functions in multiple pathways for the maintenance of genome stability." Genetics **173**(3): 1447-54.

Colaiacovo, M. P., A. J. MacQueen, et al. (2003). "Synaptonemal complex assembly in C. elegans is dispensable for loading strand-exchange proteins but critical for proper completion of recombination." Dev Cell **5**(3): 463-74.

Cooper, K. W. (1964). "Meiotic conjunctive elements not involving chiasmata." Proc. Natl. Acad. Sci., USA **52**: 1248-1255.

Couteau, F., K. Nabeshima, et al. (2004). "A component of C. elegans meiotic chromosome axes at the interface of homolog alignment, synapsis, nuclear reorganization, and recombination." Curr Biol **14**(7): 585-92.

Couteau, F. and M. Zetka (2005). "HTP-1 coordinates synaptonemal complex assembly with homolog alignment during meiosis in C. elegans." Genes Dev **19**(22): 2744-56.

Critchlow, S. E., R. P. Bowater, et al. (1997). "Mammalian DNA double-strand break repair protein XRCC4 interacts with DNA ligase IV." Curr Biol **7**(8): 588-98.

Csink, A. K. and S. Henikoff (1998). "Large-scale chromosomal movements during interphase progression in Drosophila." J Cell Biol **143**(1): 13-22.

Dart, D. A., K. E. Adams, et al. (2004). "Recruitment of the cell cycle checkpoint kinase ATR to chromatin during S-phase." J Biol Chem **279**(16): 16433-40.

Das, C., M. S. Lucia, et al. (2009). "CBP/p300-mediated acetylation of histone H3 on lysine 56." Nature **459**(7243): 113-7.

de Vries, S. S., E. B. Baart, et al. (1999). "Mouse MutS-like protein Msh5 is required for proper chromosome synapsis in male and female meiosis." Genes Dev **13**(5): 523-31.

Dernburg, A. F., K. McDonald, et al. (1998). "Meiotic recombination in *C. elegans* initiates by a conserved mechanism and is dispensable for homologous chromosome synapsis." Cell **94**(3): 387-98.

Dernburg, A. F., J. W. Sedat, et al. (1996). "Direct evidence of a role for heterochromatin in meiotic chromosome segregation." Cell **85**: 135-146.

Ding, X., R. Xu, et al. (2007). "SUN1 is required for telomere attachment to nuclear envelope and gametogenesis in mice." Dev Cell **12**(6): 863-72.

Dobzhansky, T. (1931). "The decrease of crossing-over observed in translocations, and its probable explanation." Am. Nat. **65**: 214-232.

Doherty, A. J. and S. P. Jackson (2001). "DNA repair: how Ku makes ends meet." Curr Biol **11**(22): R920-4.

Edelmann, W., P. E. Cohen, et al. (1999). "Mammalian MutS homologue 5 is required for chromosome pairing in meiosis." Nat Genet **21**(1): 123-7.

Fung, J. C., W. F. Marshall, et al. (1998). "Homologous chromosome pairing in Drosophila melanogaster proceeds through multiple independent initiations." J Cell Biol **141**(1): 5-20.

Fung, J. C., B. Rockmill, et al. (2004). "Imposition of crossover interference through the nonrandom distribution of synapsis initiation complexes." Cell **116**(6): 795-802.

Gerton, J. L. and R. S. Hawley (2005). "Homologous chromosome interactions in meiosis: diversity amidst conservation." Nat Rev Genet **6**(6): 477-87.

Ghabrial, A., R. P. Ray, et al. (1998). "*okra* and *spindle-B* encode components of the RAD52 DNA repair pathway and affect meiosis and patterning in Drosophila oogenesis." Genes & Dev. **12**(17): 2711-23.

Ghabrial, A. and T. Schupbach (1999). "Activation of a meiotic checkpoint regulates translation of Gurken during Drosophila oogenesis." Nat Cell Biol. **1**(6): 354-357.

Goday, C. and S. Pimpinelli (1989). "Centromere organization in meiotic chromosomes of Parascaris univalens." Chromosoma **98**(3): 160-6.

Gong, W. J., K. S. McKim, et al. (2005). "All Paired Up with No Place to Go: Pairing, Synapsis, and DSB Formation in a Balancer Heterozygote." PLoS Genet **1**(5): e67.

Gonzalez-Reyes, A., H. Elliot, et al. (1997). "Oocyte determination and the origin of polarity in *Drosophila*: the role of the *spindle* genes." Development **124**: 4927-4937.

Gorski, M. M., R. J. Romeijn, et al. (2004). "Disruption of Drosophila Rad50 causes pupal lethality, the accumulation of DNA double-strand breaks and the induction of apoptosis in third instar larvae." DNA Repair (Amst) **3**(6): 603-15.

Gowen, M. S. and J. W. Gowen (1922). "Complete linkage in *Drosophila melanogaster*." American Naturalist **61**: 286-288.

Grell, R. F. and J. W. Day (1970). "Chromosome pairing in the oogonial cells of *Drosophila melanogaster*." Chromosoma **31**: 424-445.

Grushcow, J. M., T. M. Holzen, et al. (1999). "Saccharomyces cerevisiae checkpoint genes MEC1, RAD17 and RAD24 are required for normal meiotic recombination partner choice." Genetics **153**(2): 607-20.

Hall, J. C. (1972). "Chromosome segregation influenced by two alleles of the meiotic mutant *c(3)G* in *Drosphila melanogaster*." Genetics **71**: 367-400.

Harper, L., I. Golubovskaya, et al. (2004). "A bouquet of chromosomes." J Cell Sci **117**(Pt 18): 4025-32.

Hawley, R. S. (1980). "Chromosomal sites necessary for normal levels of meiotic recombination in *Drosophila melanogaster*. I. Evidence for and mapping of the sites." Genetics **94**: 625-646.

Henderson, K. A. and S. Keeney (2004). "Tying synaptonemal complex initiation to the formation and programmed repair of DNA double-strand breaks." Proc Natl Acad Sci U S A **101**(13): 4519-4524.

Henderson, K. A. and S. Keeney (2005). "Synaptonemal complex formation: where does it start?" Bioessays **27**(10): 995-8.

Herman, R. K. and C. K. Kari (1989). "Recombination between small X chromosome duplications and the X chromosome in Caenorhabditis elegans." Genetics **121**(4): 723-37.

Heyer, W. D., K. T. Ehmsen, et al. (2003). "Holliday junctions in the eukaryotic nucleus: resolution in sight?" Trends Biochem Sci **28**(10): 548-57.

Hillers, K. J. (2004). "Crossover interference." Curr Biol **14**(24): R1036-7.

Hillers, K. J. and A. M. Villeneuve (2003). "Chromosome-wide control of meiotic crossing over in C. elegans." Curr Biol **13**(18): 1641-7.

Hiraoka, Y., A. F. Dernburg, et al. (1993). "The onset of homologous chromosome pairing during *Drosophila melanogaster* embryogenesis." Journal of Cell Biology **120**: 591-600.

Hoffmann, E. R. and R. H. Borts (2004). "Meiotic recombination intermediates and mismatch repair proteins." Cytogenet Genome Res **107**(3-4): 232-48.

Hollingsworth, N. M. and S. J. Brill (2004). "The Mus81 solution to resolution: generating meiotic crossovers without Holliday junctions." Genes Dev **18**(2): 117-25.

Huynh, J. and D. St. Johnston (2000). "The role of BicD, Egl, Orb and the microtubules in the restriction of meiosis to the Drosophila oocyte." Development **127**(13): 2785-2794.

Jaklevic, B. R. and T. T. Su (2004). "Relative contribution of DNA repair, cell cycle checkpoints, and cell death to survival after DNA damage in Drosophila larvae." Curr Biol **14**(1): 23-32.

James, P., J. Halladay, et al. (1996). "Genomic libraries and a host strain designed for highly efficient two-hybrid selection in yeast." Genetics **144**(4): 1425-36.

Jang, J. K., D. E. Sherizen, et al. (2003). "Relationship of DNA double-strand breaks to synapsis in Drosophila." J. Cell. Sci. **116**: 3069-3077.

Jones, G. H. (1984). "The control of chiasma distribution." Symp Soc Exp Biol **38**: 293-320.

Joshi, N., A. Barot, et al. (2009). "Pch2 links chromosome axis remodeling at future crossover sites and crossover distribution during yeast meiosis." PLoS Genet **5**(7): e1000557.

Joyce, E. F. and K. S. McKim (2009). "Drosophila PCH2 Is Required for a Pachytene Checkpoint That Monitors Double-Strand-Break-Independent Events Leading to Meiotic Crossover Formation." Genetics **181**(1): 39-51.

Joyce, E. F., S. N. Tanneti, et al. (2009). "Drosophila Hold'em Is Required for a Subset of Meiotic Crossovers and Interacts With the DNA Repair Endonuclease Complex Subunits MEI-9 and ERCC1." Genetics **181**(1): 335-40.

Kanda, T., K. F. Sullivan, et al. (1998). "Histone-GFP fusion protein enables sensitive analysis of chromosome dynamics in living mammalian cells." Curr Biol **8**(7): 377-85.

Keeney, S. (2001). "Mechanism and control of meiotic recombination initiation." Curr Top Dev Biol **52**: 1-53.

King, R. C. (1970). Ovarian development in *Drosophila melanogaster*. New York, Academic Press, Inc.

Kinner, A., W. Wu, et al. (2008). "Gamma-H2AX in recognition and signaling of DNA double-strand breaks in the context of chromatin." Nucleic Acids Res **36**(17): 5678-94.

Kleckner, N., D. Zickler, et al. (2004). "A mechanical basis for chromosome function." Proc Natl Acad Sci U S A **101**(34): 12592-7.

Klovstad, M., U. Abdu, et al. (2008). "Drosophila brca2 is required for mitotic and meiotic DNA repair and efficient activation of the meiotic recombination checkpoint." PLoS Genet **4**(2): e31.

Kneitz, B., P. E. Cohen, et al. (2000). "MutS homolog 4 localization to meiotic chromosomes is required for chromosome pairing during meiosis in male and female mice." Genes Dev **14**(9): 1085-97.

Kunz, C. and P. Schar (2004). "Meiotic recombination: sealing the partnership at the junction." Curr Biol **14**(22): R962-4.

Kusch, T., L. Florens, et al. (2004). "Acetylation by Tip60 is required for selective histone variant exchange at DNA lesions." Science **306**(5704): 2084-7.

Lake, C. M., K. Teeter, et al. (2007). "A genetic analysis of the Drosophila mcm5 gene defines a domain specifically required for meiotic recombination." Genetics **176**(4): 2151-63.

Lancaster, O. M., C. F. Cullen, et al. (2007). "NHK-1 phosphorylates BAF to allow karyosome formation in the Drosophila oocyte nucleus." J Cell Biol **179**(5): 817-24.

Lantz, V., J. S. Chang, et al. (1994). "The Drosophila ORB RNA-binding protein is required for the formation of the egg chamber and establishment of polarity." Genes & Dev. **8**: 598-613.

LaRocque, J. R., B. Jaklevic, et al. (2007). "Drosophila ATR in double-strand break repair." Genetics **175**(3): 1023-33.

Laurencon, A., A. Purdy, et al. (2003). "Phenotypic analysis of separation-of-function alleles of MEI-41, Drosophila ATM/ATR." Genetics **164**(2): 589-601.

Lavin, M. F. (2007). "ATM and the Mre11 complex combine to recognize and signal DNA double-strand breaks." Oncogene **26**(56): 7749-58.

Lee, J. H. and T. T. Paull (2006). "Purification and biochemical characterization of ataxia-telangiectasia mutated and Mre11/Rad50/Nbs1." Methods Enzymol **408**: 529-39.

Li, X. and J. C. Schimenti (2007). "Mouse pachytene checkpoint 2 (trip13) is required for completing meiotic recombination but not synapsis." PLoS Genet **3**(8): e130.

Lieber, M. R., Y. Ma, et al. (2003). "Mechanism and regulation of human non-homologous DNA end-joining." Nat Rev Mol Cell Biol **4**(9): 712-20.

Lindsley, D. L. and G. G. Zimm (1992). The Genome of *Drosophila melanogaster*. San Diego, CA, Academic Press, Inc.

Liu, H., J. K. Jang, et al. (2000). "Two genes required for meiotic recombination in Drosophila are expressed from a dicistronic message." Genetics **154**(4): 1735-46.

Liu, H., J. K. Jang, et al. (2002). "*mei-P22* encodes a chromosome-associated protein required for the initiation of meiotic recombination in *Drosophila melanogaster*." Genetics **162**: 245-258.

Lucchesi, J. C. and D. T. Suzuki (1968). "The interchromosomal control of recombination." Ann. Rev. Genet. **2**: 53-86.

MacQueen, A. J., M. P. Colaiacovo, et al. (2002). "Synapsis-dependent and -independent mechanisms stabilize homolog pairing during meiotic prophase in C. elegans." Genes Dev **16**(18): 2428-42.

Macqueen, A. J., C. M. Phillips, et al. (2005). "Chromosome Sites Play Dual Roles to Establish Homologous Synapsis during Meiosis in C. elegans." Cell **123**(6): 1037-50.

Madigan, J. P., H. L. Chotkowski, et al. (2002). "DNA double-strand break-induced phosphorylation of Drosophila histone variant H2Av helps prevent radiation-induced apoptosis." Nucleic Acids Res **30**(17): 3698-705.

Manheim, E. A., J. K. Jang, et al. (2002). "Cytoplasmic localization and evolutionary conservation of MEI-218, a protein required for meiotic crossing over in Drosophila." Mol. Biol. Cell **13**: 84-95.

Manheim, E. A. and K. S. McKim (2003). "The Synaptonemal Complex Component C(2)M Regulates Meiotic Crossing over in Drosophila." Curr Biol **13**(4): 276-85.

Marshall, W. F., A. F. Dernburg, et al. (1996). "Specific interactions of chromatin with the nuclear envelope: positional determination within the nucleus in *Drosophila melanogaster*." Mol Biol Cell **7**(5): 825-42.

Martinez-Perez, E. and A. M. Villeneuve (2005). "HTP-1-dependent constraints coordinate homolog pairing and synapsis and promote chiasma formation during C. elegans meiosis." Genes Dev **19**(22): 2727-43.

Matsuoka, S., B. A. Ballif, et al. (2007). "ATM and ATR substrate analysis reveals extensive protein networks responsive to DNA damage." Science **316**(5828): 1160-6.

McCaffrey, R., D. St Johnston, et al. (2006). "Drosophila mus301/spindle-C Encodes a Helicase With an Essential Role in Double-Strand DNA Break Repair and Meiotic Progression." Genetics **174**(3): 1273-85.

McKee, B. D. and G. H. Karpen (1990). "Drosophila ribosomal RNA genes function as an *X-Y* pairing site during male meiosis." Cell **61**: 61-72.

McKim, K., E. F. Joyce, et al., Eds. (2008). Cytological analysis of meiosis in fixed Drosophila ovaries. Methods in Molecular Biology. Totowa, NJ, Humana Press.

McKim, K. S., J. B. Dahmus, et al. (1996). "Cloning of the *Drosophila melanogaster* meiotic recombination gene *mei-218*: a genetic and molecular analysis of interval 15E." Genetics **144**: 215-228.

McKim, K. S., B. L. Green-Marroquin, et al. (1998). "Meiotic synapsis in the absence of recombination." Science **279**: 876-878.

McKim, K. S. and A. Hayashi-Hagihara (1998). "*mei-W68* in *Drosophila melanogaster* encodes a Spo11 homolog: evidence that the mechanism for initiating meiotic recombination is conserved." Genes & Dev. **12**(18): 2932-42.

McKim, K. S., A. M. Howell, et al. (1988). "The effects of translocations on recombination frequency in *Caenorhabditis elegans*." Genetics **120**: 987-1001.

McKim, K. S., J. K. Jang, et al. (2002). "Meiotic recombination and chromosome segregation in Drosophila females." Annu. Rev. Genet. **36**: 205-232.

McKim, K. S., K. Peters, et al. (1993). "Two types of sites required for meiotic chromosome pairing in *Caenorhabditis elegans*." Genetics **134**: 749-768.

McKim, K. S. and A. M. Rose (1990). "Chromosome I duplications in Caenorhabditis elegans." Genetics **124**(1): 115-32.

Mehrotra, S., R. S. Hawley, et al. (2007). Synapsis, double strand breaks and domains of crossover control in females. Recombination and meiosis, crossing-over and disjunction. R. Egel and D. Lankenau. Berlin, Springer-Verlag**:** 125-152.

Mehrotra, S. and K. S. McKim (2006). "Temporal analysis of meiotic DNA double-strand break formation and repair in Drosophila females." PLoS Genet **2**(11): e200.

Meneely, P. M., A. F. Farago, et al. (2002). "Crossover distribution and high interference for both the X chromosome and an autosome during oogenesis and spermatogenesis in Caenorhabditis elegans." Genetics **162**(3): 1169-77.

Mitra, N. and G. S. Roeder (2007). "A novel nonnull ZIP1 allele triggers meiotic arrest with synapsed chromosomes in Saccharomyces cerevisiae." Genetics **176**(2): 773-87.

Mitsis, P. G. (1995). "Phosphorylation and localization of replication protein A during oogenesis and early embryogenesis of Drosophila melanogaster." Dev Biol **170**(2): 445-56.

Moens, P. B., N. K. Kolas, et al. (2002). "The time course and chromosomal localization of recombination-related proteins at meiosis in the mouse are compatible with models that can resolve the early DNA-DNA interactions without reciprocal recombination." J Cell Sci **115**(Pt 8): 1611-22.

Muller, H. J. (1916). "The mechanism of crossing-over." American Naturalist **50**: 193-434.

Nabeshima, K., A. M. Villeneuve, et al. (2005). "Crossing over is coupled to late meiotic prophase bivalent differentiation through asymmetric disassembly of the SC." J Cell Biol **168**(5): 683-9.

Nabeshima, K., A. M. Villeneuve, et al. (2004). "Chromosome-wide regulation of meiotic crossover formation in Caenorhabditis elegans requires properly assembled chromosome axes." Genetics **168**(3): 1275-92.

Nagai, S., K. Dubrana, et al. (2008). "Functional targeting of DNA damage to a nuclear pore-associated SUMO-dependent ubiquitin ligase." Science **322**(5901): 597-602.

Namiki, Y. and L. Zou (2006). "ATRIP associates with replication protein A-coated ssDNA through multiple interactions." Proc Natl Acad Sci U S A **103**(3): 580-5.

Neale, M. J. and S. Keeney (2006). "Clarifying the mechanics of DNA strand exchange in meiotic recombination." Nature **442**(7099): 153-8.

Neuman-Silberberg, F. S. and T. Schupbach (1993). "The Drosophila dorsoventral patterning gene gurken produces a dorsally localized RNA and encodes a TGF alpha-like protein." Cell **75**(1): 165-74.

Newman, B. L., J. R. Lundblad, et al. (2002). "A Drosophila homologue of Sir2 modifies position-effect variegation but does not affect life span." Genetics **162**(4): 1675-85.

Novitski, E. and G. Braver (1954). "An analysis of crossing over within a heterozygous inversion in Drosophila melanogaster." Genetics **39**: 197-209.

Oikemus, S. R., J. Queiroz-Machado, et al. (2006). "Epigenetic telomere protection by Drosophila DNA damage response pathways." PLoS Genet **2**(5): e71.

Page, S. L. and R. S. Hawley (2001). "*c(3)G* encodes a *Drosophila* synaptonemal complex protein." Genes & Dev. **15**: 3130-3143.

Page, S. L. and R. S. Hawley (2004). "The genetics and molecular biology of the synaptonemal complex." Annu Rev Cell Dev Biol **20**: 525-58.

Papamichos-Chronakis, M., J. E. Krebs, et al. (2006). "Interplay between Ino80 and Swr1 chromatin remodeling enzymes regulates cell cycle checkpoint adaptation in response to DNA damage." Genes Dev **20**(17): 2437-49.

Penkner, A., L. Tang, et al. (2007). "The nuclear envelope protein Matefin/SUN-1 is required for homologous pairing in C. elegans meiosis." Dev Cell **12**(6): 873-85.

Peretz, G., L. G. Arie, et al. (2009). "The Drosophila hus1 gene is required for homologous recombination repair during meiosis." Mech Dev **126**(8-9): 677-86.

Petukhova, G. V., P. J. Romanienko, et al. (2003). "The Hop2 protein has a direct role in promoting interhomolog interactions during mouse meiosis." Dev Cell **5**(6): 927-36.

Phillips, C. M. and A. F. Dernburg (2006). "A Family of Zinc-Finger Proteins Is Required for Chromosome-Specific Pairing and Synapsis during Meiosis in C. elegans." Dev Cell **11**(6): 817-29.

Phillips, C. M., C. Wong, et al. (2005). "HIM-8 Binds to the X Chromosome Pairing Center and Mediates Chromosome-Specific Meiotic Synapsis." Cell **123**(6): 1051-63.

Queenan, A. M., G. Barcelo, et al. (1999). "The transmembrane region of Gurken is not required for biological activity, but is necessary for transport to the oocyte membrane in Drosophila." Mech Dev **89**(1-2): 35-42.

Queiroz-Machado, J., J. Perdigao, et al. (2001). "tef: a mutation that causes telomere fusion and severe genome rearrangements in Drosophila melanogaster." Chromosoma **110**(1): 10-23.

Radford, S. J., E. Goley, et al. (2005). "Drosophila ERCC1 is required for a subset of MEI-9-dependent meiotic crossovers." Genetics **170**(4): 1737-45.

Ramesh, M. A., S. B. Malik, et al. (2005). "A phylogenomic inventory of meiotic genes; evidence for sex in Giardia and an early eukaryotic origin of meiosis." Curr Biol **15**(2): 185-91.

Rasmussen, S. W. (1977). "The transformation of the Synaptonemal Complex into the 'elimination chromatin' in Bombyx mori oocytes." Chromosoma **60**(3): 205-21.

Ray, R. P. and T. Schupbach (1996). "Intercellular signaling and the polarization of body axes during Drosophila oogenesis." Genes Dev **10**(14): 1711-23.

Riechmann, V. and A. Ephrussi (2001). "Axis formation during Drosophila oogenesis." Curr Opin Genet Dev **11**(4): 374-83.

Roberts, P. A. (1970). "Screening for X-ray induced crossover suppressors in *Drosophila melanogaster*: Prevalence and effectiveness of translocations." Genetics **65**: 429-448.

Roberts, P. A. (1972). "Differences in the synaptic affinity of chromosome arms of *Drosophila melanogaster* revealed by differential sensitivity to translocation heterozygosity." Genetics **71**: 401-415.

Roeder, G. S. and J. M. Bailis (2000). "The pachytene checkpoint." Trends Genet **16**(9): 395-403. _00002080 _00002080.

Rogakou, E. P., C. Boon, et al. (1999). "Megabase chromatin domains involved in DNA double-strand breaks in vivo." J. Cell Biol. **146**(5): 905-16.

Rose, A. M., D. L. Baillie, et al. (1984). "Meiotic pairing behavior of two free duplications of linkage group I in *Caenorhabditis elegans*." Mol. Gen. Genet. **195**: 52-56.

Rosenberg, M. I. and S. M. Parkhurst (2002). "Drosophila Sir2 is required for heterochromatic silencing and by euchromatic Hairy/E(Spl) bHLH repressors in segmentation and sex determination." Cell **109**(4): 447-58.

Rosenbluth, R. E. and D. L. Baillie (1981). "Analysis of a reciprocal translocation, *eT1(III;V)*, in Caenorhabditis elegans." Genetics **124**: 415-428.

San-Segundo, P. A. and G. S. Roeder (1999). "Pch2 links chromatin silencing to meiotic checkpoint control." Cell **97**(3): 313-24.

Sandler, L., D. L. Lindsley, et al. (1968). "Mutants affecting meiosis in natural populations of *Drosophila melanogaster*." Genetics **60**: 525-558.

Sapir, A., R. Schweitzer, et al. (1998). "Sequential activation of the EGF receptor pathway during Drosophila oogenesis establishes the dorsoventral axis." Development **125**(2): 191-200.

Sekelsky, J. J., K. S. McKim, et al. (1995). "The Drosophila meiotic recombination gene *mei-9* encodes a homologue of the yeast excision repair protein Rad1." Genetics **141**: 619-627.

Sherizen, D., J. K. Jang, et al. (2005). "Meiotic recombination in Drosophila females depends on chromosome continuity between genetically defined boundaries." Genetics **169**(2): 767-81.

Shiloh, Y. (2006). "The ATM-mediated DNA-damage response: taking shape." Trends Biochem Sci **31**(7): 402-10.

Sibon, O. C., A. Laurencon, et al. (1999). "The Drosophila ATM homologue Mei-41 has an essential checkpoint function at the midblastula transition." Curr Biol **9**(6): 302-12.

Sijbers, A. M., W. L. de Laat, et al. (1996). "Xeroderma Pigmentosum Group F caused by a defect in a structure-specific DNA repair endonuclease." Cell **86**: 811-822.

Silva, E., S. Tiong, et al. (2004). "ATM is required for telomere maintenance and chromosome stability during Drosophila development." Curr Biol **14**(15): 1341-7.

Slijepcevic, P. (2006). "The role of DNA damage response proteins at telomeres--an "integrative" model." DNA Repair (Amst) **5**(11): 1299-306.

Song, Y. H., G. Mirey, et al. (2004). "The Drosophila ATM ortholog, dATM, mediates the response to ionizing radiation and to spontaneous DNA damage during development." Curr Biol **14**(15): 1354-9.

Spradling, A. C. (1993). Developmental genetics of oogenesis. The Development of Drosophila melanogaster. M. Bate and A. M. Arias. Cold Spring Harbor, NY, Cold Spring Harbor Laboratory Press**:** 1--70.

Spradling, A. C. (1993). "Germline cysts: communes that work." Cell **72**(5): 649-51.

Stack, S. M. and L. K. Anderson (2002). "Crossing over as assessed by late recombination nodules is related to the pattern of synapsis and the distribution of early recombination nodules in maize." Chromosome Res **10**(4): 329-45.

Staeva-Vieira, E., S. Yoo, et al. (2003). "An essential role of DmRad51/SpnA in DNA repair and meiotic checkpoint control." Embo J **22**(21): 5863-74.

Stahl, F. (1996). "Meiotic recombination in yeast: coronation of the double-strand-break repair model." Cell **87**(6): 965-8.

Stapleton, M., G. Liao, et al. (2002). "The Drosophila gene collection: identification of putative full-length cDNAs for 70% of D. melanogaster genes." Genome Res **12**(8): 1294-300.

Storlazzi, A., S. Tesse, et al. (2003). "Meiotic double-strand breaks at the interface of chromosome movement, chromosome remodeling, and reductional division." Genes Dev **17**(21): 2675-87.

Stucki, M. and S. P. Jackson (2006). "gammaH2AX and MDC1: anchoring the DNA-damage-response machinery to broken chromosomes." DNA Repair (Amst) **5**(5): 534-43.

Sturtevant, A. H. (1915). "The behavior of the chromosomes as studied through linkage." Z. Induktive Abstammungs Vererbungslehre **13**: 234-87.

Szauter, P. (1984). "An analysis of regional constraints on exchange in Drosophila melanogaster using recombination-defective meiotic mutants." Genetics **106**(1): 45-71.

Tesse, S., A. Storlazzi, et al. (2003). "Localization and roles of Ski8p protein in Sordaria meiosis and delineation of three mechanistically distinct steps of meiotic homolog juxtaposition." Proc Natl Acad Sci U S A **100**(22): 12865-70.

Tracey, W. D., Jr., X. Ning, et al. (2000). "Quantitative analysis of gene function in the Drosophila embryo." Genetics **154**(1): 273-84.

Tsubouchi, H. and G. S. Roeder (2003). "The importance of genetic recombination for fidelity of chromosome pairing in meiosis." Dev Cell **5**(6): 915-25.

Tsubouchi, T., A. J. Macqueen, et al. (2008). "Initiation of meiotic chromosome synapsis at centromeres in budding yeast." Genes Dev **22**(22): 3217-26.

Van Doren, M., A. L. Williamson, et al. (1998). "Regulation of zygotic gene expression in Drosophila primordial germ cells." Curr Biol **8**(4): 243-6.

Villeneuve, A. M. (1994). "A cis-acting locus that promotes crossing over between X chromosomes in Caenorhabditis elegans." Genetics **136**(3): 887-902.

von Wettstein, D., S. W. Rasmussen, et al. (1984). "The synaptonemal complex in genetic segregation." Annual Review of Genetics **18**: 331-413.

Wakimoto, B. T. and M. G. Hearn (1990). "The effects of chromosome rearrangements on the expression of heterochromatic genes in chromosome *2L* of *Drosophila melanogaster*." Genetics **125**: 141-154.

Walker, M. Y. and R. S. Hawley (2000). "Hanging on to your homolog: the roles of pairing, synapsis and recombination in the maintenance of homolog adhesion." Chromosoma **109**(1-2): 3-9.

Ward, I. M. and J. Chen (2001). "Histone H2AX is phosphorylated in an ATR-dependent manner in response to replicational stress." J Biol Chem **276**(51): 47759-62.

Webber, H. A., L. Howard, et al. (2004). "The cohesion protein ORD is required for homologue bias during meiotic recombination." J Cell Biol **164**(6): 819-29.

Whitby, M. C. (2005). "Making crossovers during meiosis." Biochem Soc Trans **33**(Pt 6): 1451-5.

Wojtasz, L., K. Daniel, et al. (2009). "Mouse HORMAD1 and HORMAD2, two conserved meiotic chromosomal proteins, are depleted from synapsed chromosome axes with the help of TRIP13 AAA-ATPase." PLoS Genet **5**(10): e1000702.

Wu, H. Y. and S. M. Burgess (2006). "Two distinct surveillance mechanisms monitor meiotic chromosome metabolism in budding yeast." Curr Biol **16**(24): 2473-9.

Wyman, C. and R. Kanaar (2006). "DNA double-strand break repair: all's well that ends well." Annu Rev Genet **40**: 363-83.

Xu, J., S. Xin, et al. (2001). "Drosophila Chk2 is required for DNA damage-mediated cell cycle arrest and apoptosis." FEBS Lett **508**(3): 394-8.

Yildiz, O., H. Kearney, et al. (2004). "Mutational analysis of the Drosophila DNA repair and recombination gene mei-9." Genetics **167**(1): 263-73.

Yildiz, O., S. Majumder, et al. (2002). "Drosophila MUS312 Interacts with the Nucleotide Excision Repair Endonuclease MEI-9 to Generate Meiotic Crossovers." Mol Cell **10**(6): 1503-9.

Zhimulev, I. F. and E. S. Belyaeva (2003). "Intercalary heterochromatin and genetic silencing." Bioessays **25**(11): 1040-51.

Zickler, D. (2006). "From early homologue recognition to synaptonemal complex formation." Chromosoma **115**(3): 158-74.

Zickler, D. and N. Kleckner (1998). "The leptotene-zygotene transition of meiosis." Annu Rev Genet **32**: 619-97.

Zickler, D. and N. Kleckner (1999). "Meiotic chromosomes: integrating structure and function." Annu. Rev. Genet. **33**: 603-754.

Zou, L., D. Liu, et al. (2003). "Replication protein A-mediated recruitment and activation of Rad17 complexes." Proc Natl Acad Sci U S A **100**(24): 13827-32.

Zou, Y., Y. Liu, et al. (2006). "Functions of human replication protein A (RPA): from DNA replication to DNA damage and stress responses." J Cell Physiol **208**(2): 267-73.

CURRICULUM VITAE

ERIC F. JOYCE

EDUCATION

- B.A. Genetics and Microbiology, May 2004, Rutgers, The State University of New Jersey

- Ph.D. Microbiology and Molecular Genetics, May 2010, Rutgers, The State University of New Jersey

RESEARCH EXPERIENCE

- March 2006 – May 2010: Doctoral research with Dr. Kim S. McKim, Waksman Institute, Rutgers University, New Jersey

- May 2004 – September 2005: Research technician in Dr. Kim McKim's laboratory at Rutgers University, New Jersey

PUBLICATIONS

- Joyce, E. F. & McKim, K.S. When specialized sites are important for synapsis and the distribution of crossovers. *Bioessays* 2007 Mar;29(3):217-26. Review.

- Joyce, E.F., Tanneti, N.S. & McKim, K.S. Drosophila Hold'em is required for a subset of meiotic crossovers and interacts with the DNA repair endonuclease complex subunits MEI-9 and ERCC1. *Genetics* 2009 Jan;181(1):335-40. Epub 2008 Oct 28.

- Joyce, E.F. & McKim, K.S. Drosophila PCH2 is required for a pachytene checkpoint that monitors double-strand-break-independent events leading to meiotic crossover formation. *Genetics* 2009 Jan;181(1):39-51. Epub 2008 Oct 28.

- McKim, K.S., Joyce, E.F. & Jang, J.K. Cytological analysis of meiosis in fixed Drosophila ovaries. *Methods Mol. Biol.* 2009; 558: 197-216. Review.

- Joyce, E.F., & McKim, K. Disorganized chromosome axes induce a checkpoint-mediated delay and interchromosomal effect on crossing over during Drosophila meiosis. *Plos Genetics* 2010 (*under review*).

- Joyce, E.F., Pederson, M., Tiong, S., Homola, E., Campbell, S.D., & McKim, K. ATM and ATR analysis reveal two modes of HIS2AV regulation during Drosophila oogenesis. 2010 (*In preparation*).

- Joyce, E.F., Chen, K. & McKim, K.S. Two genetically distinct pathways inhibit *lig4*-dependent repair during meiotic recombination. 2010 (*In preperation*).